Universitat de Lleida

From circulating tumour cells to metastases:
The role of Cyclin D1 and characterisation of new biomarkers

Marta Guasch Vallés

http://hdl.handle.net/10803/675443

Universitat de Lleida

From circulating tumour cells to metastases:

The role of Cyclin D1 and characterisation of new biomarkers

Marta Guasch Vallés

Memòria presentada per optar al grau de Doctor per la Universitat de Lleida

Programa de Doctorat en Salut

Director i Tutor

Dr. Eloi Garí Marsol

Directora

Dra. Neus Pedraza González

2022

Buscant el camí

El trajecte de vida
és ple de contradiccions,
hi ha nit i també dia,
vivim perseguint il·lusions.

Il·lusió aconseguida,
alegria i oblit,
a l'horitzó nova fita,
emocions i neguit.

del meu avi Francesc

Als meus pares

AGRAÏMENTS

Sembla que fos ahir que vaig trepitjar per primera vegada el laboratori de Cicle Cel·lular de l'IRB de Lleida. Era un dilluns de febrer del 2016, i la Neus C. ens explicava els seus resultats en un seminari. Jo era tot nervis i il·lusió, i començava les pràctiques del quart curs de Biomedicina. Tot eren novetats: el laboratori, el projecte, els companys... De seguida em vaig sentir part del grup i, sense saber gaire bé com, han passat sis anys. Avui, me'n vaig del laboratori amb un grapat d'aventures al cor, que sempre recordaré amb nostàlgia, i una tesi sota el braç. Demà, encararé una nova etapa amb els nervis i il·lusions que caracteritzen els començaments. Durant tot aquest temps he après molt de grans persones, i és per aquest motiu que els vull dedicar aquestes sinceres paraules.

Recordo que durant les classes d'Enginyeria Genètica de la carrera vaig pensar que si mai arribava a fer la tesi, m'agradaria que aquell professor fos el meu director. El caracteritzava l'entusiasme per la matèria, la paciència i que et feia gaudir tot el que explicava. Moltes gràcies, Eloi, per acollir-me al laboratori des de les pràctiques de grau, quan gairebé no sabia ni agafar una pipeta, fins al final de la tesi doctoral. M'has ajudat a aprendre a organitzar-me els experiments i seminaris, a saber-me expressar de manera científica, a pensar i a treballar al laboratori. Has sigut el meu guia durant tots aquests anys i, en definitiva, ets el responsable de tota la meva formació com a científica. Penso, molt sincerament, que ets el millor director de tesi que podia tenir. Moltes gràcies per ser el meu referent com a científic i com a persona.

Moltes gràcies, família de Cicle Cel·lular, pel suport que m'heu donat en tot moment, els coneixements que m'heu transmès i totes les vivències viscudes. Agrair-te, Neus P., l'estar sempre disposada a debatre la metodologia o els resultats d'un experiment i per interessar-te, dia a dia, pels meus progressos o fracassos. Aquesta tesi ha anat millorant gràcies a tu. Muchas gracias, Paco, por enseñarme a tener una visión objetiva y crítica de los resultados. Moltes gràcies al Jordi, per qüestionar-me i aportar-me idees durant els seminaris de grup; a la Neus C., per fer-me sentir una més, per oferir-me sempre la seva ajuda i per compartir amb mi tot el seu coneixement, sobretot en l'àmbit de cultius; a Celia, por sus sabias recomendaciones tras años de experiencia; i a la Gemma, per tots els seus consells. Mariel, even though we haven't shared much time in the lab, I've spent really nice moments with you. Thank you very much for them!

Moltes gràcies, Sònia R. i Marta R. per fer els dies més amens, fàcils i alegres, pels cafès, per les converses i pels consells i els ànims que des d'un principi m'heu regalat. Sònia, ets un puntal pel grup, sense tu no hagués pogut escriure aquesta tesi. Marta, ets l'essència de les bones estones i gràcies a tu el meu pas pel laboratori està farcit de grans moments. Moltes gràcies a les dues per cuidar-me!

Tània, un agraïment sincer és poc en comparació a tota l'ajuda que m'has proporcionat. Tot el que sé t'ho dec a tu. Gràcies pels teus protocols, els teus consells i els moments viscuts entre rialles, converses i cançons al fons Nord del laboratori i a la sala de cultius. Són instants de la meva vida que sempre tindran un racó al meu cor. Gràcies per formar-ne part. Moltes gràcies Turi per la teva alegria i per ensenyar-me que, de vegades, ens hem de prendre les coses amb una mica més de "ritmo caribeño". Eva, moltes gràcies per transformar les coses difícils en fàcils, les frustracions en reptes i els mals dies en bons. Tens una màgia molt bonica. Ha estat un plaer enorme compartir amb tu moments de les nostres vides tant especials. Sempre recordaré el nostre primer dia al laboratori, la IP del riure imparable, el tancament a la cambra freda i mil històries més. Gràcies per tot! Thank you Sonia A., for all your support! Gràcies, Noel, per ajudar-me en els meus primers passos al laboratori, per acollir-me i per endinsar-me en el projecte del grup durant les pràctiques del grau.

A tots els meus companys pre-docs, molts ànims amb les vostres tesis! Marc, és difícil trobar les paraules adequades per agrair-te tot el que has fet per mi. Gràcies per ser un bon company de laboratori i estar sempre disposat a ajudar-me, aportar-me idees i fer-me guanyar seguretat en mi mateixa. Gràcies per fer-me formar part del grup des d'un inici, per les converses, els debats, les confessions, els cafès, els Escape Rooms i els sopars. Moltes gràcies, amic! Només em queda demanar-te un últim favor: no deixis mai la ciència, aquest món et necessita! Roger, moltíssimes gràcies per donar-me sempre un cop de mà amb la paperassa de les beques i per transmetre'm confiança i tranquil·litat. Durant aquests anys compartits, m'has ajudat a créixer com a persona. Moltes gràcies per les teves bromes i memes, fan que treballar en el que t'agrada sigui encara més divertit. Gràcies, també, per no fallar en cap dels meus concerts! Neus PL., quan vas entrar al laboratori semblava que ja et conegués de tota la vida. Gràcies per posar-m'ho tot tant fàcil i per aportar-me ordre, organització, informacions privilegiades, detallets bonics i ganes de gaudir fent ciència! No hi ha dubte que

t'espera un gran futur en el món científic! Joan, la teva incorporació ha estat recent, però m'ha agradat molt compartir poiata, centrífuga i pipetes amb tu. Espero que tinguis molta sort en aquesta etapa!

També vull agrair als pollets del laboratori Marina, Marta V., i Íngrid el seu pas pel laboratori. M'heu aportat molt en molt poc temps i estic convençuda que el vostre trajecte per la ciència no deixarà a ningú indiferent. Molts ànims i molta sort en els vostres projectes! Marina, moltes gràcies per ajudar-me amb els experiments, els ratolins i correccions de la tesi, sense la teva ajuda una gran part d'aquesta tesi no hagués estat possible. Trobaré a faltar els teus regals de Kinder Bueno!

No puc deixar d'agrair tot el que han fet per mi a moltes persones externes al grup de Cicle Cel·lular, però que formen part de l'IRB Lleida. Coral, moltes gràcies per haver vingut a Lleida i per haver-nos conegut. Ets una persona que transmet humilitat, discreció, intel·ligència, energia i passió per la ciència. Tot aquest temps has sigut un referent per a mi i estic molt contenta d'endur-me una amiga com tu d'aquesta experiència vital. Cris P., gràcies per aportar sempre un toc d'humor i per totes les estones de les que hem gaudit. Ha estat un plaer compartir amb tu les etapes del grau i el doctorat. Molts ànims amb la recta final de la teva tesi! Alba S., ja fa deu anys que ens coneixem i sempre hem estat envoltades de ciència. Primer el grau, després el màster i ara el doctorat. Coincidirem en el futur? Espero que si. Hem compartit estones de nervis durant els estudis, de suor al gimnàs, i d'alegria o frustració a la sala de cultius. Moltes gràcies per ser-hi! Àuria, és admirable com compagines perfectament el munt d'activitats que fas: el treball al camp quan et necessiten, les associacions de les quals formes part i el doctorat. M'alegro molt d'haver coincidit amb tu, molts ànims en aquesta etapa! Moltes gràcies Isidre, Pau, Maria, Alba B., Maite i Laura per fer-me de germans grans els primers anys de tesi i acollir-me a la vostra colla des del primer dia.

Moltes gràcies a tot el grup de Patonco per l'ajuda en protocols, anticossos i ratolins que m'heu proporcionat. Gràcies, Xavi, pels teus consells i suggeriments sobre alguns experiments d'aquesta tesi. Muchísimas gracias especialmente a Raúl, por ayudarme y apoyarme des de que nos conocimos en el máster. Siempre me has aportado ideas muy interesantes, te has preocupado por mis experimentos y me has sacado muchas sonrisas. Me

gustaría mucho volver a coincidir contigo en el futuro. Simplemente, ¡gracias por tu gran talento! Muchas gracias, Cris M., por tener siempre ganas de organizar eventos en el IRB y por tu infinito entusiasmo por la ciencia. Estoy más que segura que harás un super post-doc y que serás una gran científica. Moltes gràcies Carla per ser tant bona companya de pis i per ajudar-me sempre a trobar un nou camí quan la ciència em tancava alguna porta. Esper poder conèixer na Laia ben aviat!

Tanmateix, aquesta tesi no hagués donat el seu fruit si no m'hagués sentit acompanyada en tot moment de persones tant importants i estimades per mi, alienes a tot aquest món científic. Moltíssimes gràcies Amitié: Alba, Laia, Júlia, Maria Pau i Vero per aguantar-me des que vam néixer. Ens coneixem com si fóssim germanes, i cadascuna amb les seves peculiaritats formem un grup ben bonic i divers. Gràcies per entendre la meva manca de disponibilitat, donar-me suport i interessar-vos per aquesta etapa del meu aprenentatge. Gràcies Júlia i Maria Pau, per haver començat a ampliar la nostra família amb l'arribada del Pol i l'Adrià, sou unes mares excel·lents! Gràcies a totes per ser una peça clau de la meva vida!

Roser, ens vam conèixer a l'institut i la nostra amistat segueix més viva que mai. Hem compartit moltes històries, ens hem passat molts apunts i m'has fet riure de valent amb algunes de les teves aventures. Aquests dies compartim neguits semblants: tu comences una etapa i jo n'acabo una altra. Molts ànims, estic segura que ho gaudiràs moltíssim! Gràcies per fer-me sempre costat, per interessar-te pels meus dies, per apreciar-me tant i animar-me sempre. Ets llum i fortalesa. Marta Vilanova, sardanista, veterinària i pianista, entre moltes altres coses. Si t'ho pares a pensar, tenim moltes coses en comú: la cultura catalana, la sensibilitat pels animals (segons quins), l'amor per la música, i el nom. Sembla que ens hagin fet a mida! Moltes gràcies per tot el suport i estima que m'has transmès tot aquest temps, els nostres berenars, beures i sopars són regeneradors!

Sílvia i Clàudia, Clàudia i Sílvia. Les tres bessones violinistes del conservatori. No recordo el dia que ens vam fer tant amigues, però suposo que quan et trobes bé amb algú i hi encaixes, l'amistat sorgeix per si sola. Moltes gràcies a les dues per ser-hi sempre, pel munt d'assajos d'orquestra que hem superat juntes, pels sopars i nit de nenes al pis, per les festes, per tot! Sílvia, gràcies per preguntar-me com m'anaven els experiments des del primer minut i per

voler ser la primera d'apuntar-te la data de defensa de la tesi. Clàudia, moltes gràcies per les teves correccions, sense elles no sé pas com ho hagués fet! Sense vosaltres en aquesta tesi no hi hauria posada tanta estima! Isaac, gran amic i violinista prodigi. Gràcies per interessar-te sempre pels meus avenços al laboratori tot i preguntar-me sempre què és, d'on surt i de què està feta una proteïna. No deixis mai de perseguir el teu somni!

Xavier i Francesc, vau ser uns fantàstics companys de pis i d'anècdotes increïbles. Gràcies per distreure'm després de dies durs i per fer-me riure cada dia dels que vam viure plegats. Sou com els meus germans grans! Moltes gràcies a les amigues del grau: Marina, Júlia, Laura, Adriana i Anna per encoratjar-me des de primera instància a recórrer aquest camí que ara acabo. Vaig tenir molta sort de poder compartir amb vosaltres tots els nervis i alegries. Érem i som un bon equip!

Arnau, vas aparèixer en la meva vida al mateix moment que s'iniciava una de les etapes més dures i més boniques del meu aprenentatge. Des de l'inici m'has sabut animar quan no estava contenta amb algun experiment del laboratori i m'has sabut distreure de preocupacions científiques amb bromes o qualsevol tema de conversa. Gràcies per fer-me costat i donar-me suport en tota aquesta aventura, espero que plegats en puguem compartir moltes més. T'estimo infinit! Moltes gràcies, Javi, Marta i Laura, per acollir-me a casa vostra com una filla i germana més.

Finalment, arriba el torn d'agraïments a la meva família, a qui estimo profundament i a qui ho dec absolutament tot de la meva vida. Moltes gràcies Pare i Mare per confiar en mi quan jo mateixa dubtava de les meves capacitats, per animar-me i encoratjar-me sempre a fer el que m'agradés i per posar-me a disposició tots els recursos per poder-ho tirar endavant. Gràcies per estimar-me, educar-me i ensenyar-me com heu fet tota la vida. Quim, el meu tato, dono gràcies a la mare i al pare perquè van portar-te al món i hem pogut créixer junts. El petit nen rosset que ara fa unes abraçades d'ossito que aixequen l'ànim a qualsevol. Moltes gràcies per acompanyar-me i donar-me suport en el camí de la vida. Marta, cunyada, transmets dolçor i fortalesa i tens uns valors humans immensos. Gràcies per ser de casa. Moltes gràcies a tota la família sencera: padrina, padrí, avi, tietes, tiets, cosines i cosins, per aguantar-me als dinars familiars, eixugar-me alguna que altra llàgrima i per abraçar-me i fer-

me sentir valenta. Si hagués pogut triar la família, us hagués triat a tots vosaltres. Gràcies per ser-hi sempre!

Moltes gràcies a cadascú de vosaltres per aportar el vostre granet de sorra en l'elaboració d'aquesta tesi, sense vosaltres això no hagués estat possible.

INDEX

ABBREVIATIONS

ACC	Chloroacetamide
AKT	Protein Kinase B
ANOVA	Analysis Of Variance
ATCC	American Type Culture Collection
ATP	Adenosine Triphosphate
BCL-1	Cyclin D1 or B-cell lymphoma 1 protein
BM	Binding Motif
BrdU	Bromodeoxyuridine or 5-Bromo-2'-deoxyuridine
BSA	Bovine Serum Albumin
CABLES	CDK5 and ABL1 enzyme substrate 1
Cas	CRISPR-Associated
Cas9	CRISPR Associated protein 9
CBD	Cyclin Box Domain
CBP	Creb-Binding Protein
CCND1	Cyclin D1 gene
CDK	Cyclin-Dependent Kinase
cDNA	Complementary Desoxyribonucleic Acid chain
CEEA	Ethical Committee of Animal Experimentation
CIP	CDK Interacting Protein
CKI	CDK Inhibitor
CNPPD1	Cyclin Pas1/PHO80 Domain-containing protein 1
CNTD1	Cyclin N-Terminal Domain-containing protein 1
CNTD2	Cyclin P or Cyclin N-Terminal Domain-containing protein 2
CO_2	Carbon Dioxide
CRISPR	Clustered Regularly Interspaced Short Palindromic Repeats
CRM1	Chromosomal Maintenance 1
CTC	Circulating Tumour Cells
Cx43	Connexin-43
Cyclin D1$^{-/-}$	Knock-Out of Cyclin D1
DMEM	Dulbecco's Modified Eagle's Medium
DMSO	Dimethyl Sulfoxide

DNA	Deoxyribonucleic acid
DSB	Double Strand Break
DTC	Disseminated Tumour Cells
DTT	Dithiothreitol
EDTA	Ethylene diaminetetraacetic acid
EFS	EF 1α Short
EGFR	Epidermal Growth Factor Receptor
EMT	Epithelial-to-Mesenchymal Transition
Erα	Oestrogen Receptor α
ERK	Extracellular signal-Regulated Kinase
ETSEA	Escola Tècnica Superior d'Enginyeria Agrària
FAK	Focal Adhesion Kinase
FBS	Fetal Bovine Serum
FC	Fold Change
FDR	False Discovery Rate
GAPDH	Glyceraldehyde 3-phosphate dehydrogenase
GFP	Green Fluorescent Protein
GO	Gene Ontology
GSK-3β	Glycogen Synthase Kinase-3β
GTP	Guanine Triphosphate
HCl	Hydrochloric Acid
HDF	Human Dermal Fibroblasts
HEK 293T	Human Embryonic Kidney 293T
HIF-1	Hypoxia-Inducible Factor-1
HRP	Horseradish Peroxidase
IF	Immunofluorescence
IHC	Immunohistochemistry
IFNα	Interferon-α
IRB	Institut de Recerca Biomèdica
kDa	KiloDalton
KIP	Kinase Inhibitory Protein

KLF4	Krueppel-Like Factor-4
LC-MS/MS	Liquid Chromatography Tandem Mass Spectrometry
LEF	Lymphoid Enhancer Factor
LSGS	Low Serum Growth Supplement
MAPK	Mitogen-Activated Protein Kinase
MCF-7	Michigan Cancer Foundation – 7 (adenocarcinoma human cells)
MEF	Mouse Embryonic Fibroblast
MEK	Mitogen-activated protein Kinase Kinase
MET	Mesenchymal-to-Epithelial Transition
mRNA	Messenger Ribonucleic Acid
mTOR	Mammalian Target Of Rapamycin
NaCl	Sodium chloride
NF-κB	Nuclear Factor kappa-light-chain-enhancer of activated B cells
NGF	Nerve Growth Factor
NHEJ	Non-Homologous End Joining
NOTCH1	Neurogenic locus notch homolog protein 1
OCT	Optimum Cutting Temperature
P/S	Penicillin/Streptomycin
p16	CDKN2A
p21	CDKN1A
p27	CDKN1B
p57	CDKN1C
PACSIN2	Protein kinase C and casein kinase substrate in neurons protein 2
PADI2	Protein-Arginine Deiminase type-2
PAGE	Polyacrylamide Gel Electrophoresis
PAM	Protospacer Adjacent Motif
PBS	Phosphate Buffered Saline
PBST	Phosphate Buffered Saline with 0.1% Tween-20
PC3	Human Prostatic Cancer cells
PC12	Rat pheochromocytoma cells
PCA	Principal Component Analysis

PCDH7	Protocadherin 7
PCR	Polymerase Chain Reaction
PEI	Polyethylenimine
PEST	Proline (P), Glutamic acid (E), Serine (S) and Threonine (T)
PFA	Paraformaldehyde
PI3K	Phosphatidylinositol 3-Kinases
PIP$_2$	Phosphatidylinositol 4,5-Biphosphate
PRAD1	Parathyroid neoplasia gene
PTEN	Phosphatase and Tensin Homolog
PVDF	Polyvinylidene fluoride
R3327-5'A	Rat prostate tumour cells type A
R3327-5'B	Rat prostate tumour cells type B
Rac1	Ras Related C3 botulinum toxin substrate 1
RAGE	Receptor for Advanced Glycation Endproducts
Ral	Ras-related protein
RB1	Retinoblastoma 1
RB1$^{-/-}$	Knock-Out of Retinoblastoma 1
RhoA	Ras-homolog gene family, member A
RNA	Ribonucleic Acid
ROCKII	Rho-associated protein kinase II
RT	Room Temperature
RUNX	Runt-related transcription factor-1
S6K1	S6 Kinase 1
SCID	Severe Combined Immunodeficiency
SCR	Scramble
SD	Standard of molecular weight
SD	Standard Deviation
SDF-1	Stromal cell-Derived Factor-1
SDS	Sodium Dodecyl Sulphate
SDS-PAGE	Sodium Dodecyl Sulphate – Polyacrylamide Gel Electrophoresis
SECR	Secretome

SEM	Standard Error of the Mean
sgRNA	Single-Guide Ribonucleic Acid
shAdseverin	shRNA against Adseverin
shD1	shRNA against Cyclin D1
shRB1	shRNA against Retinoblastoma 1
shRNA	Short Hairpin RNA
SMAD3	Mothers Against Decapentaplegic homolog-3
spCas9	*Streptococcus pyogenes* CRISPR Associated protein 9
SPF	Specific-Pathogen Free
STAT1	Signal Transducer and Activator of Transcription 1
STRING	Search Tool for the Retrieval of Interacting Genes
TCA	Trichloroacetic Acid
TCF	T-Cell Factor
TDE	Tumour-Derived Exosomes
TEMED	Tetramethylethylenediamine
TGF-β	Transforming Growth Factor–β
TIF	Tumour Interstitial Fluid
TKR	Tyrosine Kinase Receptors
TNFα	Tumour Necrosis Factor-α
tracrRNA	Trans-Activating crRNA
WCE	Whole Cell Extract

ABSTRACTS

Metastasis is the process in which malignant cells escape from a primary tumour, intravasate into the bloodstream and disseminate to a distant tissue, where the ones that survive establish and proliferate generating a secondary tumour. It is known that, during the metastasis stages, the composition of the tumour microenvironment is fundamental for the establishment and growth of metastatic cells. In this way, some proteins of this microenvironment could be used as metastasis markers or therapeutic targets.

During cancer progression, cells acquire new mutations and molecular functions that confer aggressive characteristics to the cell, such as the ability to migrate or invade surrounding tissues, leading to metastasis. For instance, Cyclin D1 is an oncogene that is overexpressed in many cancers. Its function in the cell nucleus is to initiate the cell cycle through the phosphorylation and inactivation of Retinoblastoma 1, promoting cell proliferation. In addition, in our lab it has been previously described that cytoplasmic Cyclin D1 also promotes metastasis through Paxillin phosphorylation.

The main objectives of this thesis are to characterise the role of Cyclin D1 and Retinoblastoma 1-dependency in dissemination, establishment, and growth of metastatic cells, and to detect proteins that belong to the tumour microenvironment that may be involved in the regulation of the metastatic colonisation. In this work, we conclude that Cyclin D1 causes the survival and establishment of disseminated tumour cells independently of Retinoblastoma 1. This cyclin also favours metastatic nodule growth, but in this case in a Retinoblastoma 1-dependent way. Moreover, we also describe that tumour interstitial fluid of metastatic lungs is enriched in cytoskeleton proteins, such as Fascin and Adseverin, which are secreted by the metastatic nodules. Furthermore, we have observed that Adseverin is also important for the survival and establishment of disseminated tumour cells and nodule growth.

Finally, in the last part of this thesis, we have studied the role of Cyclin D1 and Retinoblastoma 1 in the barley β-Glucan-mediated signalling pathways involved in cell proliferation. Our data indicate that this polymer induces a transitory arrest in human fibroblast proliferation in a Retinoblastoma 1-dependent and Cyclin D1-independent manner. At the same time, barley β-Glucan promotes migration on fibroblasts. We have also demonstrated that the topical application of this polymer increases wound healing in mice, suggesting a possible therapeutic application in skin ulcers.

La metàstasi és el procés a través del qual unes cèl·lules malignes escapen d'un tumor primari, entren al torrent sanguini i es disseminen en un teixit distant, on les que sobreviuen s'estableixen i proliferen formant un tumor secundari. Es coneix que durant aquestes etapes la composició del microambient tumoral és fonamental per l'establiment i creixement de les cèl·lules metastàtiques. Per aquest motiu, algunes proteïnes que el conformen podrien servir com a marcadors de metàstasi o fins i tot com a dianes terapèutiques.

Durant la progressió del càncer, les cèl·lules adquireixen noves mutacions i funcions moleculars que els confereixen característiques d'agressivitat, com la capacitat de migrar o d'envair teixits del voltant, produint metàstasis. Per exemple, la Ciclina D1 és un oncogen que està sobreexpressat en molts càncers. La seva funció en el nucli és iniciar el cicle cel·lular a través de la fosforilació i inactivació del Retinoblastoma 1, la qual cosa dona lloc a la proliferació cel·lular. Tanmateix, al nostre laboratori, prèviament, s'ha descrit que la Ciclina D1 citoplasmàtica afavoreix la formació de metàstasis a través de la fosforilació de la Paxilina.

Els objectius principals d'aquesta tesi són caracteritzar el paper de la Ciclina D1 i la dependència del Retinoblastoma 1 en la disseminació, l'establiment i el creixement de les cèl·lules metastàtiques, i, detectar proteïnes que formin part del microambient tumoral que estiguin involucrades en la regulació de la colonització metastàtica. En aquest treball, arribem a la conclusió que la Ciclina D1 promou la supervivència i l'establiment de les cèl·lules tumorals disseminades independentment del Retinoblastoma 1. Aquesta ciclina també afavoreix el creixement dels nòduls metastàtics, però, en aquest cas, de forma dependent del Retinoblastoma 1. A més, descrivim que el fluid intersticial de tumor de pulmons amb metàstasis està enriquit en proteïnes del citoesquelet, com la Fascina i l'Adseverina, les quals són secretades pels nòduls metastàtics. Així, hem pogut observar que l'Adseverina també és important per la supervivència i l'establiment de les cèl·lules tumorals disseminades i el creixement dels nòduls.

Finalment, en la darrera part de la tesi, hem estudiat el rol de la Ciclina D1 i el Retinoblastoma 1 en la senyalització mitjançada pel β-Glucà d'ordi sobre la capacitat proliferativa de les cèl·lules. Les nostres dades indiquen que aquest polímer provoca una aturada transitòria en la proliferació de fibroblasts humans de manera dependent del Retinoblastoma 1 i independent de la Ciclina D1. Al mateix temps, el β-Glucà d'ordi indueix la migració dels

fibroblasts. També hem demostrat que aquest polímer aplicat tòpicament incrementa la cicatrització de ferides en ratolins, per la qual cosa es suggereix una possible aplicació terapèutica en ulceracions de la pell.

La metástasis es el proceso a través del cual unas células malignas escapan de un tumor primario, entran al torrente sanguíneo y se diseminan en un tejido lejano, donde las que sobreviven se establecen y proliferan formando un tumor secundario. Se conoce que durante estas etapas, la composición del microambiente tumoral es fundamental para el establecimiento y crecimiento de las células metastáticas. Por este motivo, algunas proteínas que lo conforman podrían ser útiles como marcadores de metástasis o como dianas terapéuticas.

Durante la progresión del cáncer, las células adquieren nuevas mutaciones y funciones moleculares que les confieren características de agresividad, como la capacidad de migrar o de invadir tejidos de alrededor, generando metástasis. Por ejemplo, Ciclina D1 es un oncogén que esta sobreexpresado en muchos cánceres. Su función en el núcleo es iniciar el ciclo celular a través de la fosforilación e inactivación de Retinoblastoma 1, dando lugar a la proliferación celular. Así mismo, en nuestro laboratorio, previamente, se ha descrito que Ciclina D1 citoplasmática favorece la formación de metástasis a través de la fosforilación de Paxilina.

Los objetivos principales de esta tesis son caracterizar el papel de Ciclina D1 y la dependencia de Retinoblastoma 1 en la diseminación, establecimiento y crecimiento de las células metastáticas, y, detectar proteínas que formen parte del microambiente tumoral que estén involucradas en la regulación de la colonización metastática. En este trabajo, llegamos a la conclusión de que la Ciclina D1 promueve la supervivencia y el establecimiento de las células tumorales diseminadas independientemente de Retinoblastoma 1. Esta ciclina también favorece el crecimiento de nódulos metastáticos, pero en este caso de forma dependiente de Retinoblastoma 1. Además, describimos que el fluido intersticial de tumor de pulmones con metástasis está enriquecido en proteínas del citoesqueleto, como Fascina y Adseverina, las cuales son secretadas por nódulos metastáticos. Así, hemos podido observar que Adseverina también es importante para la supervivencia y el establecimiento de células tumorales diseminadas y el crecimiento de los nódulos.

Finalmente, en la última parte de la tesis, hemos estudiado el rol de Ciclina D1 i Retinoblastoma 1 en la señalización mediada por β-Glucano de cebada sobre la capacidad proliferativa de las células. Nuestros datos indican que este polímero provoca una parada

transitoria en la proliferación de fibroblastos humanos de manera dependiente de Retinoblastoma 1 e independiente de Ciclina D1. Al mismo tiempo, el β-Glucano de cebada induce la migración de fibroblastos. También hemos demostrado que este polímero aplicado tópicamente incrementa la cicatrización de heridas en ratones, sugiriendo una posible aplicación terapéutica en ulceraciones de la piel.

INTRODUCTION

1. METASTASIS

1.1. From primary tumour to metastasis

Metastasis is the process in which malignant cells escape from the primary tumour to establish in distant sites, where they proliferate (Massagué et al. 2017). The development of metastases from a primary tumour involves intricate molecular and cellular processes that are influenced by the tissue microenvironment (Massagué and Obenauf, 2016). The study of these processes is essential to obtain valuable information on how metastases are established and to identify possible therapeutic targets.

During cancer progression, cells acquire new mutations and molecular alterations that contribute to different aspects of the tumour phenotype, conferring the cell the ability to invade surrounding tissues and metastasise, which is a feature that distinguishes malignant tumours. To easily understand the metastatic process, different stages can be defined according to the path followed by the cancerous cells from the primary tumour to the targeted secondary tissue.

Primary tumour break-away and cell intravasation

Cancerous cells have to face lots of barriers before they can seed in a new organ and cause clinical lesions. Some of these barriers are intrinsic to the cell, such as oncogene-induced genotoxic stress, upregulation of apoptotic pathways, growth inhibition and senescence or telomere erosion. Besides, extrinsic factors of the tumour microenvironment including the immune system, components of the extracellular matrix, hypoxia, and nutrient deprivation also limit tumour progression **(Figure 1)** (Gupta and Massagué, 2006).

The way in which a cancerous cell survives and adapts to all these barriers determines its metastatic potential. For instance, cells adapted to hypoxia usually have an increased Hypoxia-Inducible Factor-1 (HIF-1) expression. Among others, this factor promotes the transcription of genes involved in angiogenesis and invasion. As a result, neo-vascularization

and protease production end up disrupting the basement membrane and the extracellular matrix (Gupta and Massagué, 2006).
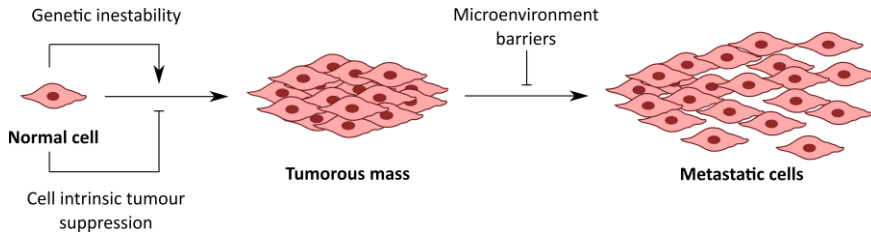
Figure 1. ***Transformation of normal cells to metastatic cells.*** The cells that integrate the normal tissue must acquire new mutations to become tumorous. Then, they must face intrinsic and extrinsic barriers in order to increase their proliferation rate and acquire migration and invasion characteristics to reach a secondary tissue where they metastasise. Image adapted from Gupta and Massagué (2006).

After overcoming the first obstacles, individual or grouped cells must escape from the primary tumour and invade the concomitant connective tissue in order to reach and enter into the blood vessels, in a process known as intravasation. This process requires cytoskeleton rearrangements and the secretion of extracellular matrix degradation enzymes (Hall, 2009; Quail and Joyce, 2013).

There are different cellular mechanisms by which cells invade surrounding tissues such as the collective, the amoeboid, or the mesenchymal invasion. In the last type, tumour cells undergo the epithelial-to-mesenchymal transition (EMT), a reversible process in which epithelial cells shift functionally and morphologically to mesenchymal. These changes contribute to the intravasation process (Thiery et al. 2009) **(Figure 2)**.

Bloodstream survival

Once in the bloodstream, circulating tumour cells (CTC) pass through the vessels (extravasation) and colonise a new tissue or organ as disseminated tumour cells (DTC). The extracellular signals and molecular pathways involved in those last steps of the metastatic process are still quite unknown.

During intravascular circulation, CTCs are surrounded by a hostile environment, where they suffer physical and oxidative stresses and have to face the immune response (Park et al. 2020). Conversely, CTCs can also receive environmental signals that ameliorate their capacity for niche colonisation in a new tissue. For instance, the interaction of CTCs with platelets further facilitates tumour cells extravasation, since platelet-derived signals promote EMT (Labelle et al. 2011) **(Figure 2)**.
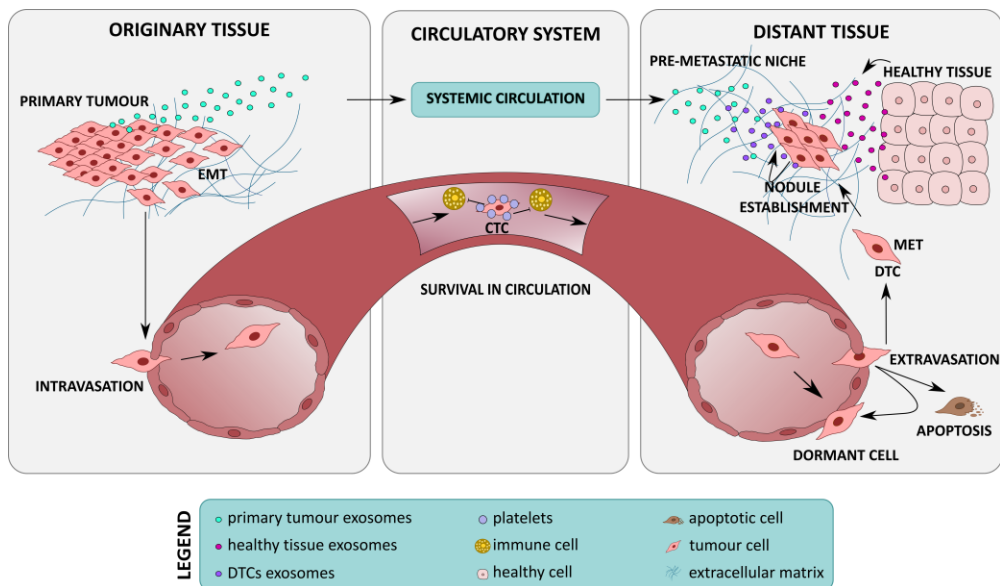
Figure 2. *Different steps of the metastatic process.* Cells from the primary tumour can suffer modifications (EMT) that allow the cell to migrate, invade, and intravasate into the bloodstream. Once in the circulatory system, tumour cells are named CTCs and interact with platelets and immunological cells, among others. The survivor cells can extravasate in a distant tissue, becoming DTCs. Then, some cells remain dormant near the blood vessels, some die through apoptosis, and some others do mesenchymal-to-epithelial transition (MET) and establish in the secondary tissue producing a metastatic nodule. It is known that the primary tumour is able to send exosomes through the circulatory system to generate a pre-metastatic niche in distant organs, thus inducing a favourable environment for the DTCs. Also, the healthy stroma and the DTCs can produce signals to enhance the survival of metastatic cells.

Extravasation and establishment in the secondary tissue

DTCs survival is compromised once they reach the new niche after extravasation, so only a few extravasated cells culminate in niche colonisation and metastasis. In fact, an

experimental study with mouse models described that most of the DTCs die by apoptosis (Wong et al. 2001). The authors intravenously injected tumour green-fluorescent cells in mice and observed that the majority of disseminated green cells in the lungs were apoptotic two days after the injection.

Surviving cells require anchorage in a supportive substrate and the reception of growth signals from the niche, which facilitates cell plasticity and immune evasion in order to initiate colonisation (Celià-Terrassa and Kang, 2018). Alternatively, DTCs can attach to the external vessel walls and remain dormant in a perivascular niche (Ghajar et al. 2013) **(Figure 2)**.

The hypothesis of "seed and soil" (Paget, 1889) suggests that the metastatic niches may be conditioned previously to the seeding of cancerous cells. For instance, the formation of a niche rich in Fibronectin favours anchorage and triggers survival of cancerous cells through the Krueppel-Like Factor-4 (KLF4) pathway (Murgai et al. 2017). Moreover, exosomes from primary tumours have been extensively associated with the formation of pre-metastatic niches in distant tissues (Peinado et al. 2012).

The arrangement of a metastatic niche requires a continuous stroma evolution from the unaffected environment to a mature niche capable of supporting DTC growth (Sleeman, 2012). This stroma remodelling can be initiated by secreted signals from the primary tumour (pre-metastatic niche) and later continued once DTCs lodge the pre-metastatic niche. However, the total maturation of metastatic niches may occur many years after seeding of DTCs **(Figure 2)**.

1.2. The role of epithelial-to-mesenchymal transition in cancer metastasis

EMT seems to play a pivotal role in cancer metastasis, but the understanding of some of its mechanisms remains elusive to this day. During EMT, epithelial cells lose their cell polarity and cell-cell adhesion and gain migratory and invasive properties, becoming malignant cells.

Along with the attainment of a mesenchymal phenotype, EMT is associated with the acquisition of stem-cell-like characteristics (Varga and Greten, 2017; Shibue and Weinberg,

2017). Classically, EMT has been associated with various tumour functions including tumour initiation, malignant progression, tumour stemness, cell migration, intravasation to the blood, metastasis, and resistance to therapy. However, the MET, which is the opposite of EMT, has been suggested to play an essential role in metastatic dissemination and colonisation (Pastushenko and Blanpain, 2019).

EMT has been understood as a binary process with two cell phenotypes: epithelial and mesenchymal. Frequently, it is defined as the loss of the epithelial marker, E-cadherin, and the gain of the expression of the mesenchymal marker, Vimentin. Nonetheless, recent studies indicate that EMT is not a binary process. Instead, EMT is a progressive process in which cells gradually acquire mesenchymal phenotype, which results in the generation of "transient" populations of cells with mixed epithelial/mesenchymal phenotype (Pastushenko et al. 2018). The role of this partial or mixed EMT state in metastatic potential is still under active investigation.

On a molecular level, the reprogramming of gene expression during EMT is initiated and controlled by several signalling pathways such as Transforming Growth Factor-β (TGF-β), Cadherin, Notch and WNT/β-Catenin (Deshmukh et al. 2021). However, the current understanding of the crosstalk between signalling pathways to assemble networks that regulate EMT is still poorly comprehended.

1.3. The role of the secretome in cancer metastasis

The secretome is considered as the global group of proteins, metabolites, protein-containing vesicles, lipids, micro-RNA, and messenger RNA secreted into the interstitial space by a cell, tissue, organ, or organism through known or unknown secretory mechanisms involving constitutive and regulated secretory organelles (Agrawal et al. 2010; Paltridge et al. 2013). Although the great majority of the secreted molecules act locally, some can have a systemic role. Due to its broad definition, the secretome is usually better conceived as the group of molecules that can be identified through mass spectrometry in cell-conditioned media in *in vitro* studies (Karagiannis et al. 2010).

The interstitial space is the cavity outside the parenchymal cells, blood, and lymphoid vessels which is full of interstitial fluid and molecules forming the extracellular matrix. The interstitial fluid contains substances either produced locally (the secretome) or transported to the organ through blood circulation. Hence, the tumour interstitial fluid (TIF) consists of the interstitial fluid in a tumorous tissue context (Wagner and Wiig, 2015).

Some studies comparing the secretomes from cancerous cells and their healthy tissues of origin have revealed that cancerous cells can often alter the secretome (Makridakis and Vlahou, 2010). Cell-secreted factors are commonly used as cell-to-cell communication mediators that could potentially promote the development of cancer (Paltridge et al. 2013). Some studies have demonstrated that malignant cancers can send signals to other cells located in distant organs to modify their phenotype (Peinado et al. 2011). In fact, TIF and specifically tumour-derived exosomes (TDE) from primary tumours have broadly been related to pre-metastatic niche formation (Nogués et al. 2018; Steinbichler et al. 2017).

For example, melanoma-derived exosomes induce the recruitment of bone marrow-derived cells toward lung pre-metastatic niches, where melanoma-derived exosomes previously promoted extracellular matrix remodelling and angiogenic events (Peinado et al. 2012). However, little is known about the role of secreted proteins and factors during metastatic niche maturation. The composition of the metastatic niche TIF may be dependent on the exosomes released by the primary tumour, but also by those secreted from DTCs and stromal cells. In this scenario, one of the roles of the secreted factors could be the regulation of the EMT status of DTCs (Steinbichler et al. 2017). As suggested by different authors, a reversion of the EMT phenotype of DTCs seeded in the niche may be important to undergo the formation of nodules (Brabletz et al. 2000; Gao et al. 2012; Wells et al. 2008).

1.4. Therapeutic approaches targeting metastatic colonisation

Most anti-metastatic therapies are focused on inhibiting secondary tumour growth, while the detection and isolation of CTCs mainly play a role in diagnosis as markers of tumour dissemination. However, therapies targeting tumour growth are inefficient against the first steps of metastatic colonisation because CTCs and DTCs, in general, do not grow and instead

remain in a quiescent state (dormancy) for extended periods of time (Celià-Terrassa and Kang, 2018).

Recently, *ex vivo* cultures and CTCs and DTCs characterisation are highlighting their potential as targets for personalised therapies against metastases (Liu et al. 2021). These strategies attempt to hamper different steps involved in metastatic colonisation, including blocking the interaction between DTCs and pre-metastatic niches, breaking the stroma-tumour connection, inhibiting DTCs dormancy, and interrupting the DTC immunosuppressive response (Celià-Terrassa and Kang, 2018).

For instance, it is described that the DTCs in the brain can establish a direct connection with astrocytes. Protocadherin 7 (PCDH7) expression in metastatic disseminated cells favours its union with Connexin-43 (Cx43), one of the main Gap Junction proteins in astrocytes, to establish a Gap Junction channel. Metastatic cells use this channel to transfer proteins which activate signalling pathways in astrocytes that favour the paracrine secretion of Interferon-α (IFNα) and Tumour Necrosis Factor-α (TNFα). These factors activate Signal Transducer and Activator of Transcription 1 (STAT1) and Nuclear Factor NF-kappa-B (NF-κB) in metastatic cells, which confer chemoresistance and promote tumour growth. The administration of Gap Junction modulators, Meclofenamate and Tonabersat, blocks this paracrine signalling and as a result, the establishment of brain metastasis (Chen et al. 2016).

Another therapeutic approach is to impede DTCs dormancy. For example, metastatic breast cells in the bone relapse many years after therapy ends. This is due to breast DTCs remaining in a dormant state in the bone. Price et al. (2016) described that the selective inhibition of both E-selectin and Stromal cell-Derived Factor-1 (SDF-1) receptor blocks breast DTCs dormancy in bone. Whereas E-selectin inhibition prevents CTCs entrance to the bone marrow, the blockage of the SDF-1-receptor promotes dormant DTCs re-enter into the bloodstream. As a result, the administration of both drugs would prevent the DTCs dormancy establishment in the bone marrow.

Many new therapies have emerged in the last years regarding CTCs and DTCs targeting. Thus, the understanding of the survival and maturation mechanisms of these cells is essential in the detection of potential markers against metastatic colonisation.

2. CYCLIN D1

2.1. Cyclins and Cyclin-Dependent Kinases

In 1982, R. Timothy Hunt was studying the cell cycle of sea urchins when he discovered various proteins whose concentration cyclically changed during the cell cycle. Due to this periodic phenomenon, he termed these proteins as cyclins (Evans et al. 1983). Human cells have more than 30 cyclins, although some of them are not involved in the cell cycle regulation, and 20 Cyclin-Dependent Kinases (CDKs).

Presently, cyclins are classified into three different groups: the canonical cyclins (D, E, A and B), which are involved in several stages of the cell cycle through its association with CDKs, even though they could perform other functions; the transcriptional cyclins (T, K, L, Q, C and H), that mainly regulate the RNA polymerase; and the atypical cyclins (CABLES, G, I, J, O, P or CNTD2, Y, YL, CNPPD1 and CNTD1) which have diverse roles such as the regulation of cell cycle progression, apoptosis, and the response to genotoxic stress, among others (Quandt et al. 2019).

Even though all the cyclins have a different amino acid sequence, the analysis of the human genome determined that cyclins share a similar motif of 100 amino acid residues. This domain is responsible for binding and activating proteins such as CDKs (Malumbres and Barbacid, 2005; Qie and Diehl, 2016). Notably, a lysine (Lys-257) and a glutamic acid (Glu-286) are conserved in almost all the cyclins in this region, which appear to be paramount for CDK binding. Moreover, the presence of other residues around these conserved amino acids seems to be essential in the distinct CDK-specificity binding (Quandt et al. 2020).

It is well established that each canonical cyclin acts in a different stage of the cell cycle, where they form active complexes with CDKs and phosphorylate specific substrates. Depending on the stage of the cell cycle they act in, canonical cyclins can be classified into several groups: cyclins from the G1/S phase (Cyclin E), S phase (Cyclin A) and M phase (Cyclin B) directly control the cell cycle process; cyclins from G1 phase (Cyclin D) are involved in the regulation of the entrance to the cell cycle in response to mitogenic signals (Sicinski et al. 1995; Sherr and Roberts, 1999).

26

CDK's principal roles are to control DNA replication and assure accurate chromosome segregation during the cell cycle progression. The CDKs manifest an oscillating action during the cell cycle because of their reversible phosphorylation/degradation and their transient association with specific cofactors like cyclins and CDK inhibitors (CKIs). Furthermore, cyclins have a double function by targeting specific substrates and being activators of CDKs.

CKIs play a role as architectural and inhibitory components. The regulation of the cell cycle is highly complex due to the existence of checkpoints or quality controls which verify that each step of the cell cycle is successfully concluded before the following one starts (Bendris et al. 2015).

2.2. Cyclins D are essential

Cyclin D1 was identified for the first time in 1991 in two different and parallel studies. One of these works distinguished Cyclin D1 for its ability to re-start the cell cycle of a human glioblastoma cDNA library introduced in *Saccharomyces cerevisiae* lacking all three G1-type cyclins (Xiong et al. 1991). The other study detected Cyclin D1 in the parathyroid adenoma as an altered gene caused by a chromosomal inversion (PRAD1), and in B-cell neoplasia as a gene affected by chromosomal translocation t(11:14) (BCL-1) (Motokura et al. 1991). These works suggested that Cyclin D1 could be of great importance in the study of the cell cycle and cancer development.

Nowadays, it is known that mammalian cells present three types of cyclins D: Cyclin D1, Cyclin D2 and Cyclin D3. Cyclin D2 and Cyclin D3 share, respectively, 62% and 51% of homology with Cyclin D1 (Musgrove et al. 2011). Although the expression and function of each D-cyclin are tissue-specific, all of them interact with CDK4 and CDK6 (Sicinski et al. 1995; Matsushime et al. 1994).

To know why mammalian cells need three distinct D-type cyclins, Sicinski's lab analysed the functionality of each cyclin D by disrupting each gene. They found that mice deficient in Cyclin D1 appeared to be viable but smaller than wild-type mice **(Figure 3)** and showed severe

retinal hypoplasia, defects in the proliferation of the mammary tissue during pregnancy and unknown neurological alterations (Bienvenu et al. 2010; Sicinski et al. 1995).
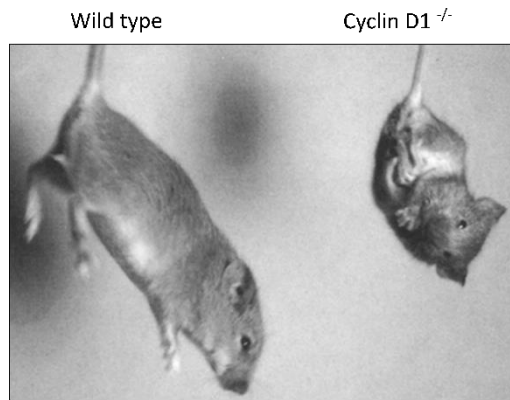
Wild type   Cyclin D1 $^{-/-}$

Figure 3. *Comparison between a wild-type mouse and a mouse lacking Cyclin D1.* Mice deficient in Cyclin D1 (Cyclin D1$^{-/-}$) are smaller than wild-type mice and show abnormal leg-clasping reflex, which indicates an alteration in the nervous system functionality. Image taken from Sicinski et al. (1995).

Cyclin D2-deficient mice were viable but sterile, as female ovarian granulosa cells failed to proliferate properly and males manifested hypoplastic testes (Sicinski et al. 1996). Cyclin D3-deficient mice could not promote normal expansion of immature T lymphocytes and presented severely hypoplastic thymuses, even though they were viable (Sicinska et al. 2003).

Mice lacking all D-type cyclins correctly developed until mid-gestation, a stage when most of the tissues and organs are already formed. This fact indicates that normal cell proliferation can occur in the absence of D-cyclins during early development. However, these mice died because of heart abnormalities and severe anaemia before the end of gestation. Thus, the lack of the three D-cyclins exacerbates the single cyclin D-deficient phenotype, showing that cyclins have some redundant functions (Kozar et al. 2004).

Furthermore, Barbacid's group showed that CDK4-deficient mice were viable, small in size, infertile, and with proliferative defects in specific endocrine cell types, resembling those phenotypes of the Cyclin D1-lacking mice (Rane et al. 1999). CDK6-deficient mice were also viable but had some defects in specific hematopoietic cell populations, similarly to the Cyclin D3-deficient mice phenotype. Finally, the CDK4 and CDK6 double-mutant mice resulted in late embryonic or postnatal lethality, even though all their organs were well-developed. This

phenotype could be due to a defect in the erythroid lineage that resulted in severe anaemia, showing a phenotype similar to that of mice lacking all D-type cyclins (Malumbres et al. 2004).

These experiments evidenced that the development of most mouse tissues can occur in a Cyclin D-CDK4/6 independent manner. For instance, fibroblasts derived from triple cyclin-D-mutant mice actively proliferated in culture, although they required higher amounts of mitogenic signals and were resistant to p16 cell cycle inhibition (CDK 4/6 inhibitor). However, these experiments also showed that the Cyclin D-CDK4/6 complex is critically required for specific tissue development (Kozar et al. 2004). Nevertheless, Cyclin D1 deficiency produces specific defects in cell polarity, like cell migration and adhesion, suggesting that the control of these functions by the cyclins is not redundant (Neumeister, 2003).

2.3. Structure of Cyclin D1

Cyclin D1 is encoded by the *CCND1* gene. It contains five coding exons and it is located in chromosome 11 in the region 11q13.3 in humans (Ramos-García, 2016; Qie and Diehl, 2016). The transcription of the five exons leads to the synthesis of Cyclin D1, integrated by a 295 amino acid chain (Malumbres and Barbacid, 2005), which has a molecular weight of 36 kDa.

Cyclin D1 contains different essential domains. The N-terminal region, from the amino acid 5 to 9, contains a Retinoblastoma 1 (RB1) binding site with the LxCxE conserved motif. The central region, from the amino acid 56 to 145, contains the Cyclin Box Domain (CBD), which allows the interaction with CDK4/6 and the CKIs (p21, p27 and p57). This CBD presents high homology between all D-type cyclins. The C-terminal part, from amino acid 241 to 290, regulates protein stability as it contains the PEST sequence: proline (P), glutamic acid (E), serine (S) and threonine (T). Particularly, the threonine residue (Thr-286) is necessary for Cyclin D1 degradation through ubiquitylation. In addition, Cyclin D1 contains two domains required for transcriptional regulation. The region between the CBD and the C-terminal domain has relevant binding sites for transcription factors. Specifically, the transcriptional activation is associated with the LxxLL motif (from amino acid 251 to 255), which is key for co-activators recruitment. However, the transcriptional repression is associated with the

presence of a repressor domain (from amino acid 142 to 253) for transcription factors **(Figure 4)** (Qie and Diehl, 2016; Knudsen et al. 2006).
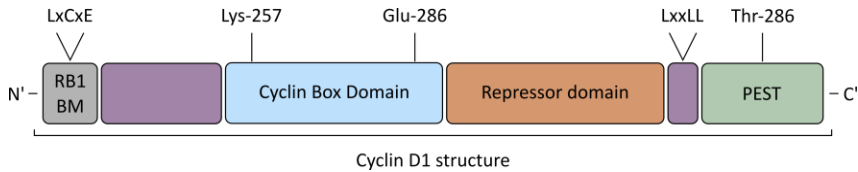
Figure 4. *Schematic representation of Cyclin D1 structure.* The RB1 binding motif (BM) LxCxE is located at the N-terminus of the protein, followed by the CBD. Then, the repressor domain and the LxxLL motif are represented. The PEST sequence and the Thr-286 are illustrated at the C-terminus part. Adapted from Knudsen et al. (2006).

A Cyclin D1 variant (Cyclin D1b) has been found in cancerous cells. It is the result of alternative splicing of the mRNA encoding for Cyclin D1 in which intron 4 is not spliced. This leads to several defective motifs in the C-terminal domain, which typically regulate Cyclin D1 turnover, including both the PEST motif and the Thr-286. Thus, Cyclin D1b becomes more stable in the nucleus, increasing its ability to regulate CDK activity and cell cycle, which is a risk factor in cancer development (Qie and Diehl, 2016; Knudsen et al. 2006).

2.4. Roles of Cyclin D1

Among all D-cyclins, Cyclin D1 has been the most studied since its gene is amplified in a wide range of cancers, including those of breast, parathyroid glands, oesophagus, bladder, and lung, becoming a major clinical problem (Alao, 2007; Sicinski et al. 1995; Baldin et al. 1993; Knudsen et al. 2006; Vermeulen et al. 2003).

Therefore, Cyclin D1 controls many functions: cell proliferation, migration, DNA damage, metabolism and differentiation (Musgrove et al. 2011). Some Cyclin D1 roles take place in the nucleus, whereas others happen in the cytoplasm. Similarly, Cyclin D1 can act in a dependent or independent way of CDK4 activity and cell cycle machinery. Some Cyclin D1 functions are detailed in **Figure 5**.
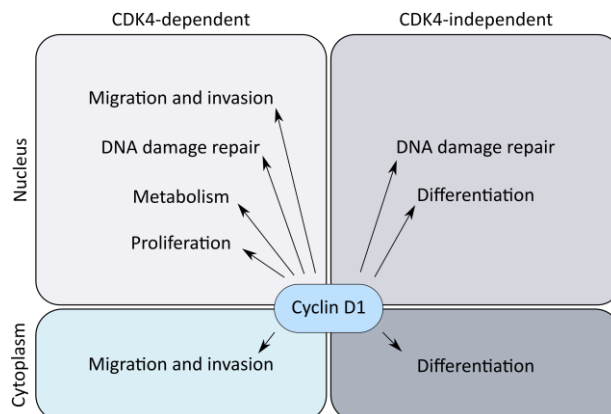
Figure 5. *Scheme of Cyclin D1 functions*. Nuclear (up) and cytoplasmic (down) functions are represented. Roles that are CDK4-dependent (left) or CDK4-independent (right) are shown.

Role of Cyclin D1 in cell proliferation

Cyclin D1, unlike the other periodically expressed cyclins, is not an integral component of the cell cycle mechanisms. Its expression is induced when the cells are exposed to extracellular mitogens, whereas it declines rapidly when these factors are withdrawn (Sherr, 1993; Sicinski et al. 1995). So, this regulation suggests that the principal function of Cyclin D1 is to link the presence of mitogenic signals with the cell cycle mechanisms (Sherr and Roberts, 1999).

The association between Cyclin D1 and CDK4/6 forms a complex which regulates the G1 to S phase transition in the cell cycle (Malumbres and Barbacid, 2005). At the end of the G1 phase, the first checkpoint of the cell cycle tests that the cell has accumulated enough mass and metabolites for DNA replication during the S phase.

When Cyclin D1-CDK4/6 complexes are active, they perform two main functions **(Figure 6).** The most recognised function is catalytic, in which the complex inhibits by multiple phosphorylations the RB1. Thus, RB1 releases the transcription factor E2F and allows it to promote the transcription from a wide range of genes, some of which are expressed in the G1/S transition and the S phase of the cell cycle (Kato et al. 1993). For instance, Cyclin E-induced expression is one target of E2F. This cyclin forms an active complex with CDK2 to

promote hyperphosphorylation of RB1, making the G1/S transition irreversible and favouring the cell cycle entry (Malumbres and Barbacid, 2005; Sherr and Roberts, 1999).

The other principal function of Cyclin D1-CDK4/6 complexes is to sequestrate the CKIs p21 (CIP) and p27 (KIP). During the G1 phase, Cyclin D1 expression increases, favouring its binding with CKIs. Hence, CKIs release Cyclin E, promoting its activation and association with CDK2 at the end of the G1 phase, which also favours the cell cycle entrance (Sherr and Roberts, 1999).
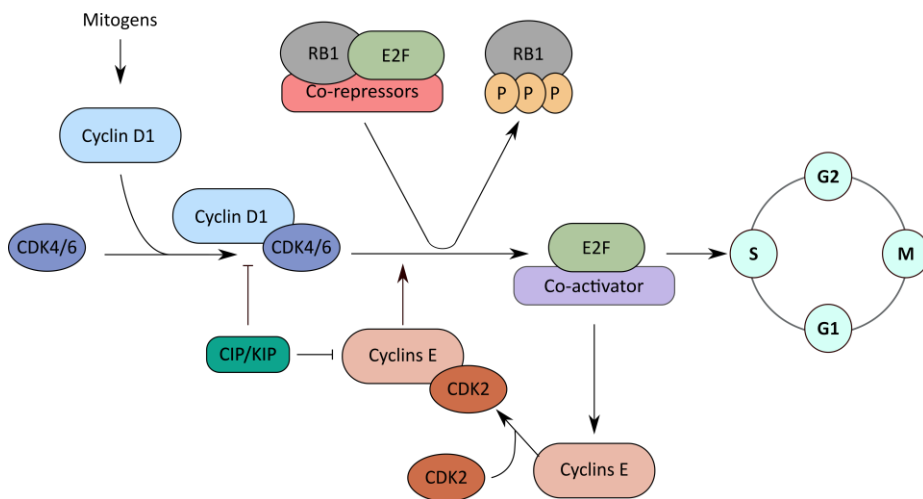
Figure 6. *Schematic representation of G1 to S phase transition in the cell cycle.* Extracellular mitogens activate the Cyclin D1 expression, which forms an active complex with CDK4/6. This complex phosphorylates RB1 in multiple sites and promotes the release of the E2F transcription factor, which induces the expression of Cyclin E and other essential genes for the S phase entrance. In association with CDK2, Cyclin E also inactivates RB1 by hyperphosphorylation, facilitating cell proliferation.

Cyclin D1-CDK4 complex can also interact with different transcription factors to regulate the proliferation of specific cell lineages in a cell-cycle independent way. Some of these transcription factors include the transcriptional modulators Mothers Against Decapentaplegic homolog-3 (SMAD3), Runt-related transcription factor-1 (RUNX) and GATA4 family members (Zhang et al. 2008; Nakajima et al. 2011; Matsuura et al. 2004).

Moreover, Cyclin D1 can regulate proliferation through the transcriptional induction of some transcription factors in a CDK4-independent way. For instance, Cyclin D1 binds to the Oestrogen Receptor (ERα) stimulating the ERα-dependent transcription in breast cancerous cells (Neuman et al. 1997).

Role of Cyclin D1 in cell migration and invasion

Different literature reports show that Cyclin D1 can regulate cell migration and invasion through diverse targets involving nuclear and cytoplasmic pathways (Li et al. 2006a; Fusté et al. 2016a).

Nuclear

Mouse embryonic fibroblasts (MEFs) and macrophages deficient in Cyclin D1 present difficulties in the polarity establishment, resulting in flattened, rounded, and less elongated cells **(Figure 7)**. Moreover, these cells are more adhered to the extracellular matrix and show reduced migration and invasion in comparison to wild-type cells, meaning that Cyclin D1 has a role in controlling these processes (Li et al. 2006a; Neumeister, 2003). These authors also demonstrate that this phenotype is dependent on CDK4 activity.
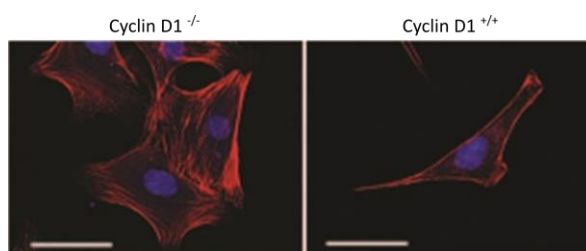
Figure 7. *The phenotype of Cyclin D1-deficient MEFs.* Cyclin D1-deficient fibroblasts (Cyclin D1$^{-/-}$) show a flattened, rounded, and less elongated morphology than wild-type fibroblasts (Cyclin D1$^{+/+}$). The scale bar is 50 µm. The image is taken from Li et al. (2006a).

These phenotypes have been associated with the nuclear function of Cyclin D1 as a transcriptional regulator (Li et al. 2006a), but in an independent way of the cell proliferation regulation (Velasco-Velázquez et al. 2011). For instance, Cyclin D1 negatively regulates the transcription of several genes coding for proteins which inhibit migration. Two of them are Rho-associated protein kinase II (ROCKII) and Thrombospondin 1 (Li et al. 2006a).

ROCKII is an effector of Ras-homolog gene family member A (RhoA) GTPases that negatively influences cell migration by regulating Actin cytoskeleton inducing the formation of stress fibres and focal adhesions (Allen et al. 1997). Thrombospondin 1 is a glycoprotein of the extracellular matrix that inhibits angiogenesis and migration (Streit et al. 2000). Cyclin D1-deficient MEFs increase their number of focal adhesions and decrease their migration due to the upregulation of ROCKII and Thrombospondin 1. In contrast, the overexpression of Cyclin D1 or the inhibition of ROCKII and Thrombospondin 1 increased cell migration **(Figure 8)** (Li et al. 2006a).
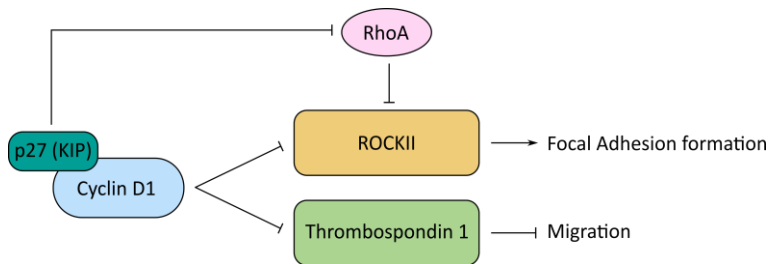
Figure 8. *Cyclin D1 regulation of ROCKII and Thrombospondin 1.* Cyclin D1 negatively regulates ROCKII and Thrombospondin 1 transcription, promoting cell migration and focal adhesion regulation. Cyclin D1 post-transcriptionally regulates RhoA through p27 stabilization. Figure adapted from Li et al. (2006a).

Moreover, it has been shown that Cyclin D1 induces migration through the regulation of post-transcriptional mechanisms. Cyclin D1 associates with the CKI member p27, and induces its abundance and stability, leading to p27 accumulation (Li et al. 2006b). This allows p27 to interact directly and inhibit RhoA in the cytoplasm, thereby inducing cell migration **(Figure 8)** (Besson et al. 2004). Thus, Cyclin D1-deficient MEFs show reduced levels of p27, consistently with the increase of RhoA activation in p27-deficient cells (Li et al. 2006b; Besson et al. 2004).

Cytoplasmic

Recently, different works have suggested that Cyclin D1 could exert some functions in the cytoplasm, where it can physically interact with cytoplasmic and membranous proteins that regulate cell migration and invasion. Many of these proteins are Filamin A, Ras-related protein (Ral) GTPases, PACSIN2, Paxillin and RhoA. All these proteins are involved in the modulation and rearrangement of the cytoskeleton, suggesting that Cyclin D1 may be participating in the cytoplasmic regulation of cell adhesion, migration, and invasion (Zhong et al. 2010; Fernández et al. 2011; Fusté et al. 2016a; Meng et al. 2011; Besson et al. 2004).

A work with metastatic breast cancer cell lines demonstrated that Cyclin D1 and Filamin A co-localise and interact in the membrane ruffles of migrating cells. Moreover, it shows that Cyclin D1 levels affect cell attachment, migration, and invasion (Zhong et al. 2010). Another study showed that Cyclin D1 interacts, co-localises, and activates Ral GTPases (Ral A and B) in the cytoplasm and the cell membranes of different cell types. Thus, Cyclin D1 enhances Ral stimulation allowing the assemblage of the exocyst and integrin recycling, which in turn promote cell motility and detachment (Fernández et al. 2011).

Furthermore, a study about Paxillin showed that this protein co-localises with Cyclin D1-CDK4 complex in membrane ruffles and that Paxillin phosphorylation in Ser-83 by this kinase complex decreases cell attachment and increases cell migration and invasion (Fusté et al. 2016a). Consequently, Paxillin induces the activation of Ras related C3 botulinum toxin substrate 1 (Rac1) GTPase, which is a membrane ruffle inductor required for migration and invasion. Thus, the Cyclin D1-CDK4 complex regulates cell migration by phosphorylating Paxillin and activating Rac1 (Chen et al. 2004; Deakin and Turner, 2008; Fusté et al. 2016a).

Role of Cyclin D1 in cell differentiation

Nuclear

Cyclin D1 contributes to cell differentiation by acting as a transcriptional regulator, in a cell-cycle and CDK4-independent way. In this case, Cyclin D1 interacts with DNA through DNA-bound transcription factors. Several years ago, a study demonstrated that Cyclin D1,

independently of CDK4, upregulates the transcription of the Neurogenic locus notch homolog protein 1 *(NOTCH1)* gene during retinal development in mice, where Notch1 signalling is paramount for the proliferation of retinal progenitor cells. Accordingly, *NOTCH1* gene depletion in retinal progenitor cells leads to unsuccessful differentiation and retinal hypoplasia, similar to the phenotype observed when the *CCND1* gene is deleted in the same cells. Hence, this study showed that Cyclin D1 regulates Notch1 expression through the recruitment of Creb-Binding Protein (CBP) Histone Acetyltransferases to *NOTCH1,* which activates *NOTCH1* gene expression by promoting the acetylation of histone residues. So, the presence of Cyclin D1 allows the proliferation and differentiation of retinal progenitors to diverse retinal cell types by controlling *NOTCH1* transcription (Bienvenu et al. 2010).

Cytoplasmic

The presence of Cyclin D1 in the cytoplasm has also been associated with the cellular differentiation process (Sumrejkanchanakij et al. 2003; Fernández-Hernández et al. 2013). During brain development, neural stem cells proliferate and change their polarity to lose adhesion capacity and increase migration and differentiation to become specific neurones (Singh and Solecki, 2015). It has been described that Cyclin D1 is delocalised from the nucleus to the cytoplasm in cortical neurons during *in vitro* differentiation (Sumrejkanchanakij et al. 2003). This, suggested that cytoplasmic Cyclin D1 could have a role in neuronal differentiation. For instance, Cyclin D1 is relevant for neurite growth in rat pheochromocytoma cells (PC12 cells) stimulated with Nerve Growth Factor (NGF) (Marampon et al. 2008). In addition, it has been shown that mice deficient in Cyclin D1 are viable but have neurological abnormalities (Sicinski et al. 1995).

Similarly, the localisation of Cyclin D1 changes during epidermis differentiation. Cyclin D1 is nuclear in the basal layer of the epidermis, whereas it is delocalised to the cytoplasm while cells differentiate in the upper layers. This shift also occurs in primary keratinocytes during *in vitro* differentiation with calcium, where Cyclin D1 co-localises with β1-integrin. It seems that the presence of cytoplasmic Cyclin D1 reduces integrin-dependent adhesion to the basal membrane (Fernández-Hernández et al. 2013).

2.5. Cyclin D1 in cell signalling

Extracellular mitogens and the cell binding to the extracellular matrix stimulate the induction of Cyclin D1 expression through different signalling pathways. In the same way, the anti-proliferative signals are also integrated to dictate the levels of Cyclin D1 in the cell. This rapid induction and its intrinsic instability allow Cyclin D1 to act as a cell sensor. In addition, Cyclin D1 rapid degradation depends on the cell cycle phase and occurs when mitogenic factors withdraw or when anti-proliferative signals are transduced (Knudsen et al. 2006; Diehl et al. 1997). Thus, Cyclin D1 is a high labile protein, being its half-life of 10-30 minutes (Qie and Diehl, 2016).

Mitogens regulate Cyclin D1 at multiple levels, including its gene transcription, translation, stability, and assembly with their CDK4/6 partners (Sherr and Roberts, 2004). For instance, this regulation is mediated by Ras-dependent signalling pathways. Indeed, when growth factors bind to Tyrosine Kinase Receptors (TKR) on the cell membrane, they initiate the Ras - Mitogen-Activated Protein Kinase (MAPK) signalling cascade that induces the transcription of Cyclin D1 **(Figure 9)** (Ramos-García, 2016; Musgrove, 2006). However, other signalling pathways can also regulate Cyclin D1 expression, such as NF-κB and Wnt/β-Catenin (Guttridge et al. 1999; Shtutman et al. 1999). Particularly, the complex formed between β-Catenin and Lymphoid Enhancer Factor/T-cell factor (LEF/TCF) targets the *CCND1* gene promoter to drive Cyclin D1 expression. NF-κB can act in a similar way (Qie and Diehl, 2016).

Glycogen Synthase Kinase-3β (GSK-3β) can phosphorylate Cyclin D1 on Thr-286 and facilitate its nuclear export by promoting its association with the nuclear exportin Chromosomal Maintenance 1 (CRM1). Once in the cytoplasm, Cyclin D1 is ubiquitylated and marked for degradation through proteasome (Alao, 2007). The stabilization of Cyclin D1 can be enhanced by the Phosphatidylinositol 3-Kinases and Protein Kinase B (PI3K/Akt) signalling pathway, which can also be Ras-mediated. On the one hand, Akt prevents Cyclin D1 degradation by phosphorylating GSK3β and blocking its kinase activity, thereby promoting Cyclin D1 accumulation in the nucleus (Vivanco and Sawyers, 2002). On the other hand, Akt promotes Cyclin D1 mRNA translation through the stimulation of mammalian Target Of Rapamycin (mTOR), which activates the S6 Kinase 1 (S6K1). Hence, this kinase is responsible for Cyclin D1 expression (Musgrove, 2006).

For accurate proliferation, apart from mitogens, some cells need signalling derived from adhesions to the extracellular matrix. Integrins are the adhesion signalling mediators. When integrins are in contact with elements of the extracellular space, they become active and exacerbate Cyclin D1 expression through the activation of Ras-MAPK and PI3K/Akt/GSK3β pathways (Schwartz and Assoian, 2001; D'Amico et al. 2000; Musgrove, 2006).
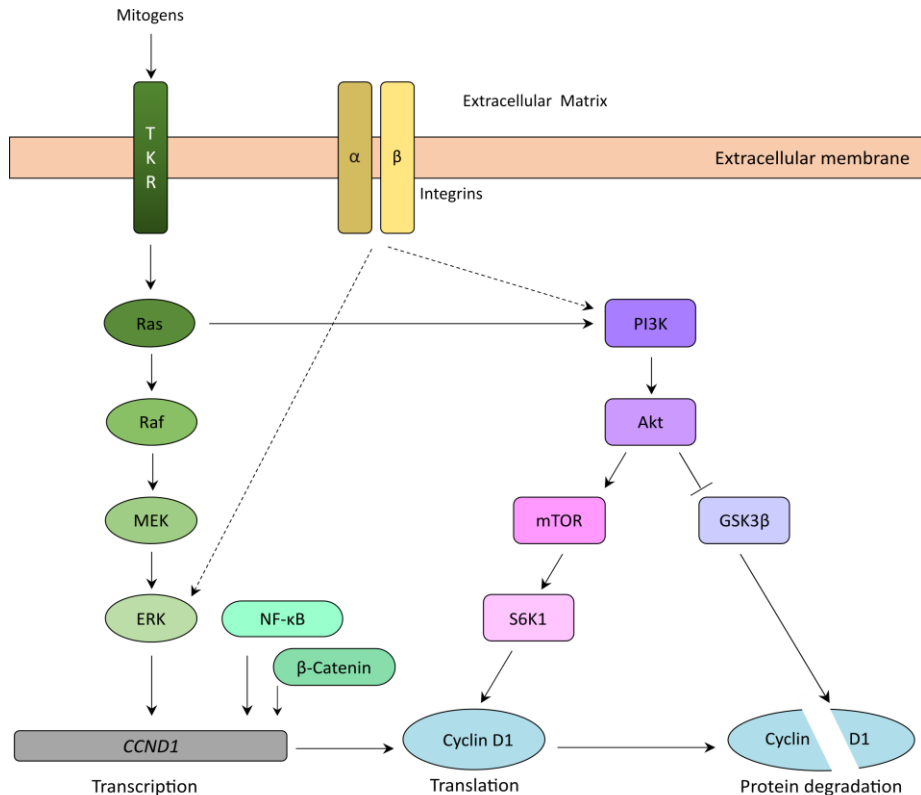
Figure 9. *Scheme of signalling pathways regulating Cyclin D1.* Mitogens activate the TKR and induce the MAPK pathway, which promotes *CCND1* gene transcription. NF-κB and β-Catenin also promote the transcription of *CCND1*. Ras activates PI3K, which induces Cyclin D1 translation through mTOR and inhibits Cyclin D1 degradation through the inactivation of GSK3β. Integrins mediate Cyclin D1 expression through Ras-MAPK and PI3K/Akt pathways. Adapted from Musgrove (2006).

As mentioned, Cyclin D1 has always been categorised as a downstream target of many different cell-signalling pathways. However, a recent study has shown that cytoplasmic Cyclin D1 could promote Rac1 activation through the phosphorylation of Paxillin, suggesting that Cyclin D1 can act upstream in cell signalling (Fusté et al. 2016a). Hence, the role of Cyclin D1 as a cell-signalling mediator is an open question.

3. CYCLIN D1 IN CANCER

3.1. Cyclin D1 gene rearrangements in cancer

Cyclin D1 has been associated with the cancerous transformation of some cells, as its gene can suffer genomic alterations that can lead to the appearance of mantle cell lymphoma, pancreatic, breast and endometrial cancer, non-small cell lung carcinoma, parathyroid adenoma, melanoma, and colorectal carcinoma, among others (Qie and Diehl, 2016).

As previously mentioned, Cyclin D1b variant derived from misleading splicing is present during the development of some cancers, as this protein is very stable in the nucleus. It has been described in carcinomas of the breast, oesophagus, colorectal, and prostate (Lu et al. 2003; Qie and Diehl, 2016).

Moreover, some rearrangements of the *CCND1* gene exist in a great variety of cancers. For instance, the chromosomal translocation t(11;14)(q13;q32) changes the *CCND1* locus in chromosome 11q13 for the immunoglobulin heavy chain gene in 14q32, which leads to Cyclin D1 overexpression. This translocation typically appears in mantle cell lymphoma, a B-cell lymphoma (Resnitzky et al. 1996). Another example is the chromosomal inversion of *CCND1* in parathyroid adenoma. This chromosome rearrangement provides *CCND1* re-location under a potent tissue-specific enhancer, which drives Cyclin D1 overexpression and, consequently, cancer development (Motokura et al. 1991).

CCND1 amplification has been implicated in human breast cancer appearance. The 11q13.4 to 11q13.5 is the most common *CCND1* amplified region. This section can be expanded in tandem extra copies from 3 to 10 times, leading to Cyclin D1 overexpression (Arnold and Papanikolau, 2005). The amplification of *CCND1* has also been described in pancreatic and endometrial cancers, melanoma, and lung and colorectal carcinomas, among others (Qie and Diehl, 2016).

3.2. Cyclin D1 and the oncogenic signalling

The expression of Cyclin D1 can be regulated by many signalling pathways. The alteration of these mechanisms can produce Cyclin D1 overexpression, also favouring cancer progression. For instance, mutations and amplifications of the gene encoding the Epidermal Growth Factor Receptor (EGFR) induce constitutive activation of the MAPK pathway and, consequently, Cyclin D1 transcription. This phenomenon has been described in prostate cancα (Amanatullah et al. 2000) and breast cancer (Krishnamurti and Silverman, 2014), among other cancer types. Consistently, cells overexpressing H-Ras manifest upregulated Cyclin D1 levels and a shorter G1 phase of the cell cycle, promoting a rapid proliferation (Liu et al. 1995). In fact, mutations in K-Ras are one of the most common alterations in cancer, frequently found in pancreatic and colorectal cancer, and lung adenocarcinomas (Hymowitz and Malek, 2018).

Alterations in the PI3K/Akt pathway have also been related to cancer progression. For example, Akt is amplified in breast and ovarian cancers; over-activation of PI3K has been described in ovarian, gastrointestinal, breast, and prostate cancers; and loss of Phosphatase and Tensin Homolog (PTEN), a tumour suppressor protein from the PI3K/Akt pathway, has been detected in a wide range of cancers, such as melanoma, breast, prostate, and renal cancers (Pópulo et al. 2012).

In conclusion, Cyclin D1 is an oncogene that appears overexpressed in a wide range of cancers. In agreement with this, Cyclin D1 overexpression correlates with tumour size and metastasis. This overexpression is a marker of poor prognosis in some human cancers (Qie and Diehl, 2016).

3.3. Roles of Cyclin D1 in cancer

Classically, the role of Cyclin D1 in cancer has been associated with proliferation dependent on CDK4 and RB1 pathways. Therefore, the use of CDK4 inhibitors such as Palbociclib has been approved for the treatment of several cancers to impede tumour growth (Mao et al. 2021; Gallanis et al. 2021). Nevertheless, being Cyclin D1 a multi-functional oncoprotein that

acts both in the nucleus and cytoplasm, as well as its wide association to proliferation, migration, and differentiation events, it is not difficult to imagine a broader implication of this cyclin in cancer signalling and development.

For instance, it has been observed that Cyclin D1 is delocalised in the cytoplasm of tumour cells in the invasive fronts of different tumours (Fusté et al. 2016b). In additional experiments, cytoplasmic Cyclin D1 promoted invasion of glioblastoma cells *in vivo* independently of the RB1 pathway (Cemeli et al. 2019). The expression of a membrane-targeted Cyclin D1 increased the dissemination of human glioblastoma cells orthotopically injected in the mouse brain. Moreover, the activation of Paxillin and Ral GTPases rescued the invasion capacity of human glioblastoma cells deficient in Cyclin D1 (Cemeli et al. 2019). All these data strongly suggest that Cyclin D1 influences cancer by multiple mechanisms beyond the classical role in proliferation depending on RB1.

The most unknown Cyclin D1-dependent mechanisms are those related to metastatic colonisation, although there is a positive correlation between Cyclin D1 expression and metastatic output in diverse cancers. For instance, clinical studies showed that Cyclin D1 favours metastasis from prostate tumours to the bone (Drobnjak et al. 2000). Since it is well established that Cyclin D1 promotes cell detachment and invasion of tumour cells **(see above)**, it has been assumed that Cyclin D1 is relevant in the escape of neoplastic cells from the primary tumour. The adhesion and motility functions, at least in part, are controlled by Cyclin D1 through RB1-independent mechanisms (Cemeli et al. 2019; Li et al. 2006a).

However, the relevance of Cyclin D1 in metastatic colonisation has also been stated. Two *in vivo* studies in murine models demonstrated that decreased expression of Cyclin D1 in CTCs reduced the number of lung metastatic nodules (Fusté et al. 2016a; Huang et al. 2009). These data suggest that Cyclin D1 would regulate other steps in metastasis, not only primary tumour dissemination but perhaps extravasation, survival, or establishment of CTCs. Moreover, it has been reported that these processes could be regulated by Cyclin D1 through RB1-independent mechanisms too. For instance, the expression of membrane-targeted Cyclin D1 in CTCs increased the number of lung nodules in mice (Fusté et al. 2016b). Furthermore, the hyperactivation of Paxillin in CTCs augmented the number of lung nodules

(Fusté et al. 2016a), suggesting that Cyclin D1 would promote metastatic colonisation through the Paxillin-Rac1 pathway.

Overall, the current data in the literature demonstrates that Cyclin D1 influences cancer in different ways (tumour growth, tumour dissemination and metastatic colonisation) and by multiple mechanisms, most of them still unknown.

HYPOTHESIS

The spread of cancerous cells before resection of the primary tumour is the leading cause of cancer death. Currently, there are no efficient therapies to prevent metastatic colonisation. Thus, finding biomarkers and therapeutic targets against the spread, survival, and maturation of circulating tumour cells should be a priority.

The downregulation of Cyclin D1 reduces the number of metastatic nodules in murine models. This datum suggests that Cyclin D1 controls metastatic colonisation, but the step in which this cyclin is relevant remains unknown. Since Cyclin D1 promotes cell proliferation and cell invasion, we hypothesise that Cyclin D1 is involved in the dissemination of circulating tumour cells and the growth of metastatic nodules.

First, we assume the possibility that there are several specific combinations of cellular and environmental factors that mediate the triggering of metastatic colonisation. These factors may be involved in the dissemination of circulating tumour cells and nodule formation. We propose to use our murine model of metastasis to detect biomarkers and targets against metastatic colonisation.

Second, Cyclin D1 has been classically studied as an effector downstream of signalling pathways. Based on the results obtained characterising the cytoplasmic roles of Cyclin D1, we hypothesise that Cyclin D1 also acts as a mediator of cell signalling pathways. This feature may be relevant in tumour spreading and metastasis.

OBJECTIVES

First, we are interested in assessing the role of Cyclin D1 in the dissemination, establishment, and growth of tumour cells during metastasis formation. We propose to use a murine model to check how cells with Cyclin D1 or with Cyclin D1 downregulated behave in these processes.

Second, we focus on collecting evidence to understand how Cyclin D1 regulates metastatic steps. We plan to obtain a Retinoblastoma 1 knock-out cell line to establish whether these processes are regulated by Cyclin D1 through Retinoblastoma protein.

Third, we aim to detect novel proteins and factors involved in metastatic colonisation that may ultimately be useful in diagnosis or targeted therapies. We propose a proteomic screening to detect proteins present in the metastatic lung environment that promote the spread, maturation, and growth of nodules.

Fourth, to device whether Cyclin D1 could be a mediator in signalling pathways. In collaboration with the Chemistry Department of ETSEA (University of Lleida), we are going to define the role of Cyclin D1 in the proliferation arrest caused by β-Glucan polymers.

MATERIALS AND METHODS

1. MOLECULAR BIOLOGY TECHNIQUES

1.1. Plasmid constructions

All DNA plasmids were purified with the HiSpeed Plasmid Midi Kit *(QIAGEN, #12643)* and with the HiSpeed Plasmid Maxi Kit *(QIAGEN, #12663),* following the manufacturer's instructions. The concentration of the obtained DNA was measured in the NanoDrop ND-1000 spectrophotometer *(NanoDrop Technologies)*, and its quality was evaluated by electrophoresis in agarose gels. The lentiviral vectors used in this work are shown in **Table 1**.

Name	Lentiviral Vectors	Description
pCYC2315	pL.CRISPR.EFS.PAC	Lentiviral CRISPR-Cas9 plasmid containing SpCas9 and sgRNA, puromycin resistance. EFS promoter. *(Was a gift from Benjamin Ebert. Addgene plasmid #57828; http://n2t.net/addgene:57828; RRID: Addgene_57828).*
pCYC2317	pX-evoCas9	Lentiviral CRISPR-Cas9 plasmid containing SpCas9 variant in mammalian cells (evoCas9, expressing M495V/Y515N/K526E /R661Q) and sgRNA, puromycin resistance. EFS promoter. *(Was a gift from Anna Cereseto. Addgene plasmid #107550; http://n2t.net/addgene:107550; RRID: Addgene_107550).*
pCYC2330	pCEPe9	An ApaI/PmlI fragment in pCYC2315 was substituted with an ApaI/PmlI fragment from pCYC2317. New construct checked by sequencing.
pCYC2111	shRNA SCR (Scramble)	Control vector shRNA SCR pLKO.1-puro *(Sigma-Aldrich).*
pCYC2133	FSV in lentivirus	FSPsi without puromycin and with GFP. *(Obtained from Mario Encinas-IRB Lleida).*
pCYC2140	627 – packaging helper (ΔR)	Packaging helper pHR'82ΔR that codifies for gag and pol proteins. *(Obtained from Xavier Dolcet-IRB Lleida).*
pCYC2141	628 – envelope helper (VSV)	Vector pMD2G that codifies for the virus envelope pVSV.G. *(Obtained from Xavier Dolcet-IRB Lleida).*
shD1	Mouse Cyclin D1 shRNA	shRNA against mouse Cyclin D1 in pLKO.1-puro vector TRCN0000040038 *(Sigma-Aldrich).*

ShAdseverin	Mouse Adseverin shRNA	shRNA against mouse Adseverin in pLKO.1-puro vector TRCN0000091314 *(Sigma-Aldrich).*
shRB1	Human Retinoblastoma shRNA	shRNA against human Retinoblastoma in pLKO.1-puro vector TRCN0000040167 *(Sigma-Aldrich).*

Table 1. *Lentiviral vectors.*

1.2. CRISPR/Cas

The CRISPR/Cas system

Clustered Regularly Interspaced Short Palindromic Repeats (CRISPR) sequences were described for the first time in 1987 in the *Escherichia coli* genome (Ishino et al. 1987). The identification of these evolutionarily conserved sequences among phylogenetically distant prokaryotic cells confirmed their biological relevance (Mojica et al. 2000).

The CRISPR loci are classically formed by discontinuous repeats divided by variable sequences (protospacers) which are frequently close to nuclease *CAS* genes (CRISPR-associated). Some experiments have elucidated that the spacers presented homology with foreign sequences, such as infectious plasmid sequences and bacteriophages. Hence, the role of the nucleases is to cleave the external nucleic acids into small pieces by providing immune protection to the cell. These generated short sequences are integrated into the genome's CRISPR arrays and can be used to directly cleave the same DNA if a future re-infection occurs (Barrangou et al. 2007). In this case, the Cas nuclease would process the CRISPR array to generate a guide RNA (gRNA) against the exogenous organism, forming a CRISPR/Cas complex. Then, the gRNA guide directs the CRISPR/Cas complex to the foreign DNA through the Watson-Crick base pairing. The target sequence is always located upstream of a 3-5 nucleotide-protospacer adjacent motif (PAM), which is crucial for Cas binding. Once the CRISPR/Cas complex is attached to the specific sequence, it generates a double-strand break (DSB) that forces the destruction of the extrinsic DNA (Ran et al. 2013).

The CRISPR/Cas genome edition

The components of the CRISPR/Cas machinery are widely diverse among the species. The type II CRISPR/Cas system is the most used in gene editing and consists of a nuclease Cas9 and a gRNA formed by two types of RNA: crRNA and tracrRNA (trans-activating crRNA). The crRNA or targeting gRNA binds to the target DNA through sequence homology. The tracrRNA or scaffold gRNA links the crRNA and Cas9 (Deltcheva et al. 2011). However, in many systems used for CRISPR-delivery, crRNA and tracrRNA are fused into a single-guide RNA (sgRNA).

The pL-CRISPR.EFS.PAC32 (pCYC2315) **(Table 1)** (Heckl et al. 2014) is a lentiviral vector that includes the *Streptococcus pyogenes* Cas9 (SpCas9) as well as the scaffold sgRNA. A useful characteristic of this vector is that the gene that provides resistance to puromycin is translationally coupled to Cas9 via a P2A cleaving peptide (Kim et al. 2011), which allows the specific selection of those cells that are expressing the Cas9 nuclease.

The pX-evoCas9 vector (pCYC2317) **(Table 1)** (Casini et al. 2018) contains a variant that differs from SpCas9 in four punctual mutations: M495V, Y515N, K526E, R661Q. These alterations generate a high-fidelity SpCas9 nuclease (evoCas9). A cleavage with Apa1 and Pml1 restriction enzymes was performed in both plasmids to eliminate the SpCas9 from pL-CRISPR.EFS.PAC32 and insert the evoCas9 from pX-evoCas9, creating the pCEPe9 vector (pCYC2330) **(Table 1)**.

Each specific sgRNA was cloned between two BsmBI restriction sites in the pCEPe9 downstream the human U6 promoter. The Cas9 cleavage results in DSB that may be repaired by non-homologous end joining (NHEJ) usually leading to frameshifts and the appearance of premature stop codons. Hence, when a gene knock-out is desirable, first exons of genes are targeted with CRISPR/Cas. Thus, selected sgRNA were from exons 1 and 3 **(Table 2)**. They were designed with the Benchling software (https://benchling.com) and the correct insertion was determined by PCR.

Exon	Strand	Sequence	PAM
Exon 1	Reverse	AGAGAGAGCTTGGCTAACGT	GGG
Exon 3	Forward	AGCATTATCAACTTTGGTAC	TGG

Table 2. *Sequences of sgRNA.*

2. CELL BIOLOGY TECHNIQUES

2.1. Cell cultures

Cell culture processing includes defreezing, maintenance, and freezing of cells. Normally, cells were stored in cryotubes at liquid nitrogen. To defreeze cells, cryotubes were taken from the liquid nitrogen and incubated in a 37ºC bath. Once cells were thawed, they were transferred into a 15 mL tube, medium was added, and cells were centrifuged at 1000 rpm during 5 minutes. Then, the cell pellet was resuspended with the adequate medium, and cells were seeded onto plates containing medium.

Cell lines were grown in Dulbecco's Modified Eagle's Medium (DMEM) *(GIBCO-Thermo Fisher Scientific)* supplemented with 4 mM glutamine, 100 µg/mL penicillin/streptomycin (P/S) and 10% of Fetal Bovine Serum (FBS) *(GIBCO-Thermo Fisher Scientific)*, at 5% CO_2 and 37ºC in a humid chamber. To maintain the cells, passages were performed every 3 or 4 days, when cells were at 90% of confluence.

In the passage proceeding, the medium in the cell plates was discarded and cells were washed with phosphate buffer saline (PBS) to eliminate the serum. To detach cells, 0.25% trypsin-ethylene diaminetetraacetic acid (EDTA) was added into the plates and cells were incubated for 5 minutes at 5% CO_2 and 37ºC. Afterwards, trypsin was inactivated by the addition of DMEM with 10% FBS and antibiotics. Then, cells were collected in a tube and centrifuged at 1000 rpm during 5 minutes. Once the supernatant was removed, the cell pellet was resuspended in 1 mL of DMEM with antibiotics and 10% FBS, and cells were counted in a Neubauer's Chamber or directly seeded in a dilution between 1:10 and 1:20 depending on the cell type. Finally, cells were incubated in the humid chamber at 5% CO_2 and 37ºC.

Primary fibroblasts were grown in Medium 106 *(GIBCO- Thermo Fisher Scientific)* supplemented with Low Serum Growth Supplement (LSGS) *(GIBCO- Thermo Fisher Scientific)*, 100 µg/mL P/S and 10 µg/mL gentamycin. As their proliferation rate was low, cells were passaged once per week when they were at 90% of confluence. After the elimination of the medium and the cells washing, trypsin was added for 5 minutes at 5% CO_2 and 37ºC to detach the cells. Then, trypsin was inactivated by the addition of 0.5 mg/mL soybean trypsin inhibitor

solution and cells were pelleted. Finally, cells were resuspended in Medium 106, counted or seeded in a 1:4 dilution and incubated in the humid chamber at 5% CO_2 and 37ºC.

To freeze cells, a freezing medium containing 90% FBS 10% dimethyl sulfoxide (DMSO) was added to the pellet obtained by centrifugation in a normal passage. Then, cells were transferred into cryotubes and stored at least 24 hours at -80ºC freezer. Finally, cryotubes were relocated to liquid nitrogen.

Human embryonic kidney 293T cells

The human embryonic kidney (HEK 293T) cell-line grows fast and is easily transfected. It is a variant of HEK 293 that expresses SV40 large T-antigen and other adenovirus genes. Thus, those transfected plasmids carrying the SV40 origin of replication can be transiently maintained at high copy number. This is the reason why in this work this cell line is used for lentiviral production. However, these cells detach very rapidly and they must be seeded on plates coated with collagen 100 µg/mL and 0.02 M acetic acid. These cells were obtained from the American Type Culture Collection (ATCC).

R3327-5'A and R3327-5'B cells

R3327-5'A and R3327-5'B are two rat prostate adenocarcinoma cell lines cloned from the same heterogeneous parental cell line (Luo et al. 1997). Whereas R3327-5'B cells grow in epithelial-like clusters and produce subcutaneous tumours poorly metastatic and invasive, R3327-5'A cells maintain a fibroblast-like phenotype, do not produce subcutaneous tumours and are highly metastatic and invasive. These cell lines were kindly provided by M. Hendrix.

Human dermal fibroblast cells

The human dermal fibroblasts (HDF) are isolated from adult skin and are grown in Medium 106. These primary cells were obtained from Thermo Fisher Scientific *(GIBCO, C0135C).*

2.2. Cell transfection

Transfection is possible through different reagents, although the most used in this work are polyethylenimine and lipofectamine. Quantities of each reagent are shown in **Table 3.**

Polyethylenimine

Polyethylenimine (PEI) *(Sigma-Aldrich)* is a cationic lipid used for packaging plasmid DNA neutralizing its negative charges and avoiding the action of nucleases. The resulting complexes have positive charges and are able to interact with the negative-charged membrane phospholipids, leading to their endocytosis and posterior release of DNA inside the cell. PEI have a high transfection efficiency in HEK 293T cells.

Normally, transfection starts when plates present 70-80% of cell confluence. PEI and DNA were diluted distinctly in opti-MEM *(GIBCO-Thermo Fisher Scientific)*, which is a reduced-serum medium. Both dilutions were mixed and incubated 10 minutes at room temperature (RT), so PEI-DNA complexes were generated. After that, the mixture was added to cells and incubated for 1 hour in the humid chamber at 5% CO_2 and 37ºC. Finally, the transfection mixture was removed and DMEM with 10% FBS and antibiotics was added.

Lipofectamine

Lipofectamine 2000 *(Invitrogen)* is a reagent containing neutral and positive liposomes that wraps nucleic acids. Due to its properties, liposomes can fuse with the cell membrane to deposit their cargo inside. This method is widely used for cells with a medium transfection ratio, as R3327-5'A and R3327-5'B.

The lipofectamine transfection procedure is similar to PEI's, but with some time changes, even though plates also need to present 70-80% of cell confluence. Lipofectamine was mixed with opti-MEM and incubated for 5 minutes at RT. Then, this mixture was combined to DNA-opti-MEM mix and incubated for 20 minutes at RT, in order to form the DNA-lipofectamine complexes. The resulting solution was added to cells and incubated for 20 minutes in the

humid chamber at 5% CO_2 and 37ºC. Finally, the transfection mixture was removed and DMEM with 10% FBS and antibiotics was added.

	Reagents	35 mm Ø	60 mm Ø	100 mm Ø
PEI	DNA + opti-MEM	4 µg + 250 µL	8 µg + 500 µL	24 µg + 1500 µL
	PEI + opti-MEM	40 µL + 210 µL	80 µL + 420 µL	240 µL + 1260 µL
Lipofectamine	DNA + opti-MEM	4 µg + 250 µL	8 µg + 500 µL	24 µg + 1500 µL
	Lipofectamine + opti-MEM	10 µL + 250 µL	20 µL + 500 µL	60 µL + 1500 µL

Table 3. *Transfection reagents.* Amounts of each reagent according to plate size.

2.3. Lentivirus production and infection

Lentivirus production

HEK 29T cells were seeded in collagen plates so as to reach 70-80% of confluence the next day. Twenty-four hours later, cells were transfected with lentiviral expression plasmids, wrapping vector pVSV.G and packaging vector pHR'82ΔR (encoding gag and pol viral proteins) in a 2:1:1 proportion, using the PEI protocol described before.

Once the virus are generated, cells release them into the medium. So, the medium of the plates was collected after 3 days of transfection, and was filtered with a 0.45 µm nitrocellulose membrane. Finally, it was stored at -80ºC for posterior usage. The virus collection and manipulation were performed in a BioIIA hood.

Cell infection

The desired number of cells were seeded on plates with medium, lentivirus solution, and polybrene *(Sigma-Aldrich)*. Polybrene is hexadimethrine bromide, a cationic polymer that increases infection efficiency. Medium was changed after 24 hours, and the effect produced by the lentivirus infection is assessed after 72 hours by immunoblot or immunofluorescence. The quantities of each product are shown in **Table 4.**

Plates	Medium	Virus solution	Polybrene
35 mm	1 mL	1 mL	3.5 µL
60 mm	2.5 mL	2.5 mL	8 µL
100 mm	5 mL	5 mL	16 µL

Table 4. *Lentiviral infection.* Amount of medium, lentivirus solution, and polybrene needed for each plate size.

2.4. Retinoblastoma 1 knock-out generation

Twenty-four hours after R3327-5'A cells were seeded in 35 mm plates, they were transfected with the pCEPe9 vector **(Table 1)** containing sgRNA of RB1 exon 1, pCEPe9 vector containing sgRNA of RB1 exon 3, and the pCEPe9 vector without any sgRNA as a control. Some R3327-5'A were not transfected and were used as a control, also. The seeding and transfection were done in duplicates.

Afterwards, one duplicate was titrated with 4 µg/mL of puromycin and the other with 8 µg/mL. Five days after the treatment with puromycin, cells were trypsinised and seeded in low density in a 100 mm plate until they formed clones. Then, each clone was taken to a 96-well plate (20 clones from exon 1, 20 clones from exon 3, 8 clones without sgRNA and 8 clones without plasmid). All the clones were amplified and obtained for immunoblot analysis. Candidate clones that did not show expression of RB1 were sequenced by the Sanger method to confirm that they were knock-out for RB1.

2.5. Cell proliferation and viability

Proliferation assay

To determine the proliferation, 10^5 cells were seeded in four 35 mm plates in serum-containing medium and incubated in a humid chamber at 5% CO_2 and 37ºC. Each plate corresponded to a time point: 0 hours, 24 hours, 48 hours and 72 hours. Hence, 24 hours after the seeding, cells from the first plate (time 0) were trypsinised and counted in a Neubauer's Chamber. For experiments with the inhibitor Palbociclib, this drug or DMSO (control) were added at time 0.

Proliferation assay with BrdU incorporation

Bromodeoxyuridine or 5-bromo-2'-deoxyuridine (BrdU) *(Sigma-Aldrich)* is a synthetic thymidine analogue that cells incorporate into their new chains of DNA during the S phase of the cell cycle instead of thymidine. Hence, BrdU integration is further used to detect proliferative cells.

BrdU 8 µg/mL was added to cells for 8 hours. After this time, cells were fixed with 4% of paraformaldehyde (PFA) for 15 minutes at RT, permeabilised during 3 minutes at RT with 0.2% Triton-X-100 and washed three times with PBS. In order to facilitate the primary antibody to recognise the BrdU, DNA was denatured and broken with HCl 2 M for 30 minutes. Afterwards, the addition of sodium tetraborate 0.1 M (pH 8.5) for 2 minutes into the cells neutralises the HCl. Then, cells were blocked with 3% of Bovine Serum Albumin (BSA) *(Sigma-Aldrich)* during 1 hour, washed three times with PBS and incubated with the primary antibody (anti-BrdU, 1:200 dilution) **(Table 7)** overnight.

The following day, cells were washed three times with PBS and were incubated for 1 hour at RT with the secondary antibody (Alexa Fluor 488, 1:1000 dilution) **(Table 7)** and Hoechst *(Sigma-Aldrich)* at 0.5 µg/mL of final concentration with BSA 0.3%. Hoechst was used due to its ability to bind to DNA, as it permits the nuclei detection. Finally, cells were washed three times with PBS, and BrdU-positive or BrdU-negative cells were quantified relative to the total

nuclei (stained with Hoechst). Images were taken with the inverted Olympus IX71 microscope with 10x and 20x objectives.

Viability assay with trypan blue

Trypan blue *(Sigma-Aldrich)* is a dye that is incorporated in the cell when its membrane is damaged, being dead cells exclusively blue-coloured. Hence, this staining is frequently used to differentiate live and dead cells in proliferation and viability assays.

Three thousand cells per well were seeded on a 24-well plate and incubated at 37ºC and 5% CO_2. Cells were counted at 24 hours, 48 hours, and 72 hours after treatment. To perform the quantification, seeded cells were washed with PBS, trypsinised, and diluted in 300 µL of medium with trypan blue 0.4% in a 1:1 proportion. Once the staining was done, stained cells (dead) and non-stained cells (live) were counted in the Neubauer's Chamber.

Colony formation assay

The colony formation assay checks the ability of a single cell to divide and form a colony. This assay was performed to analyse how the loss of some proteins can affect the cell establishment and proliferation.

In this protocol, 500 isolated cells were seeded in 35 mm plates and incubated with DMEM supplemented with FBS and antibiotics for a week. Once colonies were formed and were macroscopically visible, cells were fixed for 20 minutes with 4% of PFA and stained with 0.5% of crystal violet during 1 hour. Then, some washes with water were performed to remove all the residual staining. Colonies number and area were quantified using the ImageJ software.

2.6. Cell migration assay

In migration assays, cells are required to cross through a porous membrane in order to study their migratory ability. In this protocol, cells were trypsinised, and fifty thousand cells were diluted in 20 µL of PBS, for each condition. Then, cells were seeded on the bottom side of an 8 µm pore filter of 6.5 mm diameter Transwell *(Corning)*, and incubated for 4 hours in the humid chamber at 5% CO_2 and 37ºC for cells adhesion into the surface of the filter.

Afterwards, Transwells were placed in 24-well plates and 400 µL of serum-containing medium was added between the Transwell and the well, whereas 200 µL of serum-free medium was added inside the Transwell. In this way, the cells present in the bottom side of the filter were attracted to the upper side of the filter due to the serum. This filter assembly was incubated for 24 hours in the humid chamber at 5% CO_2 and 37ºC. Under these conditions, some cells migrated from the bottom side of the filter to the upper side.

Cells which could not migrate and persisted at the bottom of the filter were removed with a cotton stick. Migrated cells present in the upper side of the filter were fixed with 8% of PFA for 15 minutes at RT, and stained with Hoechst for 15 minutes at RT. Finally, nuclei were observed under the microscope and counted with Image J software. The percentage of migrated cells is relative to the total amount of cells.

2.7. Secretome obtaining

The secretome study *in vitro* consists of obtaining the molecules that cells release into the medium. To perform this, cells were seeded in a 100 mm plate and were grown until they reached 80% of confluence. Then, cells were washed three times with PBS and three times with serum-free DMEM with antibiotics to eliminate as much serum as it was possible. Cells were incubated with serum-free DMEM for 24 hours in the humid chamber at 5% CO_2 and 37ºC. The following day, medium was collected and filtered through 0.45 µm filter, and cells attached into the plate were collected for immunoblot analysis **(Figure 10)**.
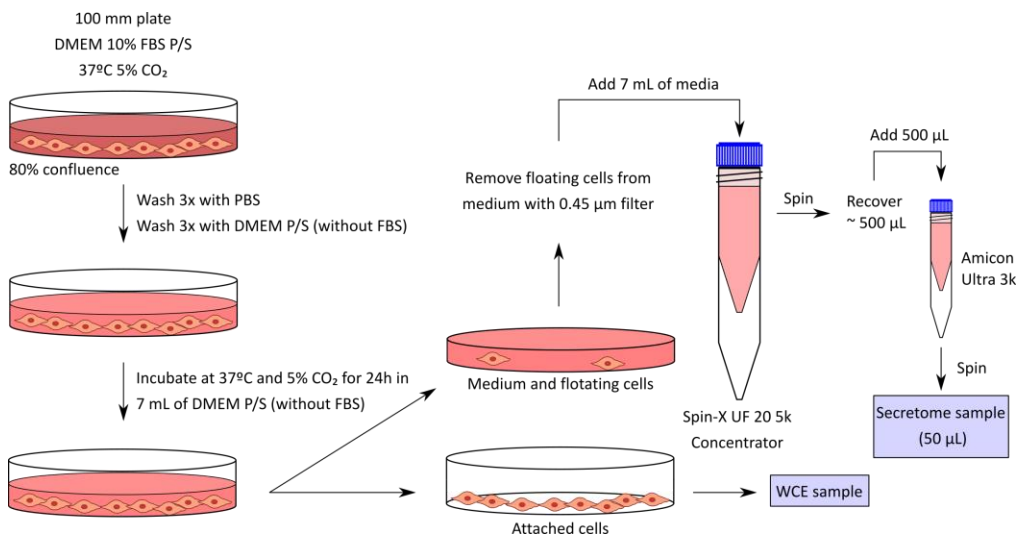
Figure 10. *Secretome obtaining methodology***.** Cells at 80% of confluence were washed with PBS and DMEM containing antibiotics without FBS and incubated for 24h with DMEM containing antibiotics without FBS. Then, cells and medium were collected separately. The medium was filtered and concentrated until up to 50 µL. Whole Cell Extract (WCE).

The medium obtained, approximately 7 mL, was concentrated with the Spin-X UF 20 5k Concentrator *(Sigma-Aldrich)* during 75 minutes, at 8000 g and 4ºC. After centrifugation, 500 µL of media was recovered and concentrated with the Amicon Ultra 3k tubes *(Millipore)* during 30 minutes, at 14000 g and 4ºC, to obtain 50 µL of concentrated medium **(Figure 10)**.

3. PHARMACOLOGICAL TREATMENTS

3.1. Palbociclib

Palbociclib or PD-332991 *(Selleckchem)* is a highly selective inhibitor of the cyclin-dependent kinases CDK4 and CDK6 that acts as an ATP-competitive inhibitor. We used Palbociclib for *in vitro* treatments, even though it has been extensively used as a clinical treatment of cancer. Palbociclib in powder was dissolved in sterile DMSO at a stock concentration of 2.5 mM and was maintained in the dark at -80ºC. During *in vitro* experiments, cells were treated with 4 µM of this drug, which was diluted in the medium. Control cells were treated with DMSO.

3.2. Barley β-Glucan

β-Glucans are carbohydrate polymers that can be found in cell walls of many organisms and display important functions in the modulation of the immunological and the wound healing responses. For this work, barley β-Glucan (1→3),(1→4) was produced by Dra. M. Moralejo (ETSEA – University of Lleida).

For *in vitro* experiments, 10 mg of β-Glucan powder were solubilised in 1 mL of sterile water, heated and stirred in a water bath at 90ºC for 5 minutes. Then, shaking continued for 10 minutes without heating. Some proliferation assays, cell migration assays, and BrdU incorporation assays were performed with 400 µg/mL solution of barley β-Glucan.

For *in vivo* experiments, a 30 mg/mL aqueous solution was prepared in the same way.

3.3. Methylcellulose and amylopectin

Methylcellulose *(Sigma-Aldrich #M7027)* is a synthetic compound derived from cellulose. Amylopectin *(Sigma-Aldrich #10120)* is a polysaccharide highly-branched which forms starch together with amylose. Both of them were prepared at a final stock of 10 mg/mL in water at RT. A proliferation assay was performed with 400 µg/mL solution of methylcellulose or amylopectin.

4. BIOCHEMICAL TECHNIQUES

4.1. Protein extraction and western blot

SDS protein extraction

Proteins were extracted from cells growing on culture plates. In order to have an efficient extraction, cells were washed with cold PBS and collected with 1xSR (2% sodium dodecyl sulphate (SDS) and 0.125 M Tris-HCl at pH 6.8). SDS inactivates and denatures enzymes present in the protein extract, like proteases, that could degrade and damage the sample.

The volume of 1xSR necessary to have a good extraction depends on the size of the plate containing the cells. For instance, 60 μL were used in a 4-well plate (16 mm of diameter), or 100 μL in a 35 mm plate. Finally, samples were sonicated with an MSE Soniprep 150 sonicator during 10 seconds at power 8, twice. With this process, genomic DNA is disrupted and, consequently, the sample lose its viscosity.

Protein quantification

After sonication, samples were quantified by the Lowry method *(DC Protein Assay, Bio-Rad)*, widely used to determine the total amount of protein in an extract. Three μL of each sample or 5 μL of BSA as a control were added in each well in a 96-well plate. Then, reagent A and reagent B were added in each well, following the manufacturer instructions, and incubated for 15 minutes at RT in the dark. Finally, absorbance was read at 595 nm wavelength and the obtained values were extrapolated to protein concentrations using the calibration line.

SDS-Polyacrylamide gel electrophoresis

Once quantified, loading buffer 4x (20% sucrose and 0.02% bromophenol blue) was added to the samples at a final concentration of 1x. In addition, β-mercaptoethanol (1% final concentration) was added. Then, these samples were boiled for 5 minutes at 95ºC to completely denature proteins, so they were totally prepared for being loaded into SDS-Polyacrylamide gel electrophoresis (PAGE) gels.

SDS-PAGE gels were prepared with 30% of acrylamide and 2% of bis-acrylamide solution *(Bio-Rad)*. The addition of 0.1% of tetramethylethylenediamine (TEMED) *(Sigma-Aldrich)* was necessary as a polymerization initiator, and 0.05% of ammonium persulfate as a catalyst of the reaction.

A gel is formed by two main parts: the stacking gel or the upper part, and the separating gel or the lower part. The stacking gel is where the samples are loaded. Its function is to package different-sized proteins in the front, so as they could enter at the same time into the

separating gel. It consists of a solution of 5% of acrylamide in 125 µM of Tris-HCl at neutral pH (6.8). The separating gel is where the proteins separate by molecular weight. It is prepared using different quantities of acrylamide, among 7.5% to 15%, in 375 µM of Tris-HCl at basic pH (8.8), depending on the molecular weight of the proteins of interest.

Once the gels were prepared, they were put on the bucket of the MiniProtean system *(Bio-Rad)*, filled with an electrophoretic solution containing 25 mM Tris, 1.44% glycine and 0.1% SDS. Then, samples were loaded in the stacking gel, and a constant current of 20 mA per gel was applied. Thus, samples migrate from the negative pole to the positive one through the polyacrylamide matrix, being separated by their molecular weight. As a molecular weight marker and standard (SD), 2 µL of the PageRuler™ Prestained Protein Ladder *(ThermoFisher #26616)* was also loaded.

Protein transfer and blocking

When the electrophoresis was finished, proteins separated in the gel were transferred in a polyvinylidene fluoride (PVDF) membrane *(Immobilon-P, Millipore)*. Membranes were activated with methanol and equilibrated with the transfer buffer (192 mM glycine, 25 mM Tris, 10 or 20% ethanol). For the protein transfer, a semi-dry system with a constant current of 60 mA per gel for 1 hour was used.

Once the transfer was done, the protein-containing membranes were blocked in a solution of 3% BSA in phosphate buffered saline with 0.1% Tween-20 (PBST) for 1 hour.

Protein immunodetection

After blocking, membranes were washed several times with PBST. Then, the primary antibody of interest was added and incubated overnight at 4ºC. Antibody dilutions are shown in **Table 5**. The following day, membranes were washed three times with PBST. The secondary antibody diluted in 0.3% of BSA in PBST was added and incubated at least 1 hour. Normally,

secondary antibodies are conjugated with Horseradish Peroxidase (HRP) *(GE Healthcare UK Ltd)* and used in a 1:10000 dilution. Then, membranes were washed with PBST three times.

Finally, membranes were incubated with HRP Chemiluminescent substrate *(Immobilon Western, Millipore)* for 5 minutes. The chemiluminescent signal of the studied proteins was detected with the Chemidoc™ MP Imaging System *(Bio-Rad)*. The protein band quantification was performed with the software ImageLab, associated to the Chemidoc System.

Antibodies

The following table shows the primary and secondary antibodies used in the western blot technique:

Primary antibody	Reference	Dilution
Anti-α-Tubulin	Mouse monoclonal, B-5-1-2, *Sigma-Aldrich, #T5168*	1/10000
Anti-β-Actin	Mouse monoclonal, C-4, *Millipore #MAB1501R*	1/1000
Anti-Adseverin	Mouse monoclonal, C-2, *Santa Cruz, #sc-376136*	1/1000
Anti-CDK4	Rabbit polyclonal, C-22, *Santa Cruz #sc-260*	1/250
Anti-Clusterin	Goat polyclonal, M18, *Santa Cruz, #sc-6420*	1/1000
Anti-Cyclin D1	Mouse monoclonal, DCS-6, *BD Pharmingen, #556470*	1/1000
Anti-E-Cadherin	Mouse monoclonal, HECD-1, *Calbiochem, #205601*	1/1000
Anti-Fascin	Mouse monoclonal, 55K-2, *Santa Cruz, #sc-21743*	1/1000
Anti-GAPDH peroxidase	Mouse monoclonal, 71.1, *Sigma-Aldrich #G9295*	1/40000
Anti-p38	Rabbit polyclonal, *Cell Signaling, #9212*	1/500
Anti-pho-p38 (Thr-180/Tyr-182)	Mouse monoclonal, 28B10, *Cell Signaling, #9216*	1/500
Anti-PADI2	Rabbit polyclonal, *Proteintech, #12110-1-AP*	1/1000
Anti-Paxillin	Mouse monoclonal, 349, *BD Biosciences, #610051*	1/1000
Anti-RB1	Mouse monoclonal, G3-245, *BD Pharmingen, #554136*	1/500

Anti-pho-RB1 (Ser-780)	Mouse monoclonal, J146-35, *BD Pharmingen, #558385*	1/500
Anti-S100B	Mouse monoclonal, C-3, *Santa Cruz, sc-393919*	1/1000
Anti-Vinculin	Mouse monoclonal, VIN-11-5, *Sigma-Aldrich*, *#V4505*	1/1000

Secondary antibody	Reference	Dilution
Goat anti-Mouse	IgM-HRP, *Santa Cruz, sc-2973*	1/10000
Donkey anti- Rabbit	IgG-HRP, *Amersham Biosciences, NA934*	1/10000
Horse anti-Goat	IgG-HRP, *Vector Laboratories, PI-9500*	1/10000

Table 5. *Primary and secondary antibodies used in western blot technique.* All antibodies were diluted in 0.3% BSA.

5. MICROSCOPY TECHNIQUES

5.1. Sample processing

Once animals were sacrificed, lungs were obtained and included in paraffin blocks, in cryofrozen cassettes or fixed with Bouin solution.

For paraffin blocks, the extracted lungs were fixed immediately with formol overnight at 4ºC. The next day, the samples were placed in cassettes and taken to the Anatomical Pathology Unit, where they prepared the samples. Lungs were gradually dehydrated in different alcohols (from ethanol 70º to ethanol 100º), treated with xylene and included in paraffin. Next, paraffin blocks were sectioned at 3 μm of thickness and lung samples were placed in slides and dried for 1 hour at 65ºC. Then, samples were deparaffinised with xylene, gradually rehydrated in alcohols (from ethanol 100º to ethanol 70º), and washed with PBS. To study the lung histology, samples were observed under the microscope after haematoxylin-eosin or immunohistochemistry staining.

For cryofrozen cassettes, the extracted lungs were fixed with 4% PFA overnight at 4ºC. Afterwards, lungs were placed in a 30% sucrose buffer until they were dehydrated. Finally, they were included in cassettes with optimum cutting temperature reagent (OCT) *(Tissue-Tek*

O.C.T. Compound, VWR Cat #25608-930) and frozen at -80ºC until cut in 16 µm section in the cryostat.

For Bouin treatment, the extracted lungs were incubated with the Bouin solution for 48 hours and then were washed with PBS several times. Bouin solution was used to maintain the lung structure and macroscopically observe metastasis.

5.2. Immunohistochemistry

Antibodies

The following table contains the primary and secondary antibodies used in the immunohistochemistry methodology:

Primary antibody	Reference	Dilution
Anti-Adseverin	Mouse monoclonal, C-2, *Santa Cruz, #sc-376136*	1/100
Anti-Cleaved Caspase 3 (Asp-175)	Rabbit polyclonal, *Cell Signaling, #9661*	1/100
Anti-Cyclin D1	Rabbit monoclonal, EP12, *Dako, #M3642*	1/400
Anti-pho-FAK (Tyr-397)	Rabbit monoclonal, 31H5L17, *Invitrogen, #700255*	1/100
Anti-Fascin	Mouse monoclonal, 55K-2, *Santa Cruz, #sc-21743*	1/100
Anti-PADI2	Rabbit polyclonal, *Proteintech, #12110-1-AP*	1/200
Anti-pho-Paxillin (Ser-83)	Rabbit polyclonal, *ECM biosciences, #PP1341*	1/100
Anti-RB1	Mouse monoclonal, G3-245, *BD Pharmingen, #554136*	1/100
Anti-S100B	Mouse monoclonal, C-3, *Santa Cruz, sc-393919*	1/100

Secondary antibody	Reference	Dilution
Goat anti-Rabbit	EnVision+System-HRP labelled polymer, *Dako, #K4003*	1/1000
Goat anti-Mouse	EnVision+System-HRP labelled polymer, *Dako, #K4001*	1/1000

Table 6. *Primary and secondary antibodies used in immunohistochemistry technique.* Both primary and secondary antibodies were diluted in an Antibody Diluent Ready-to-use *(Agilent #S080983-2)*.

Immunohistochemistry

The immunohistochemistry technique allowed us to detect some specific antigens in cells contained in a lung section. The deparaffinised samples placed in slides were incubated in the commercial buffer EnVision Flex Target Retrieval Solution *(Dako, Agilent)* containing Tris/EDTA 50x at pH 9 for 20 minutes at 95ºC, in order to perform an epitope retrieval. The purpose of this step is to expose the masked antigens during the sample preparation. Then, endogenous peroxidase was blocked by incubating sections in 3% H_2O_2 and three washes of PBS were performed before the incubation with the primary antibody **(Table 6)** for 30 minutes at RT.

Next, three more washes of PBS were done and samples were incubated for 30 minutes with the peroxidase-conjugated secondary antibody **(Table 6)**. Finally, diaminobenzidine chromogen was used as a substrate to visualise the presence of antigen through the EnVision FLEX Detection Kit *(Dako, Agilent)*, and a haematoxylin counterstaining was done to see the cell nucleus. The tissue controls were performed without the addition of the primary antibody.

In this work, staining of Cyclin D1, Paxillin Pho-Ser-83, Focal Adhesion Kinase (FAK) Pho-Tyr-397, Cleaved Caspase 3, Adseverin, Fascin, Protein-Arginine Deiminase type-2 (PADI2), and S100B were analysed. Images from the immunohistochemistry results were taken with the Leica DMD108 microscope.

5.3. Immunofluorescence

Antibodies

The following table contains the primary and secondary antibodies used in both cell and tissue immunofluorescences:

Primary antibody	Reference	Dilution
Anti-BrdU	Rat monoclonal, BU1/75 (ICR1), *Bio-Rad #MCA2060*	1/200[1]
Anti-GFP	Rabbit polyclonal, *Invitrogen #A21311*	1/200[2]
Anti-Cyclin D1	Mouse monoclonal, *Santa Cruz, #72-13G*	1/200[1]

Secondary antibody	Reference	Dilution
Goat anti-Rat	Alexa Fluor ® 488, *Molecular Probes, A-11006*	1/1000[1]
Goat anti-Rabbit	Alexa Fluor ® 488, *Molecular Probes, A-11008*	1/500[3]
Donkey anti-Mouse	Alexa Fluor ® 594 *Thermo Fisher, A-21203*	1/1000[1]

Table 7. *Primary and secondary antibodies used in the immunofluorescence technique.* [1] Antibodies diluted in 0.3% BSA; [2] antibodies diluted in 4% BSA 0.04% Tween-20; [3] antibodies diluted in PBS.

Cell immunofluorescence

For the immunofluorescence technique, cells were seeded in 8-well glass-bottom plates to be able to see the cells at the confocal microscope. Cells were washed with PBS and fixed with 4% PFA for 15 minutes at RT. Wells were washed three times with PBS, and cells were permeabilised with 0.2% Triton-X100 for 3 minutes at RT and blocked with 3% BSA in PBS for 30 minutes at RT. Then, cells were incubated overnight at 4ºC with primary antibodies in a 1:200 dilution in 0.3% BSA. Primary antibodies are shown in **Table 7**.

The following day, cells were washed three times with PBS. Secondary antibodies marked with Alexa 488 or Alexa 594 *(Molecular Probes)* **(Table 7)** were added in a 1:1000 dilution in 0.3% BSA and were incubated for 1 hour at RT in the dark, together with Hoechst, to stain the cellular nuclei. Finally, three washes of PBS were performed in each well and SlowFade antifade reagent *(Molecular Probes)* was added to avoid photobleaching.

In this work, the anti-BrdU and the anti-Cyclin D1 antibodies were used, and images were acquired with 40x and 60x objectives in an Olympus FV1000 microscope.

Tissue immunofluorescence

Cryofrozen lung samples cut in 16 μm section in the cryostat were used for tissue immunofluorescence. First, samples were thawed at RT and washed with PBS before being fixed with 4% PFA for 5 minutes at RT. Then, after washing with PBS, samples were permeabilised with methanol-acetone for 2 minutes at -20ºC. Finally, samples were blocked with 4% BSA with 0.2% Tween-20.

Primary antibodies in a 1:200 dilution in 4% BSA and 0.04% Tween-20 were added on the samples and were incubated overnight at 4ºC. Used antibodies are shown in **Table 7**. The following day, three washes of PBS were done. The corresponding Alexa 488 and Alexa 594 *(Molecular Probes)* secondary antibodies were added into the samples and incubated in a 1:500 dilution in PBS for 1 hour, at 4ºC and in the dark, together with Hoechst.

Finally, three washes with PBS were done and the slides were mounted. In this work, the antibody against Green Fluorescent Protein (GFP) was used and pictures were taken using the Olympus FV1000 confocal microscope.

6. EXPERIMENTAL ANIMALS

6.1. Previous considerations

The *in vivo* studies performed in this work using laboratory animals have been developed according to the following legal regulations:

- **Catalan Government:** 5/1995 law, of 21st June, on animals' protection used in animal experimentation and other scientific finalities.
- **Catalan Government:** Decree 214/1997, of 31st July, on regulation of animal usage for experimentation and other scientific finalities.
- **Spanish Government:** Royal Decree 53/2013, of 1st February, which establish the applicable basic rules for the protection of animals used in experimentation and other scientific finalities, including teaching.

- **Spanish Government:** Order ECC/566/2015, of 20th March, that establish the training requirements that personnel managing animals used, bred or supplied for experimental and other scientific purposes, including teaching, must have.
- **European Parliament and Council:** Directive 2010/63/EU, of 22nd September, on the protection of animals used for scientific purposes.

The procedures with mice have been conducted under the supervision of the responsible personnel at our centre, always respecting current legal and ethical guidelines. Furthermore, this work has been approved by the Ethical Committee of Animal Experimentation (CEEA) from University of Lleida.

All animals were maintained in cycles of 12 hours of light and darkness, at 20±2ºC of temperature, in humidity of 50±5%, and *ad libitum* access to food and water. All the procedures were performed under pathogen-free conditions.

6.2. Animals

SCID mice

Severe combined immunodeficiency (SCID) mice have a genetic autosomal recessive mutation (Prkdc^{SCID}) located in the chromosome 16, that prevent the accurate VDJ recombination. As mice are homozygous for this mutation, they cannot produce functional B and T lymphocytes and develop a serious immunodeficiency. Functionally, this mutation prevents immune system of maturation, so mice cannot reject tumours and transplants or fight infections. For this reason, these mice are widely used as an animal model for the subcutaneous or xenografted tumours study. In our lab, SCID mice were yielded by Dr. Xavier Dolcet (IRB Lleida).

In this work, SCID male mice were used as experimental animals. They have been hosted in specific-pathogen free (SPF) conditions.

C57BL/6 mice

The C57BL/6 mouse strain is a subline derived from the C57BL line established in 1921 by Dr. C. C. Little, and introduced to the Jackson Laboratory in 1948. In our lab, these mice were yielded by Dr. Mario Encinas (IRB Lleida).

6.3. Metastasis assay

The metastasis assay allows us to observe whether the circulating cells are able to reach the tissue and form a nodule.

Survival assay

In the survival experiment, mice were retro-orbitally injected with 250.000, 500.000, 750.000 or 1.000.000 of R3327-5'A or R3327-5'B cells and euthanised when they had a weight loss, showing a clear decline of their health. Once sacrificed, the lungs were collected. One lung of each mouse was fixed with Bouin solution, and the other lung was prepared to be included in paraffin.

Metastasis analysis

To assess the number and size of lung metastasis, SCID mice were retro-orbitally injected with 400.000 R3327-5'A, R3327-5'A shD1, R3327-5'A shAdseverin, R3327-5'A knock-out RB1 (RB1$^{-/-}$), R3327-5'A RB1$^{-/-}$ shD1 or R3327-5'B cells. In all cases, cells were co-infected with FSV (produces the green fluorescent protein). Injection of PBS was used as a control. Mice were euthanised one, two, or fifteen days after the injection. For observational experiments, one lung of each mouse was cryofrozen to perform immunofluorescences, and the other lung was included in paraffin to carry out haematoxylin-eosin staining and immunohistochemistries. For proteomic analysis of the TIF, one lung of each mouse was cryofrozen, 1/3 of one lung was included in paraffin, and 2/3 of lung were used for TIF obtaining.

6.4. Tumour interstitial fluid obtaining

The study of the cancerous secretome *in vivo* requires the TIF obtaining. During the last years, different techniques have been used for TIF isolation, although the most commonly practised are elution and centrifugation. TIF isolation could be difficult, as it depends on many variables. For this reason, the establishment of a TIF obtaining workflow is important. Recently, our group has set up a centrifugation method for TIF isolation from skin squamous carcinomas (Matas-Nadal et al. 2020). In this work, we have adapted this method to obtain TIF from metastatic lungs.

We collected mice lungs and washed them with cold PBS until the blood was removed. Then, they were dried with absorbent paper, cut in small sections and centrifuged with ClearSpin filter microtubes *(DD Biolab #007859ACL)* for 20 minutes at 10000 rpm at 4ºC (Matas-Nadal et al. 2020). The volume of obtained TIF varied between 3 and 10 µL depending on the sample. In each case, PBS and proteases inhibitors were added to reach a final volume of 50 µL. From the total volume, 10 µL were separated and mixed with 10 µL of 2xSSR (4% SDS, Tris-HCl 0.25 M pH 6.8, 10% sucrose, 2% β-mercaptoethanol, and 0.01% bromophenol blue) to be checked in an SDS-PAGE followed by gel staining. The rest of the sample was stored at -20ºC for a posterior usage.

To obtain a cellular extract of each sample, each tissue remaining on the filter was collected and mixed with 50 µL of urea 5 M and glass beads. Samples were shaken in the Mini-Beadbeater-16 *(Biospec)* for 40 seconds in two cycles to break the tissues. To elute all the proteins, 50 µL of 1xSR were added into the samples and boiled at 95ºC for 3 minutes. Then, samples were sonicated for 30-40 seconds at power 8, and loading buffer with β-mercaptoethanol was added. Finally, all the samples were stored at -20ºC.

6.5. Wound closure assay

To appreciate the cutaneous healing capacity of the mice, two wounds of 6 mm were generated in the lumbar skin of each animal using a biopsy punch, after previous hair removing and disinfection with 70% ethanol. During the process, mice were anesthetised

with 3% isofluorane and subcutaneous injected with 0.05 mg/kg of buprenorphine as an analgesic measure. The lumbar wounds were treated with water, as control, or 30 mg/mL of aqueous solution of barley β-Glucan every three days during two weeks. Images were taken the same day of treatment and wounds area was measured with Image J software.

7. PROTEOMIC ANALYSIS

7.1. Protein analysis of tumour interstitial fluid

A proteomic analysis was performed with the TIFs obtained from mice lungs in the Proteomic Unit from Josep Carreras Leukaemia Research Institute. Forty µL of each sample were mixed with 80 µL of urea 6 M Tris 0.1 M. Then, samples were sonicated for 10 cycles of 30 seconds On/Off with a bioruptor to disrupt membranes and solubilise proteins. After that, samples were centrifuged for 5 minutes at 5000 g at RT to discard the pellet that contains the ruptured membranes. Supernatant was collected, treated for 1 hour at 4ºC with trichloroacetic acid (TCA) to precipitate the protein, and centrifuged. Hence, the pellet was saved and treated with 400 µL of acetone to dehydrate the protein. At this point, samples were frozen and vortexed four times every 30 minutes, and then they were left at -20ºC overnight. The following day, samples were dried in the SpeedVac and quantified with RCDC Protein Assay kit *(BioRad #5000-120)* following manufacturer's instructions.

To digest proteins, samples were mixed with urea 6 M Tris 0.1 M and dithiothreitol (DTT) 10 mM in the thermo-mixer at 650 rpm for 1 hour at 30ºC to reduce proteins, and then mixed with chloroacetamide (ACC) for 30 minutes at 30ºC for alkylation reactions. Afterwards, samples were diluted to a final concentration of urea 2 M and were digested overnight at 37ºC and 650 rpm with 0.2 µg/µL endoproteinase Lys-C *(WAKO, #125-05061)*. Then, samples were diluted again to urea 1 M and were digested with 0.2 µg/µL trypsin *(Promega, #V5280)* at 37ºC in the thermo-mixer at 650 rpm the following 8 hours. After this time, trypsin was inhibited with formic acid and peptides were desalted and purified with Pierce™ C18 Tips *(Thermo Fisher #87782)* following manufacturer's instructions. Finally, purified peptides were

dried in the SpeedVac and analysed by liquid chromatography tandem mass spectrometry (LC-MS/MS).

7.2. Protein analysis of exosomes from tumour interstitial fluid

To analyse which proteins detected in TIFs were being secreted in exosomes, three TIF samples from mice injected with PBS and three TIF samples from mice injected with R3327-5'A were collected and analysed by LC-MS/MS in the Proteomic Unit from Josep Carreras Leukaemia Research Institute. For exosomes isolation, they used the qEV Original / 70 nm SEC Columns for Exosomes Separation and Purification *(Izon)*.

Columns were equilibrated and exosomes were eluted and concentrated following manufacturer's instructions. Once exosomes were separated, proteins were extracted with urea 8 M Tris 0.1 M and precipitated and digested as explained in **Section 7.1.** Peptides were purified and desalted with PolyLC C18 pipette tips *(PolyLC. INC. #P/N TT10C18.96)* following manufacturer's instructions and LC-MS/MS analysis was performed.

8. BIOINFORMATIC TOOLS

8.1. Image J

Image J is an image processing program of a JAVA public domain, which permits the visualization and managing of images obtained from the microscope. It is really helpful because it can measure surfaces, distances and points, edit the image by contrast or sharpening it, and set scales among multiple other functions (Schneider et al. 2012).

We used this tool to measure both the number of DTCs in the lung parenchyma two days after the tumour cells injection and the number and size of metastatic nodules after fifteen days of cells injection. Moreover, it allowed us to measure the number of BrdU-positive cells and migrated cells. <u>Website:</u> https://imagej.nih.gov/ij/

8.2. Uniprot

Uniprot (Universal Protein Resource) is a group of databases that contain validated data about protein sequences and functional information from a great variety of species (Bateman, 2019). It also allows comparing distinct protein sequences. In this work it has been used to check the consensus DNA or protein sequence and functional pathways of some proteins obtained in the TIF proteomic analysis.   Website: https://uniprot.org

8.3. STRING

The Search Tool for the Retrieval of Interacting Genes (STRING) is an online database that includes a wide range of predicted and known associations of physical and functional interactions between proteins. It obtains the information from literature, other databases, and computational predictions of interactions (Szklarczyk et al. 2021). In this work, this application has been used to analyse the candidates list obtained in the TIFs analysis.

Website: https://string-db.org/

8.4. ShinyGo

ShinyGO is a novel web application sustained on a database derived from Ensembl and STRING that contains information about 315 organisms (Xijin et al. 2020). This application allows us the study of protein-to-protein interactions, the analysis of enrichment results with graphical visualization, and the identification of statistically significant differences in gene characteristics of our interest from background genes. We made usage of this website to check the enrichment of the proteins obtained in the TIFs.

Website: http://bioinformatics.sdstate.edu/go/

8.5. ExoCarta

ExoCarta is an exosome online database that gathers all the compounds that have been identified until the moment in isolated exosomes from multiple species (Keerthikumar et al. 2016). We used this platform in order to check whether the proteins we found in our proteomic screenings had been previously detected in other works.

<u>Website:</u> http://www.exocarta.org/

8.6. DeepVenn

DeepVenn is an online application which compares different lists of proteins and generates proportional Venn diagrams (Hulsen et al. 2008). In this work, we have used this website to compare protein lists from TIFs and exosomes analysis, and observe which proteins detected in the TIFs were also found in exosomes.   <u>Website:</u> https://deepvenn.com/

RESULTS

CHAPTER 1.

ROLE OF THE CYCLIN D1 IN METASTASIS

1. Setting up an *in vivo* metastasis model

To analyse the importance of Cyclin D1 in the regulation of metastasis, we first looked for an *in vitro* cellular model to work. R3327-5'A and R3327-5'B are two cell types that were isolated from the same heterogeneous rat prostate tumour (Luo et al. 1997). R3327-5'A cells exhibit a fibroblast-like phenotype and are highly metastatic and invasive, whereas R3327-5'B cells grow in an epithelial-like phenotype and are poorly metastatic and invasive **(Figure 11A).** Since the two cell lines show a great difference in the metastatic response despite sharing the same origin, they are a reliable model.
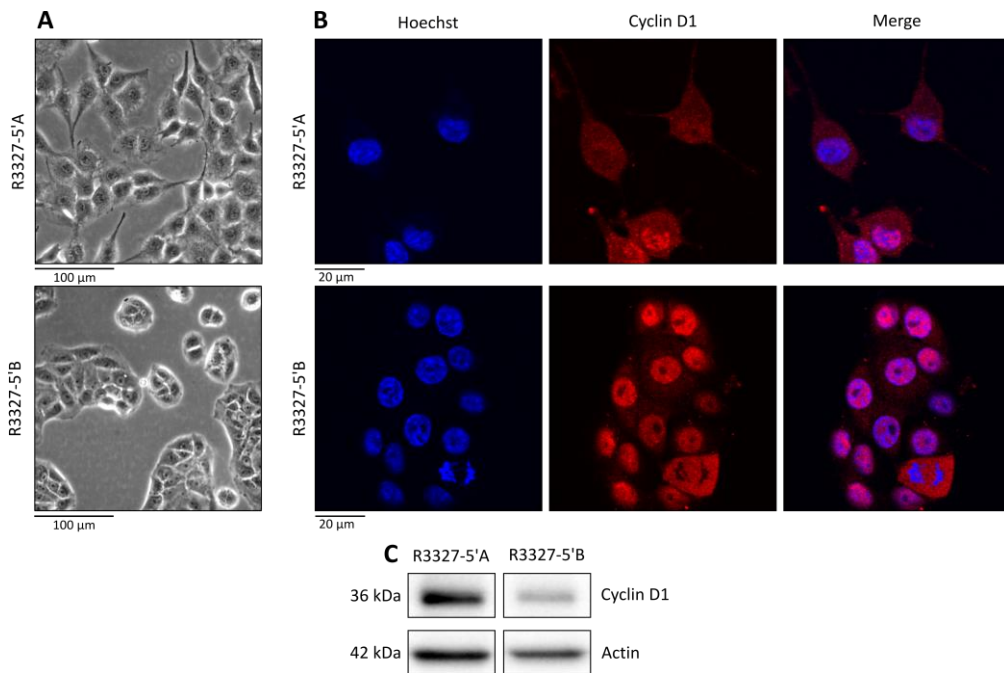
Figure 11. *Cyclin D1 has a differential expression and location in R3327-5'A and R3327-5'B cells.* **A)** R3327-5'A and R3327-5'B cells were cultured in DMEM with antibiotics and 10% of FBS. The image was taken 48 hours after the seeding. **B)** An immunofluorescence against Cyclin D1 (red) was performed in R3327-5'A and R3327-5'B cells, and images were taken in the confocal microscope. Nuclei were stained with Hoechst (blue). **C)** Cyclin D1 and Actin expressions were assessed by immunoblot containing R3327-5'A and R3327-5'B cells protein samples.

Moreover, we have determined the Cyclin D1 levels and localisation in the previous stated cells. As observed in **Figures 11B and 11C**, R3327-5'A cells present higher levels of Cyclin D1,

and it is located in the nucleus and cytoplasm, whereas R3327-5'B cells have less Cyclin D1 and it appears mainly in the nucleus. This difference is quite interesting because cytoplasmic Cyclin D1 is a marker of invasiveness (Fusté et al. 2016b).

Once the cellular model was established, we started with the setting up of an *in vivo* model of metastasis. We injected PBS as control, and R3327-5'A or R3327-5'B cells retro-orbitally into SCID mice in different amounts (250.000 cells, 500.000 cells, 750.000 cells or 1.000.000 cells) to check at which quantity we could observe a stronger effect while causing the least possible pain to mice **(Figure 12A)**.

Remarkably, this model allows us to analyse the cells' behaviour once they are in the bloodstream, studying the CTCs. Thus, we can analyse the extravasation, survival, and establishment processes of DTCs and the growth of nodules or secondary tumours in the distant organ. In this model, we do not analyse the escape and intravasation processes from the primary tumour.

Since the loss of mass is a marker of illness, we measured mice body weight every three days after cells injection, and animals were euthanised when they started losing mass heavily and presented retarded movements, considering this point as the survival of each mouse. Overall, mice injected with R3327-5'A cells (no matter the number of injected cells) lost approximately 20% of mass before euthanasia, whereas mice injected with PBS or R3327-5'B cells did not lose body weight at any moment **(Figure 12B)**.

Moreover, R3327-5'A-injected mice needed to be euthanised between the fourteenth and the twenty-first-day post-injection, being the ones injected with 1.000.000 and 750.000 cells sacrificed earlier than the ones injected with 500.000 and 250.000 cells. In contrast, PBS and R3327-5'B-injected mice remained in good health until the end of the experiment on the twenty-first day, when we euthanised all the remaining mice. Only one R3327-5'B-injected mouse died on the fifteenth day due to external causes **(Figure 12C)**. Considering that R3327-5'A cells display invasive and metastatic potential versus R3327-5'B cells, this result was aligned with our expectations (Luo et al. 1997).
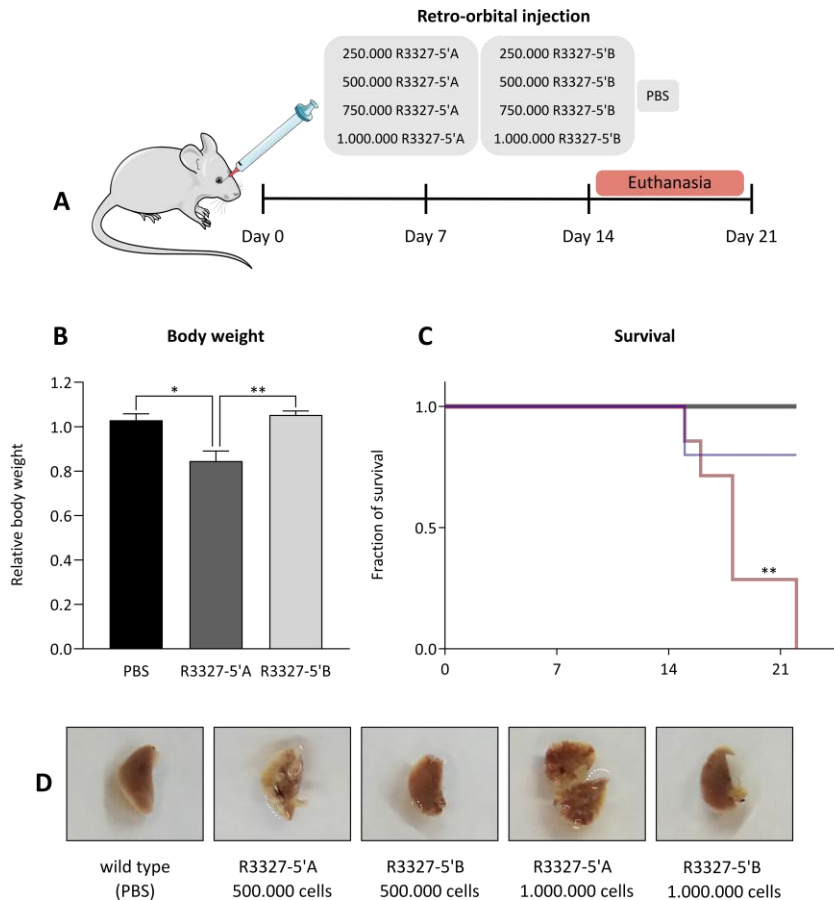
Figure 12. *Set up of a metastasis model in vivo.* **A)** PBS or different quantities (250.000, 500.000, 750.000 or 1.000.000) of R3327-5'A or R3327-5'B cells were retro-orbitally injected into SCID mice. Euthanasia was performed between the fourteenth and the twenty-first day post-injection. **B)** The body weight of R3327-5'A-injected mice (n=8), R3327-5'B-injected mice (n=6), and PBS-injected mice (n=7) was measured before euthanasia, relative to its body weight on the first day after injection. Data are the mean ± SEM, and statistical significance was determined by one-way ANOVA and Tukey-HSD post-test (*p≤0.05) (**p≤0.01). **C)** The survival of the mice in B after cells or PBS injection is represented. Statistical significance was determined by Log-Rank (Mantel-Cox) test (**p≤0.01). **D)** After euthanasia, the lungs of each mouse were macroscopically observed.

The lung is the tissue where R3327-5'A cells injected retro-orbitally usually form metastasis (Fusté et al. 2016a). Thus, we obtained the lungs from all mice after euthanasia to assess whether the injected cells produced metastases. We macroscopically observed that all mice

injected with R3327-5'A cells presented multiple lung metastasis, whereas the lungs from R3327-5'B-injected mice looked completely healthy **(Figure 12D)**. We only examined, macroscopically, the surface of the lung. Therefore, we could not determine the approximate number of nodules in the lung of each R3327-5'A-injected mouse. However, as we observed that the more cells we injected, the earlier the mice became ill **(Figure 12C)**, it would be plausible to think that the ones injected with more cells may produce more metastasis in less time.

Mice injected with 250.000 and 500.000 R3327-5'A cells remained in good health for more than fifteen days, and their lungs showed macroscopical metastasis. Consequently, we established as our model of metastasis the injection of 400.000 cells into mice and their euthanasia fifteen days later.

2. Effects of Cyclin D1 in the extravasation during metastasis

Previous experiments have shown that Cyclin D1 is important for metastatic nodule growth (Fusté et al. 2016a). Beyond these results, we were interested in addressing the role of Cyclin D1 in the different steps of lung metastasis.

For that, we injected SCID mice retro-orbitally with R3327-5'A cells, R3327-5'A cells with Cyclin D1 downregulated (shD1) **(Figure 13C)**, and R3327-5'B cells as control, all of them infected with GFP as a marker of DTCs. We euthanised all mice two days after the injection of the cells and performed immunofluorescence to detect the disseminated cells in the lung parenchyma **(Figure 13A)**.

As expected, due to its lack of EMT, any R3327-5'B cell could be detected in the lung tissue **(Figure 13B)**. Surprisingly, we observed that the lungs from mice injected with R3327-5'A cells with downregulated Cyclin D1 showed approximately twice more DTCs than the lungs from mice injected with R3327-5'A cells **(Figures 13B and 13D)**, suggesting that Cyclin D1 could restrict the cells extravasation from the capillaries to the lung tissue.
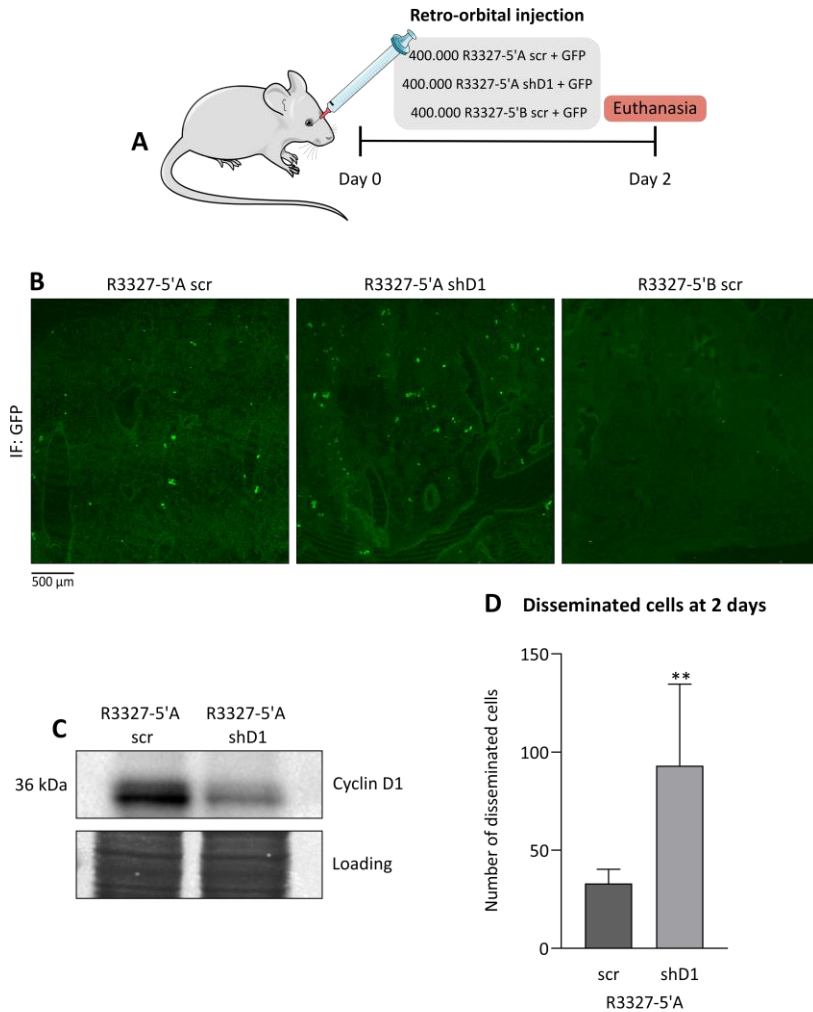
Figure 13. *Silencing Cyclin D1 increases the number of DTCs two days after mice retro-orbital injection.* A) R3327-5'A cells were infected either with lentiviruses with a scramble shRNA (scr) and GFP or with an anti-Cyclin D1 (shD1) shRNA and GFP. R3327-5'B cells were infected with scramble shRNA (scr) and GFP lentiviruses. Seventy-two hours later, cells were injected retro-orbitally into SCID mice, which were euthanised after two days. **B)** Two days after injection, lungs were cryopreserved and processed for immunofluorescence. The antibody used was anti-GFP for DTCs (green) detection, and images were acquired by confocal microscopy. **C)** R3327-5'A scramble cells and R3327-5'A cells with Cyclin D1 downregulated (shD1) were collected 72 hours after infection, and Cyclin D1 downregulation was determined by immunoblot (anti-Cyclin D1 (DCS6) antibody). **D)** From the images of seven different R3327-5'A scr lungs and nine different R3327-5'A shD1 lungs, we counted the DTCs (green). The number of DTCs is per area. Data are the mean ± SEM, and statistical significance was determined by Student t-test (**p≤0.01).

3. Cyclin D1 positively regulates disseminated tumour cells survival and establishment, and metastatic nodules growth

As we were interested not only in the role of Cyclin D1 in extravasation and dissemination but also in its role in the secondary tumour establishment and growth, we injected SCID mice retro-orbitally with PBS or R3327-5'A cells, R3327-5'A shD1 cells and R3327-5'B cells, all of them infected with GFP. Fifteen days after the injection of the cells, we euthanised the animals to obtain their lungs **(Figure 14A)**.

As expected, mice with R3327-5'B did not show any metastasis, and their lung tissue was highly similar to the lung tissue from control mice injected only with PBS **(Figure 14B)**. Mice injected with R3327-5'A cells had three times more tumours per lung than mice injected with R3327-5'A shD1 **(Figures 14B and 14C)**. Moreover, the tumours in R3327-5'A mice were larger than the tumours in R3327-5'A shD1 **(Figure 14D)**. Considering that the absence of Cyclin D1 promotes dissemination **(Figures 13B and 13D)**, these results strongly suggest that Cyclin D1 exerts a supportive role in the survival and establishment of DTCs, as well as the growth of metastatic nodules in the lung parenchyma.

Figure 14. *Cyclin D1 is required for DTCs survival, establishment, and metastatic nodules formation.* A) R3327-5'A cells were infected either with lentiviruses with a scramble shRNA (scr) and GFP or with an anti-Cyclin D1 (shD1) shRNA and GFP. R3327-5'B cells were infected with scramble shRNA (scr) and GFP lentiviruses. Seventy-two hours later, cells were injected retro-orbitally into SCID mice, and the animals were euthanised fifteen days post-injection. **B)** The panel above: two weeks after injection, one lung of each mouse was cryopreserved and processed for immunofluorescence. The antibody used was anti-GFP for tumorous cells (green) detection, and images were acquired by confocal microscopy. The panel below: two weeks after injection, the other lung of each mouse was paraffined and processed for haematoxylin-eosin staining. Tumours are shown in dark purple. Images were acquired by phase-contrast microscopy. **C)** From the immunofluorescence images of five different R3327-5'A lungs and four different R3327-5'A shD1 lungs, we have counted the green tumours. The number of tumours is per lung. Data are the mean ± SEM, and statistical significance (n=5, R3327-5'A) (n=4, R3327-5'A shD1) was determined by Student t-test (*p≤0.05). **D)** From the immunofluorescence images of five different R3327-5'A lungs and four different R3327-5'A shD1 lungs, we have quantified the area of the green tumours by using the ImageJ software. The percentage of tumours is per lung. Data are the mean ± SEM, and statistical significance (n=5, R3327-5'A) (n=4, R3327-5'A shD1) was determined by two-way ANOVA (**p≤0.01).
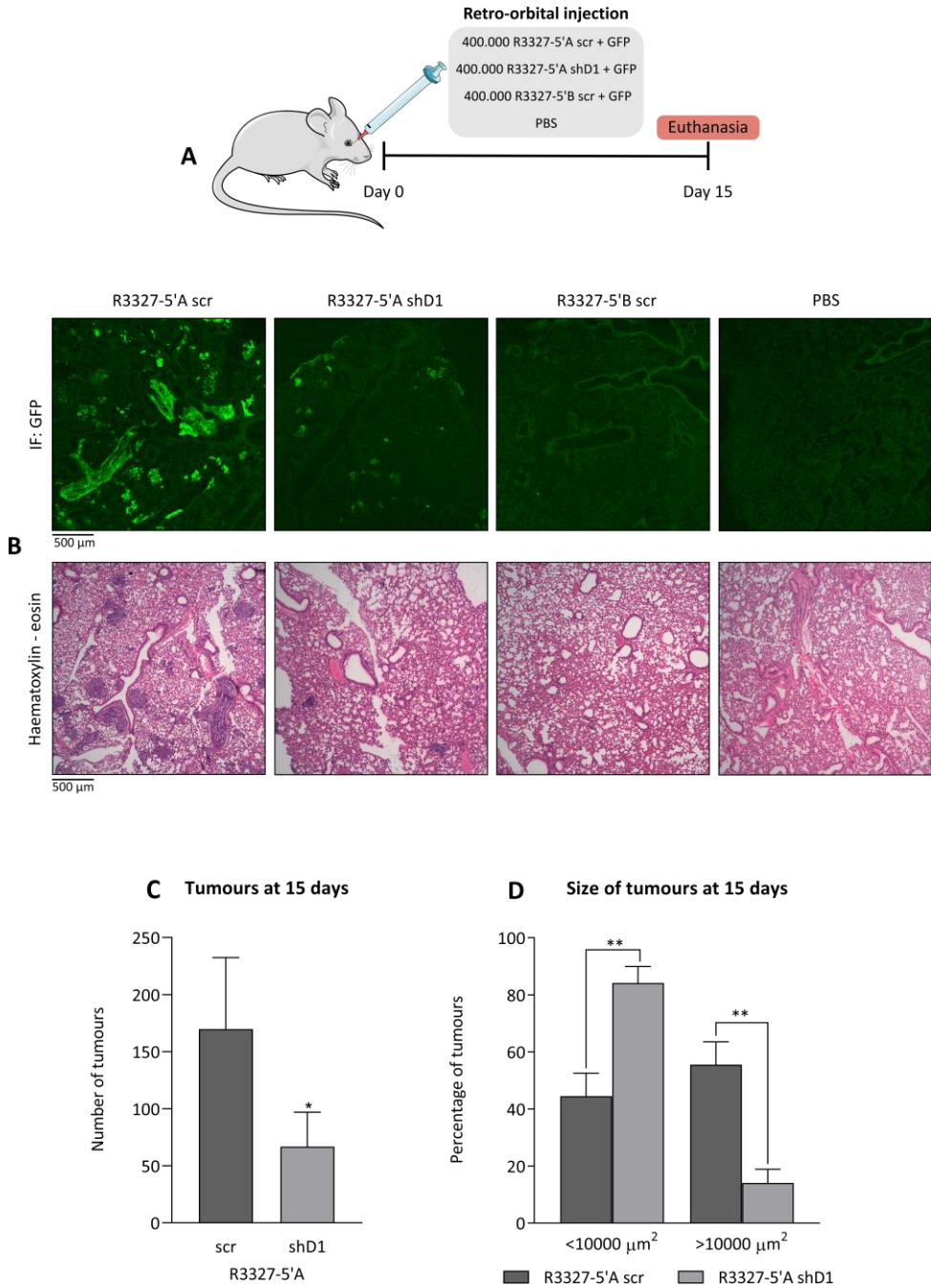
In previous studies, we described the relevance of cytoplasmic Cyclin D1 in the growth of metastatic nodules (Fusté et al. 2016a). Cyclin D1 promotes the activation of the Paxillin – FAK pathway in tumour cells. Then, we checked by immunohistochemistry the activation of the Paxillin – FAK pathway. We have determined the expression of Cyclin D1, Paxillin phosphorylated at Ser-83, and FAK phosphorylated at Tyr-397 **(Figure 15)**.
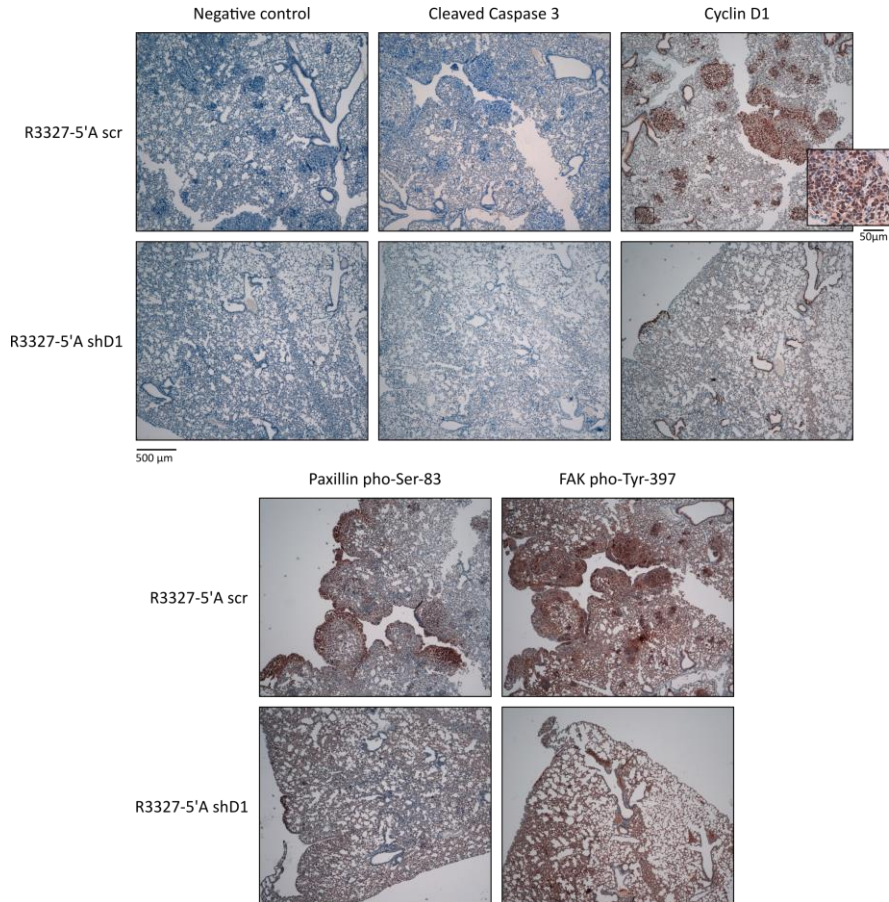
Figure 15. *Paxillin and FAK are activated in R3327-5'A lung metastasis nodules.* R3327-5'A scramble (scr) and R3327-5'A shD1 were injected retro-orbitally into SCID mice. Two weeks later, mice were euthanised, and their lungs were obtained, paraffined, and processed for immunohistochemistry. The antibodies used were: anti-Cyclin D1 (DCS6), anti-pho-Paxillin (Ser-83), anti-pho-FAK (Tyr-397), and anti-Cleaved Caspase 3.

Cyclin D1 staining was detectable in all the tumours, including the ones present in the lungs from mice injected with R3327-5'A shD1. Given that Cyclin D1 downregulation is not absolute in R3327-5'A shD1 cells, it is likely that cells with remaining Cyclin D1 are the ones with the ability to generate metastatic nodules. Moreover, the staining of Cyclin D1 was both nuclear and cytoplasmic.

The staining of Paxillin phosphorylated at Ser-83 appeared to be more intense in one side of the tumour, probably where the invasive front of the tumour was. FAK phosphorylated at Tyr-397 was positive in all the tumours, even though all the lung parenchyma showed some staining. Then, in agreement with previous results, the Paxillin – FAK pathway was activated in the presence of Cyclin D1.

Furthermore, considering the high number of extravasated R3327-5'A shD1 cells, and the small number of tumours they reach to generate, we thought that we could observe some apoptotic cells by performing a Caspase 3-Cleaved immunohistochemistry. Surprisingly, we did not observe any staining. Therefore, it is possible that the cells died previous to lung collection, or could have died through an alternative mechanism.

4. Mechanism of metastasis regulation by Cyclin D1. Dependence on Retinoblastoma 1

One of the main pathways in which Cyclin D1 is involved includes its association with CDK4/6, forming a catalytic complex. Its most recognised function is the inhibition by phosphorylation of the tumour suppressor RB1, which in turn induces cell proliferation and growth (Sherr and Roberts, 1999).

Even though we have previously described the relevance of cytoplasmic Cyclin D1-targets in the metastatic growth (Fusté et al. 2016a), we cannot discard that Cyclin D1 could regulate the DTCs establishment and growth in the lung through RB1. To address this, we generated an R3327-5'A RB1$^{-/-}$ using the CRISPR/Cas9 technique **(see methods) (Figure 16A)**.
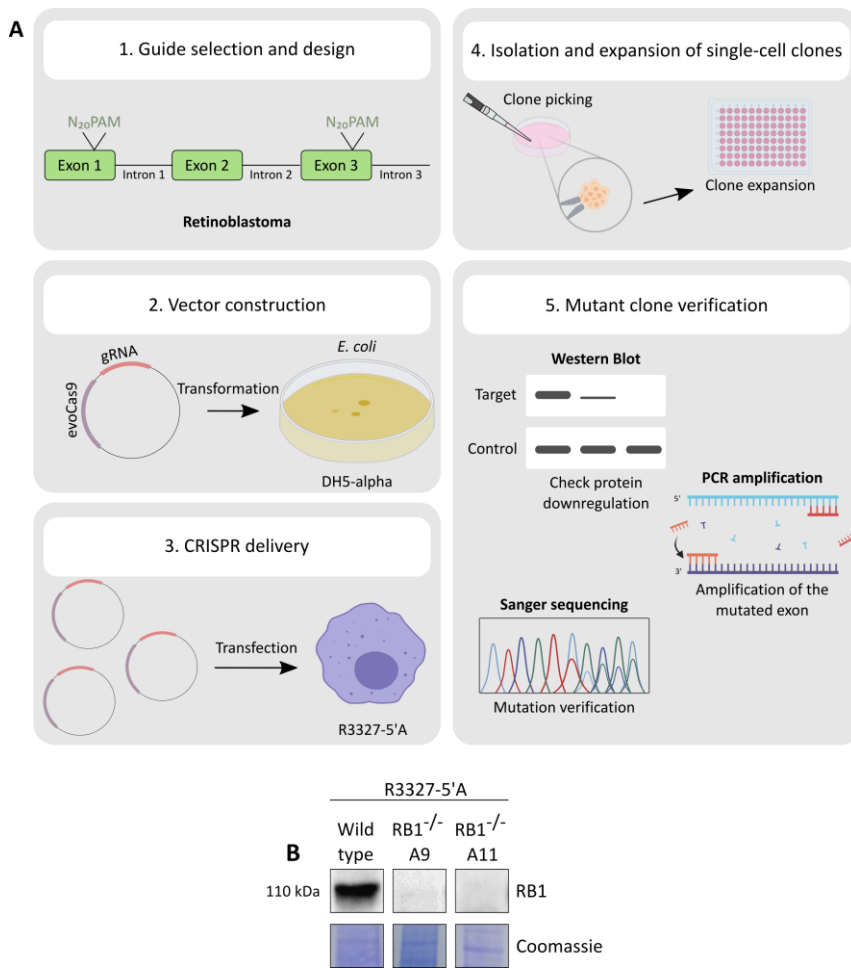
Figure 16. *Obtaining of RB1$^{-/-}$ clones in R3327-5'A cells.* **A)** Representative scheme of the CRISPR/Cas9 technique. Image adapted from Marina Ribes master thesis. **B)** An immunoblot was performed to assess the expression of RB1 in wild-type R3327-5'A cells and R3327-5'A RB1$^{-/-}$ A9 and A11 cells.

We obtained two candidate clones that did not express the RB1 protein: R3327-5'A RB1$^{-/-}$ A9 and R3327-5'A RB1$^{-/-}$ A11 **(Figure 16B)**. We performed further experiments to characterise the behaviour of each clone. Both RB1$^{-/-}$ A9 and A11 clones treated with DMSO (control) showed a slower proliferation tendency than R3327-5'A wild-type clones **(Figure 17A)**, even though it is described that RB1$^{-/-}$ cells usually increase their proliferation rate (He et al. 2016). As R3327-5'A is a highly tumorigenic cell line, these cells may have other alterations which lead to a slower proliferation when RB1 is knocked-out.
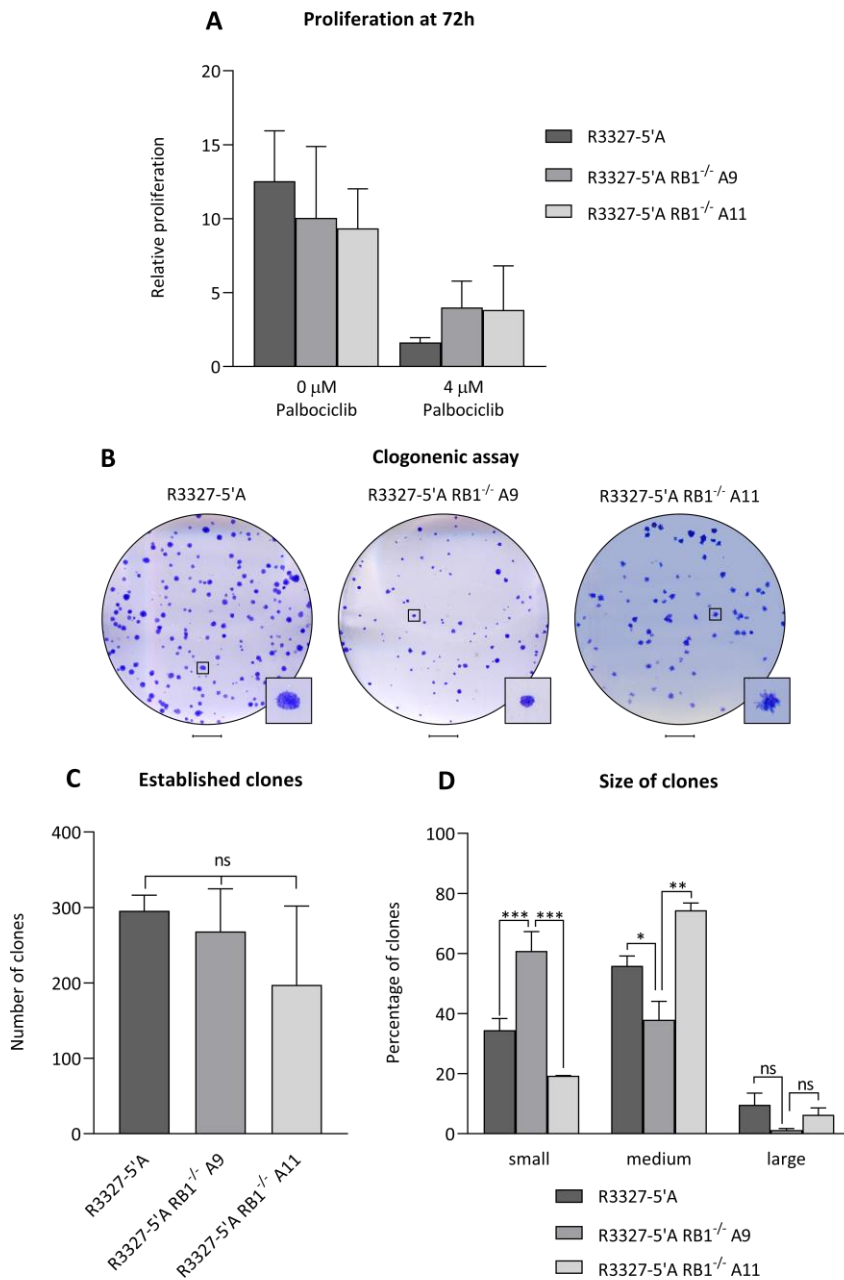
Figure 17. *Characterisation of RB1⁻/⁻ A9 and A11 clones.* **A)** One hundred thousand cells of R3327-5'A, R3327-5'A RB1⁻/⁻ A9, and R3327-5'A RB1⁻/⁻ A11 were seeded in two 35 mm plates with DMEM containing antibiotics and 10% of FBS. One plate of each cell-type was treated with DMSO as control (Palbociclib 0 µM) and 4 µM of Palbociclib was added to the other plate. Cells were kept at 37°C with 5% CO_2. After 72 hours of incubation, the number of cells was

counted. The experiment was independently repeated twice. Relative mean values ± SD are shown. **B)** Five hundred R3327-5'A, R3327-5'A RB1$^{-/-}$ A9, and R3327-5'A RB1$^{-/-}$ A11 cells were cultured in 35 mm plates for one week. Then, they were fixed with PFA 4% and stained with crystal violet 0.05% for 1 hour. Afterwards, images were taken. **C)** The number of clones in B was analysed. Data are expressed as mean ± SEM for R3327-5'A (n=10) and R3327-5'A RB1$^{-/-}$ A9 (n=10), and as mean ± SD for R3327-5'A RB1$^{-/-}$ A11 (n=2). Differences were not statistically significant (ns). **D)** The area of the clones in B was quantified using ImageJ software. Data are expressed as mean ± SEM for R3327-5'A (n=10) and R3327-5'A RB1$^{-/-}$ A9 (n=10), and as mean ± SD for R3327-5'A RB1$^{-/-}$ A11 (n=2). Significance was determined by two-way ANOVA (*p≤0.05) (**p≤0.01) (***p≤0.001).

We have also determined the resistance of RB1$^{-/-}$ clones to Palbociclib, a CDK-inhibitor, which prevents Cyclin D1-CDK4/6 to phosphorylate RB1 and, in consequence, reduces proliferation. R3327-5'A RB1$^{-/-}$ clones should be resistant to the Palbociclib effect, as they do not present RB1 and cannot be phosphorylated. As expected, in the presence of 4 μM Palbociclib, wild-type cells do not proliferate. In contrast, RB1$^{-/-}$ A9 and A11 clones showed a tendency on being resistant to Palbociclib **(Figure 17A)**.

A clonogenic assay was performed to assess the capacity of RB1$^{-/-}$ clones to form colonies. Both A9 and A11 showed a similar number of viable colonies as wild type, indicating that *in vitro,* the ability to establish and start proliferating is not affected when RB1 is deleted **(Figures 17B and 17C)**. As shown in **Figure 17D**, A9 clone formed smaller colonies than A11 and wild type, and A11 tended to have more medium-sized colonies than wild type and A9. Finally, wild-type cells were the ones that could form bigger colonies.

Once the behaviour of clones was analysed, we checked the colonies morphology. As observed in **Figure 17B**, A11 colonies presented a star shape with protrusions and prolongations, similar to the aspect of some invading cells. This fact was decisive to choose the A9 clone as the most feasible one to study the RB1-dependence in *in vivo* metastasis, even though its colonies were the smallest.
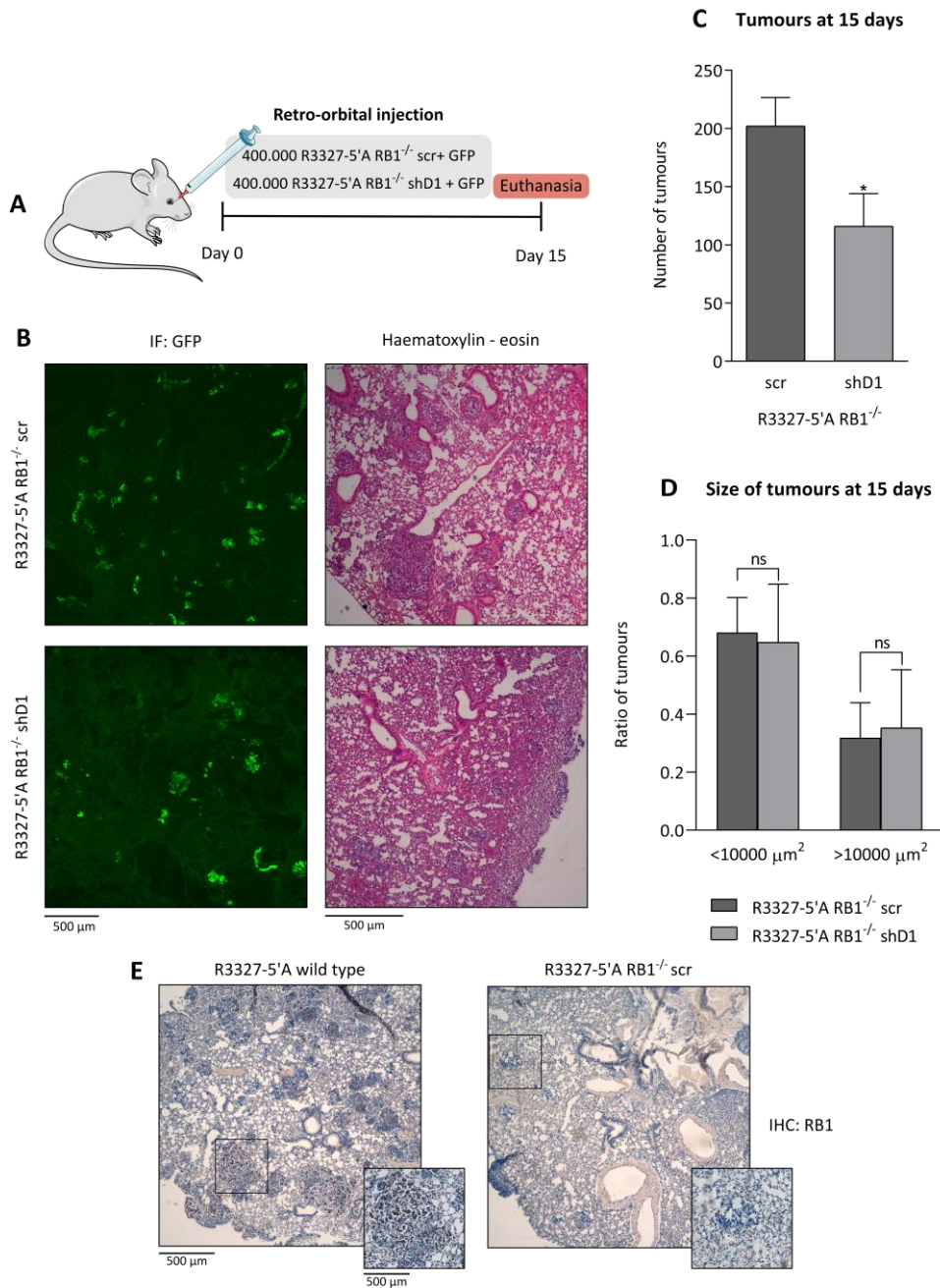
Figure 18. *Cyclin D1 role in DTCs survival and establishment is RB1 independent.* **A)** R3327-5'A RB1$^{-/-}$ A9 cells were infected with scramble shRNA (scr) and GFP or with an anti-Cyclin D1 (shD1) shRNA and GFP. Seventy-two hours later, cells were injected retro-orbitally into SCID mice, which were euthanised after fifteen days. **B)** Two weeks after injection, one lung of each mouse was cryopreserved and processed for immunofluorescence, where the used antibody was anti-GFP for tumorous cells (green) detection. The other lung was paraffined and processed for

haematoxylin-eosin staining. Immunofluorescence images were acquired by confocal microscopy and haematoxylin-eosin images by phase-contrast microscopy. **C)** From immunofluorescence images of eight different R3327-5'A RB1$^{-/-}$ A9 lungs and eight different R3327-5'A RB1$^{-/-}$ A9 shD1 lungs, we counted the green tumours. The number of tumours is relative to 25 mm^2 of the lung area. Data are the mean ± SEM, and statistical significance was determined by Student t-test (*p≤0.05). **D)** From the same images as in C, we counted the area of the green tumours by using the ImageJ software. Data are the mean ± SEM, and statistical significance (n=8) and (n=8) was determined by two-way ANOVA (ns > 0.05). **E)** We performed immunohistochemistry with the anti-RB1 antibody (G3-245) in lung samples from R3327-5'A-injected mice and R3327-5'A RB1$^{-/-}$-injected mice.

To analyse if the ability of R3327-5'A to form metastasis was dependent on RB1, the next step was to inject R3327-5'A RB1$^{-/-}$ A9 cells infected with GFP or R3327-5'A RB1$^{-/-}$ A9 cells infected with shD1 and GFP, retro-orbitally into SCID mice **(Figure 18A)**.

Fifteen days after cell injection, mice were euthanised, and their lungs were obtained. Immunohistochemistry against RB1 was performed to ensure that the injected RB1$^{-/-}$ A9 cells were definitely knocked-out for RB1. As observed in **Figure 18E**, no RB1 was detected in the nodules.

Moreover, we performed immunofluorescence and haematoxylin-eosin staining of the lungs to analyse the number and size of the generated nodules. Both R3327-5'A RB1$^{-/-}$ A9 and R3327-5'A RB1$^{-/-}$ A9 shD1 cells formed similar-sized tumours, indicating that tumour growth is dependent on RB1 **(Figures 18B and 18D)**. Surprisingly, R3327-5'A RB1$^{-/-}$ A9 shD1 cells showed nearly half of tumours than R3327-5'A RB1$^{-/-}$ A9 cells **(Figures 18B and 18C)**, suggesting that Cyclin D1 could have some effects on DTCs survival and establishment which are not dependent on RB1.

CHAPTER 2.

DESCRIBING NEW BIOMARKERS AND TARGETS OF METASTASIS

1. Obtaining tumour interstitial fluid from metastatic lungs

It has been described that the cells release many components into the extracellular space which integrate the secretome (Agrawal et al. 2010). Among the secretome constituents, we find secreted proteins that can be crucial for cell-to-cell communication and signalling. Consequently, it was of our interest to analyse the proteins that malignant cells can be secreting into the interstitial space, as it would allow us to detect possible biomarkers and to describe proteins that interestingly generate a malignant atmosphere through aberrant signalling. In previous work, we have already set up the method for obtaining the TIF by tissue centrifugation **(see methods)** (Matas-Nadal et al. 2020).
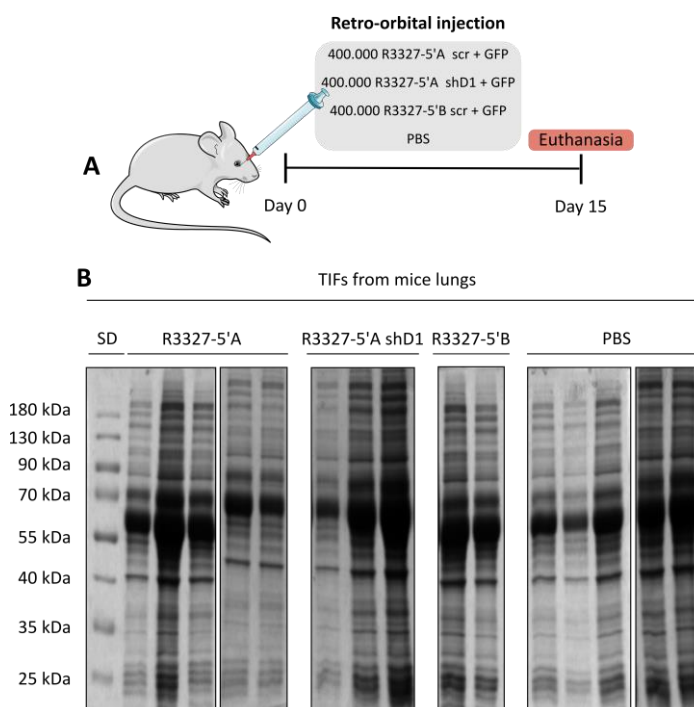
Figure 19. *Obtaining TIF from metastatic lungs.* A) R3327-5'A cells were infected with lentiviruses expressing scramble shRNA (scr) and GFP or with an anti-Cyclin D1 (shD1) shRNA and GFP, and R3327-5'B cells were infected with scramble shRNA (scr) and GFP lentiviruses. Seventy-two hours later, cells or PBS were injected retro-orbitally into SCID mice, and the animals were euthanised fifteen days post-injection. TIFs were collected by lung tissue centrifugation. **B)** The collected TIFs were run in an SDS-PAGE, and gels were stained with Coomassie blue. SD is the molecular weight marker.

To identify some of these proteins, we injected SCID mice retro-orbitally with PBS or R3327-5'A cells, R3327-5'A shD1 cells, or R3327-5'B cells, all of them infected with GFP. Fifteen days post-injection, we obtained the mice lungs and collected their TIF **(Figure 19A)**. We performed electrophoresis with these TIFs samples and stained the gels with a Coomassie blue staining, observing that we had been able to obtain enough protein using the TIF extraction method **(Figure 19B)**.

2. Proteomic analysis of tumour interstitial fluid

In collaboration with the Proteomic Unit from Josep Carreras Leukaemia Research Institute (Drs. de la Torre and Bech), TIF samples were analysed to determine which proteins were present in each condition. Totally, by analysing fifteen samples (five from R3327-5'A, three from R3327-5'A shD1, two from R3327-5'B, and five from PBS) through an LC-MS/MS system, 2818 different proteins were detected.

The principal component analysis (PCA) showed two main clusters **(Figure 20A)**. One cluster was constituted with the samples of lungs injected with R3327-5'A cells (n=5), and the second cluster was composed with the remaining samples: from lungs injected with PBS (n=5), R3327-5'A shD1 (n=3), and R3327-5'B (n=2). As expected, R3327-5'A shD1 and R3327-5'B proteomes were similar to PBS one, because R3327-5'B cells fail to form metastasis, and R3327-5'A shD1 cells generate few and small nodules. In fact, both TIFs from lungs injected with R3327-5'B and R3327-5'A shD1 share 99% of the detected proteins with PBS treatment.

Unfortunately, we only managed to get a short number of samples of R3327-5'B and R3327-5'A shD1, so we based our analysis on the comparison of R3327-5'A (metastasis condition) with PBS (healthy condition) **(Figures 20B and 20C)**. Finally, we obtained a list of candidates with 42 enriched proteins (FC > 2.0; p < 0.05) in the metastasis condition **(Table 8)**, whereas we detected 46 downregulated proteins (FC > 2.0; p < 0.05) in the same condition. In this work, we have focused on the analysis of the enriched candidates as they are likely to be produced or induced by tumour cells.
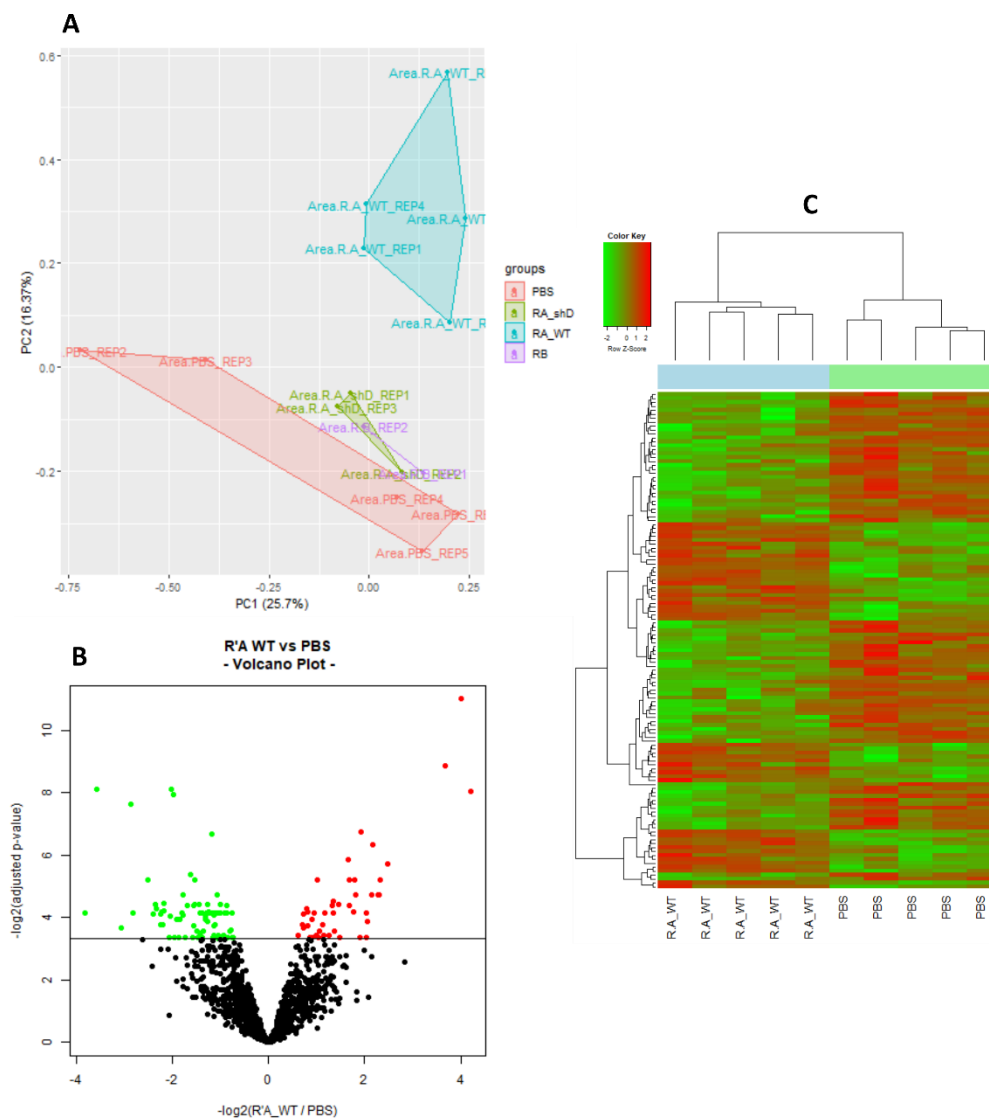
Figure 20. *Proteomic data from TIF samples.* TIFs from lungs of mice injected with R3327-5'A, R3327-5'A shD1, R3327-5'B, or PBS were analysed by proteomic tools. All the analysis was performed in the Proteomic Unit from Josep Carreras Institute. **A)** PCA analysis comparing the four conditions. **B)** Volcano plot and **C)** Heat Map, compare TIFs from mice injected with R3327-5'A and PBS, and show the proteins that are significantly upregulated (red) or downregulated (green) between the two conditions (p<0.05).

Accession	Description	FC
Q60604	Adseverin	>
P31254	Ubiquitin-like modifier-activating enzyme 1 Y	>
Q9Z2Z9	Glutamine--fructose-6-phosphate aminotransferase [isomerizing] 2	>
Q8VHX6	Filamin-C	>
P97310	DNA replication licensing factor MCM2	>
Q08642	Protein-arginine deiminase type-2	>
Q99JT2	Serine/threonine-protein kinase 26	>
P19324	Serpin H1	>
P25206	DNA replication licensing factor MCM3	>
Q61881	DNA replication licensing factor MCM7	>
Q04857	Collagen alpha-1(VI) chain	>
Q62059	Versican core protein	>
P50114	Protein S100-B	>
Q9QZ85	Interferon-inducible GTPase 1	>
Q9EQH2	Endoplasmic reticulum aminopeptidase 1	>
Q80YX1	Tenascin	>
Q05186	Reticulocalbin-1	>
P11157	Ribonucleoside-diphosphate reductase subunit	>
Q60715	Prolyl 4-hydroxylase subunit alpha-1	>
O54962	Barrier-to-autointegration factor	>
Q9CZ15	DNA replication complex GINS protein PSF1	>
P98086	Complement C1q subcomponent subunit A	>
Q8BIL5	Protein Hook homolog 1	>
Q61553	Fascin	18,41
P07091	Protein S100-A4	16,20
Q8VC30	Triokinase/FMN cyclase	12,80
Q64449	C-type mannose receptor 2	5,58
O70475	UDP-glucose 6-dehydrogenase	4,99
Q61362	Chitinase-3-like protein 1	4,92
Q9D2R0	Acetoacetyl-CoA synthetase	4,83
Q91W90	Thioredoxin domain-containing protein 5	4,46

P14106	Complement C1q subcomponent subunit B	4,42
P60843	Eukaryotic initiation factor 4A-I	3,82
P45377	Aldose reductase-related protein 2	3,50
P16045	Galectin-1	3,48
P17918	Proliferating cell nuclear antigen	3,19
P12246	Serum amyloid P-component	3,19
Q9CQ65	S-methyl-5'-thioadenosine phosphorylase	3,15
Q9CWZ3	RNA-binding protein 8A	2,77
P08030	Adenine phosphoribosyltransferase	2,55
Q60972	Histone-binding protein RBBP4	2,49
Q9DBJ1	Phosphoglycerate mutase 1	2,01

Table 8. *List of proteins that are significantly upregulated in R3327-5'A versus PBS condition.* Proteins highlighted in dark grey are the selected candidates. FC is the Fold Change. The > symbol in the third column indicates that these proteins appear only in the R3327-5'A samples. Numbers in the third column indicate the number of times that a protein is upregulated in the R3327-5'A samples versus PBS samples.

Later, we analysed the list of candidates using the STRING database (https://string-db.org), which extracts curated data from the Gene Ontology (GO) database, among others. We observed that the list in **Table 8** was enriched in Actin cytoskeleton proteins (FDR = 0.0014) and extracellular proteins (FDR = 0.026). The enrichment clusters obtained with the ShinyGO database can be observed in **Figure 21**. Our data suggest that the secretion of cytoskeleton proteins could play a role in metastatic colonisation.
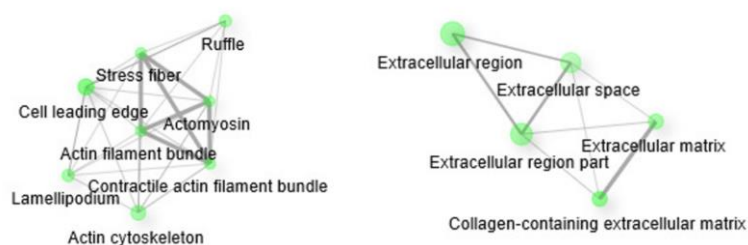
Figure 21. *Clusters representing GO: cellular component analysis of the candidates.* Analysis of the upregulated candidates in metastatic lungs versus PBS, using the ShinyGO database (http://bioinformatics.sdstate.edu/go/).

3. Exosome analysis of tumour interstitial fluid

It has been described that the secretome of a cell is composed of typical and atypical secreted proteins. The typical proteins harbour a signal peptide, whereas the atypicals do not require any known peptide for transit and secretion, such as cytoskeleton proteins (Rabouille, 2017). This feature was also observed in our list of candidates, which was enriched in typical extracellular proteins such as S100B and atypical ones such as the cytoskeleton protein Fascin. Since it is assumed that the secretion of these 'atypical' proteins is mainly produced in vesicles such as exosomes, we were interested in the characterisation of exosome protein patterns in our samples to better characterise the TIF. Therefore, we checked the proteomic composition of exosomes present in the TIFs from metastatic lungs through LC-MS/MS techniques, in collaboration with Drs. de la Torre and Bech from the Proteomic Unit from Josep Carreras Leukaemia Research Institute.

We injected three mice with PBS and three mice with R3327-5'A cells and, after fifteen days, they were euthanised and the TIFs of the lungs obtained. Exosomes were isolated from the TIFs to determine which proteins were secreted in this type of vesicles **(see methods)**. The proteomic analysis detected 1342 proteins in exosomes, from which 1010 had been previously detected in the TIFs proteomic analysis **(Figure 22)**. Unexpectedly, only 35% of the proteins in the TIF were present in exosomes.
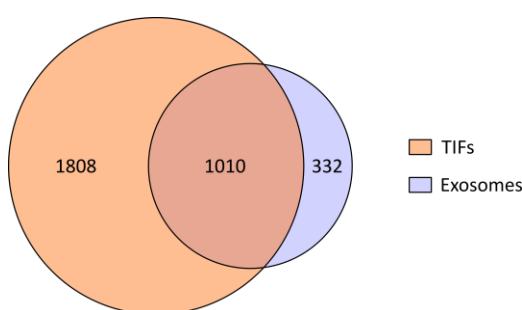
Figure 22. *Comparison between the proteins obtained in TIFs analysis and the exosomes analysis.* TIFs were obtained from mice injected with PBS or R3327-5'A, and the exosomes fraction was isolated. Proteins obtained in the exosomes fraction were compared to all the proteins obtained in the previous TIFs analysis. Venn diagrams were performed in the DeepVenn application (https://deepvenn.com).

Among these, only ten proteins **(Table 9)** from our list of enriched candidates **(Table 8)** were present in the R3327-5'A exosome fraction, for instance, Fascin. This fact could be explained by the difficulties to obtain exosomes in reliable conditions. However, most of our cytoskeleton candidates are cited in the exocarta (http://www.exocarta.org/), as they have been detected in exosomes from different experiments.

Accession	Description
P19324	Serpin H1
Q04857	Collagen alpha-1(VI) chain
Q62059	Versican core protein
Q80YX1	Tenascin
P98086	Complement C1q subcomponent subunit A
Q61553	Fascin
P07091	Protein S100-A4
P14106	Complement C1q subcomponent subunit B
P60843	Eukaryotic initiation factor 4A-I
P16045	Galectin-1

Table 9. *List of candidates that appear in the R3327-5'A exosomes fraction and that are upregulated significantly in TIFs of R3327-5'A versus PBS samples.*

4. Selection of candidates for functional analysis

Among the most enriched proteins from our list of candidates, we have selected a reduced number of proteins to initiate the functional analysis. We focused our search on cytoskeleton proteins like Adseverin, Fascin, and S100B. Both Adseverin and Fascin act as regulators of the Actin cytoskeleton and, together with S100B, participate in the microfilament reorganization. Through the control of the cytoskeleton, these proteins regulate cellular processes such as cell migration (Hashimoto et al. 2007; Jiang et al. 2011; Li et al. 2015).

By interacting with other molecules like Receptor for Advanced Glycation Endproducts (RAGEs), S100B can modify some signalling pathways which regulate cancer establishment (Donato et al. 2009). We have also selected the protein PADI2 because this protein is an

arginine deiminase that controls cellular migration through protein modification (Horibata et al. 2017).

First, to corroborate the proteomic analysis, we used the TIFs from PBS and R3327-5'A-injected mice to check whether we could detect the selected proteins (Adseverin, PADI2, Fascin, and S100B) using specific antibodies by immunoblot. The protein profile of TIFs is shown in **Figure 23A**.

Both Adseverin and Fascin were significantly increased in the R3327-5'A condition versus the PBS one **(Figure 23C)**. As expected, due to the proteomic results, Adseverin was almost indetectable in the PBS condition, while Fascin was undoubtedly upregulated in R3327-5'A. Higher levels of PADI2 were detected in R3327-5'A in comparison to PBS, although it did not appear in the TIF proteomic profile of PBS **(Figure 23B)**. In addition, even though the S100B protein appeared in the proteomics of R3327-5'A, we could not detect it by immunoblot.

Moreover, we used Vinculin as a control since it appears in the extracellular space, which enables its use as a secretion marker (Kawakami et al. 2015). Thus, its presence in the TIFs indicated that we could properly detect secreted proteins. We also checked Cyclin D1 as a marker of non-secretion. The fact that we cannot detect this protein in the TIFs (only in one of the PBS samples) implies that TIFs are not contaminated by intracellular proteins, and, consequently, the TIF collection was performed correctly **(Figure 23B)**.

Secondly, we analysed by immunohistochemistry the expression of Adseverin, PADI2, Fascin, and S100B in the lung tissue of mice injected with PBS or R3327-5'A cells. The four proteins were detected in the metastatic nodules, although S100B staining was very low. Adseverin and Fascin appeared to be both nuclear and cytoplasmic in the tumorous cells, and PADI2 and S100B seem to be present in the nucleus. Interestingly, PADI2 tended to be more localised in the periphery of nodules. This region may be recognised as the invasive front of the tumour, so PADI2 could be a marker of aggressiveness **(Figure 24)**. The four candidates were detected in the metastatic nodules, and no signal was observed in normal lung and stroma. This result suggested that our candidates could be directly secreted by R3327-5'A cells.
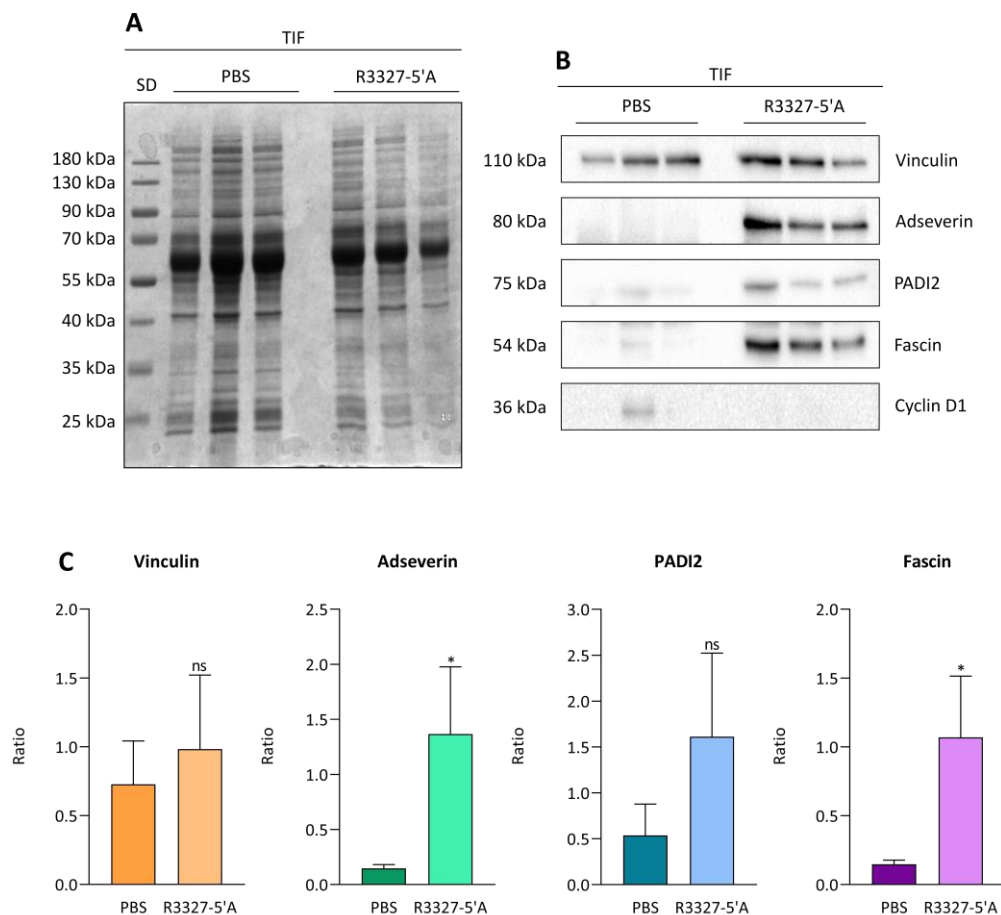
Figure 23. *Adseverin, PADI2, and Fascin are enriched in R3327-5'A TIFs.* A) Three SCID mice were injected retro-orbitally with PBS, and three other mice were injected with R3327-5'A cells. Fifteen days post-injection, mice were euthanised, and TIFs from their lungs were extracted. We performed electrophoresis using the TIFs samples, and then the gel was stained with Coomassie blue. SD is the molecular weight marker. **B)** In the TIFs samples, the expression of Vinculin, Adseverin, PADI2, Fascin, and Cyclin D1 was assessed by immunoblot. **C)** The levels of protein were determined by densitometry with the Image Lab 4.0.1 software from BioRad. Data are expressed as mean ± SEM (n=3), and statistical significance was determined by a Student t-test (*p≤0.05) (ns>0.05).
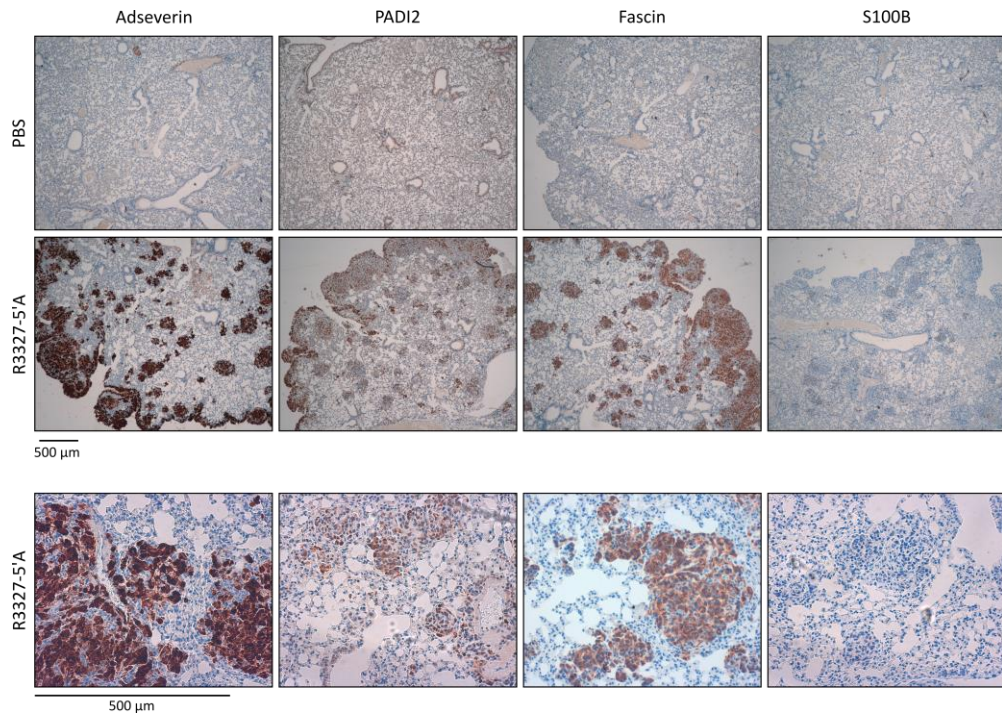
Figure 24. *Adseverin, Fascin, PADI2, and S100B are detectable in metastatic lung nodules.* Three SCID mice were injected retro-orbitally with PBS, and three other mice were injected with R3327-5'A cells. Fifteen days post-injection, mice were euthanised, and one lung of each mouse was paraffined and processed for immunohistochemistry. The antibodies against Adseverin, Fascin, PADI2, and S100B were used. The images were obtained by phase-contrast microscopy.

5. Collection and analysis of R3327-5'A cells secretome

From the previous result, we were interested in elucidating if our four candidates could be secreted directly by the tumorous R3327-5'A cells or by the lung stroma cells. To address this question, we obtained a conditioned medium from cultured tumour cells. Conditioned medium is attained by collecting and filtering the medium of a plate containing confluent cells, assuming that all the proteins that the cells release are present in the medium **(see methods)**. Once the media is collected, cells are also harvested for their posterior analysis.

To perform this experiment, we obtained secretomes from R3327-5'A and R3327-5'B cells. We used R3327-5'B cells because, even though they have the same origin as R3327-5'A, they are non-invasive and should show different secretome characteristics.

We checked the amount of protein we could collect from each secretome and its respective whole-cell extract. As observed in **Figure 25A**, the quantity of protein was similar in both secretomes and inputs. R3327-5'A and R3327-5'B secretomes showed a different protein profile, suggesting that the proteins released by these cells to the extracellular space may be distinct.

To check the quality of the collected secretomes, we performed various immunoblots. Vinculin and Clusterin were analysed as markers of secretion, as the two of them have been previously found secreted (Kawakami et al. 2015; Chen et al. 2021). As shown in **Figure 25B**, both proteins appear in the secretomes of R3327-5'A and R3327-5'B cells, indicating that we could detect secreted proteins and that the collection of the secretome was correctly done.

Furthermore, we analysed the presence of Paxillin, Glyceraldehyde 3-Phosphate Dehydrogenase (GAPDH), and Cyclin D1, well-established intracellular proteins (Fusté et al. 2016a; Sherr and Roberts, 2004; Eguchi et al. 2020). As expected, they uniquely appeared in the whole-cell extract, suggesting that the obtained secretome was free from cell lysis **(Figure 25B)**.

Finally, to confirm the differential phenotype of the R3327 cells, we checked the epithelial marker E-Cadherin. This was only found in the whole-cell extract of R3327-5'B **(Figure 25B)**, and it appeared in two bands, possibly due to the fact that the antibody could detect the pro-region of this protein before being cleaved.

Once we had the quality of secretomes checked, we wanted to analyse whether the candidate proteins obtained from the TIFs analysis (Adseverin, Fascin, PADI2, and S100B) could also be detected on the secretomes obtained *in vitro*. We were interested in this information since we wanted to know if these proteins were exclusively secreted by R3327-5 cells or if their secretion was influenced by the lung parenchyma in the *in vivo* model.
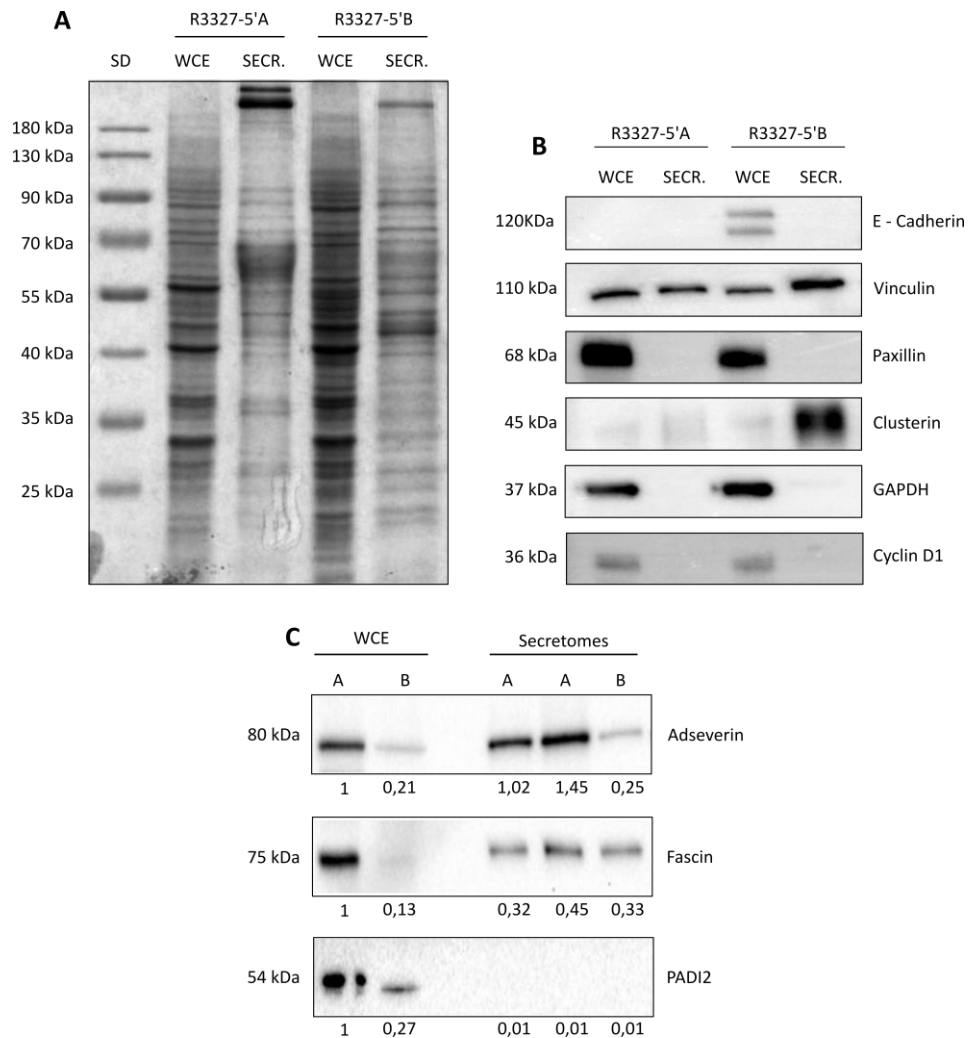
Figure 25. *Adseverin and Fascin are secreted from R3327 cells.* **A)** Secretomes of R3327-5'A cells and R3327-5'B cells and their respective whole-cell extracts were collected after 72 hours of seeding in 100 mm plates. Twenty-four hours before collection, three washes with PBS were performed to remove all the serum, and DMEM containing antibiotics without FBS was added. Samples were run in an SDS-PAGE, and the gel was stained with Coomassie blue. SD is the molecular weight marker. **B)** The presence of E-Cadherin, Vinculin, Paxillin, Clusterin, GAPDH, and Cyclin D1 in the secretomes was determined by immunoblot using specific antibodies. **C)** The presence of Adseverin, PADI2, and Fascin in the secretomes of R3327 cells was analysed by immunoblot using specific antibodies. The quantity of expressed protein was calculated by densitometry through the Image Lab 4.0.1 software from BioRad and is defined below each sample. "A" and "B" mean R3327-5'A and R3327-5'B cells, respectively.

We observed that Adseverin was five times more expressed in the whole-cell extract and in the secretome of R3327-5'A cells than in the R3327-5'B cells samples. PADI2 appeared only in the whole-cell extract, and it was almost four times more expressed in R3327-5'A cells than in R3327-5'B cells. Fascin was present in the secretomes of R3327-5'A and R3327-5'B cells in a similar way, whilst it was mainly expressed in R3327-5'A cells whole-cell extract. In this case, R3327-5'B cells may secrete all the generated Fascin, though we still do not know the importance of this process **(Figure 25C)**. Again, S100B could not be detected by immunoblot neither in the whole-cell extract nor in the secretomes of R3327-5'A and R3327-5'B cells.

First, from this result we can conclude that Adseverin and Fascin can be secreted by tumorous R3327-5'A cells. The fact that we cannot detect PADI2 in the secretomes, even though it was previously detected in the TIFs, could be explained because tumorous cells secretion could be influenced by parenchymal cells when they are growing in the lung. Second, we have observed that Adseverin, Fascin, and PADI2 are overexpressed in R3327-5'A cells compared to R3327-5'B cells. This result is consistent with the fact that these proteins have been related to tumour aggressiveness in cancer models (Liu et al. 2016; Tan et al. 2013; Wang et al. 2017).

6. Study of the relevance of Adseverin in metastatic colonisation

The differential expression of Adseverin in the whole-cell extract and secretomes of R3327-5'A and R33257-5'B cells, and its relation with cancer aggressiveness, makes this protein prone to be involved in metastatic colonisation. Thus, we decided to determine its relevance in our model. We have downregulated Adseverin expression in R3327-5'A cells (shAdseverin) by using interference of RNA **(Figure 26A)**. This downregulation caused a morphological change in R3327-5'A cells, as they become larger and more spread into the plate **(Figure 26B)**.

To check the behaviour of R3327-5'A cells in the absence of Adseverin, we performed clonogenic and proliferation assays. The clonogenic assay **(Figure 27A)** showed that cells with Adseverin downregulated, significantly formed fewer and smaller colonies than the R3327-5'A control cells **(Figures 27B and 27C).** Moreover, cells with Adseverin downregulated

tended to proliferate slower than the wild-type cells **(Figure 27D)**. Then, we concluded that Adseverin was involved in the regulation of R3327-5'A cells growth.
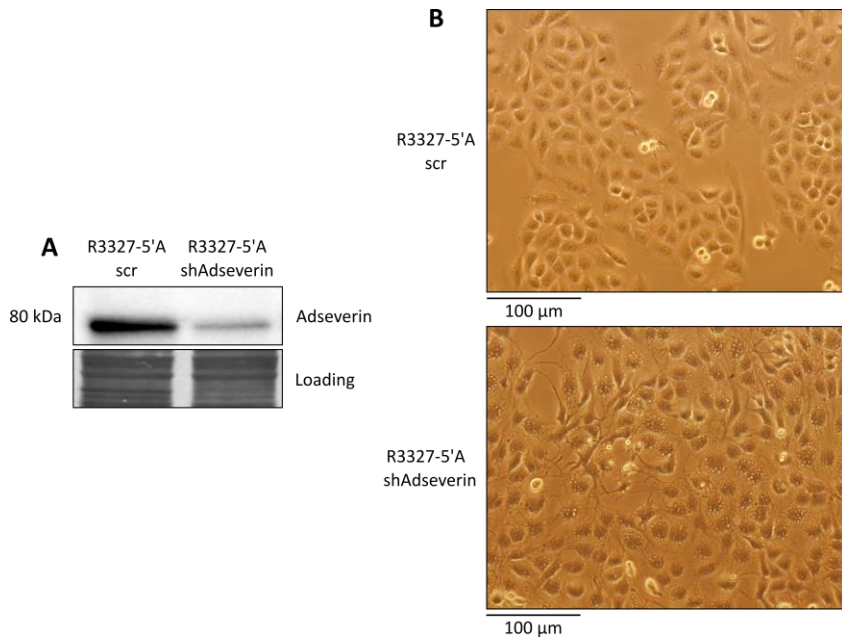
Figure 26. *Adseverin downregulation in vitro.* **A)** R3327-5'A were infected with scramble shRNA (scr) or with an anti-Adseverin shRNA (shAdseverin), and the cells were cultured with DMEM with antibiotics and 10% FBS at 37ºC and 5% CO_2. Cells were collected 72 hours after seeding, and an immunoblot anti-Adseverin was performed. Coomassie blue staining of the membrane was used as a loading control. **B)** A representative image of control (scr) R3327-5'A cells and Adseverin downregulated (shAdseverin) R3327-5'A cells 72 hours after seeding.

Figure 27. *Characterisation of the Adseverin downregulation effect in R3327-5'A cell growth.* **A)** R3327-5'A cells were infected with scramble shRNA (scr) or with an anti-Adseverin shRNA (shAdseverin). Seventy-two hours later, 500 cells of each condition were cultured in 35 mm plates. One week later, cells were fixed with PFA 4% and stained with crystal violet 0.05% for 1 hour. **B)** The number of clones in A were counted (n=3). Data are expressed as mean ± SEM, and statistical significance was determined by a Student t-test (*p≤0.05). **C)** The area of the clones in A (n=3) was measured using the ImageJ software. Data are expressed as mean ± SEM, significance was determined by a two-way ANOVA (***p≤0.001) (ns>0.05). **D)** R3327-5'A cells were infected with scramble shRNA (scr) or with an anti-Adseverin shRNA (shAdseverin). Seventy-two hours later, 100.000 cells of each condition were cultured in four 35 mm plates. Cells were counted at 24 hours, 48 hours, and 72 hours. The experiment was independently repeated twice. Data are expressed as mean ± SD.

A **Clonogenic assay**

R3327-5'A
scr

R3327-5'A
shAdseverin

B **Established clones**

C **Size of clones**

■ R3327-5'A scr
□ R3327-5'A shAdseverin

D **Cell proliferation**

Time (h)

●— R3327-5'A scr   ●— R3327-5'A shAdseverin
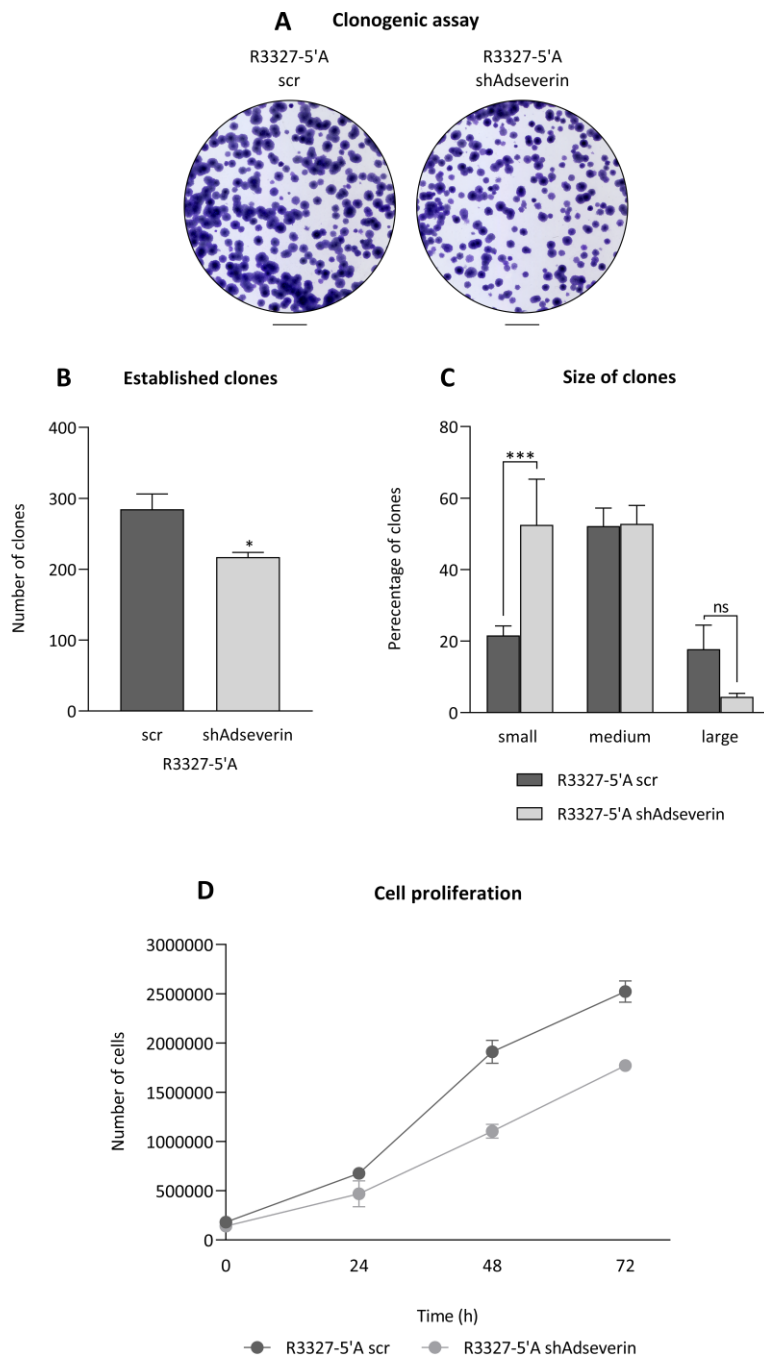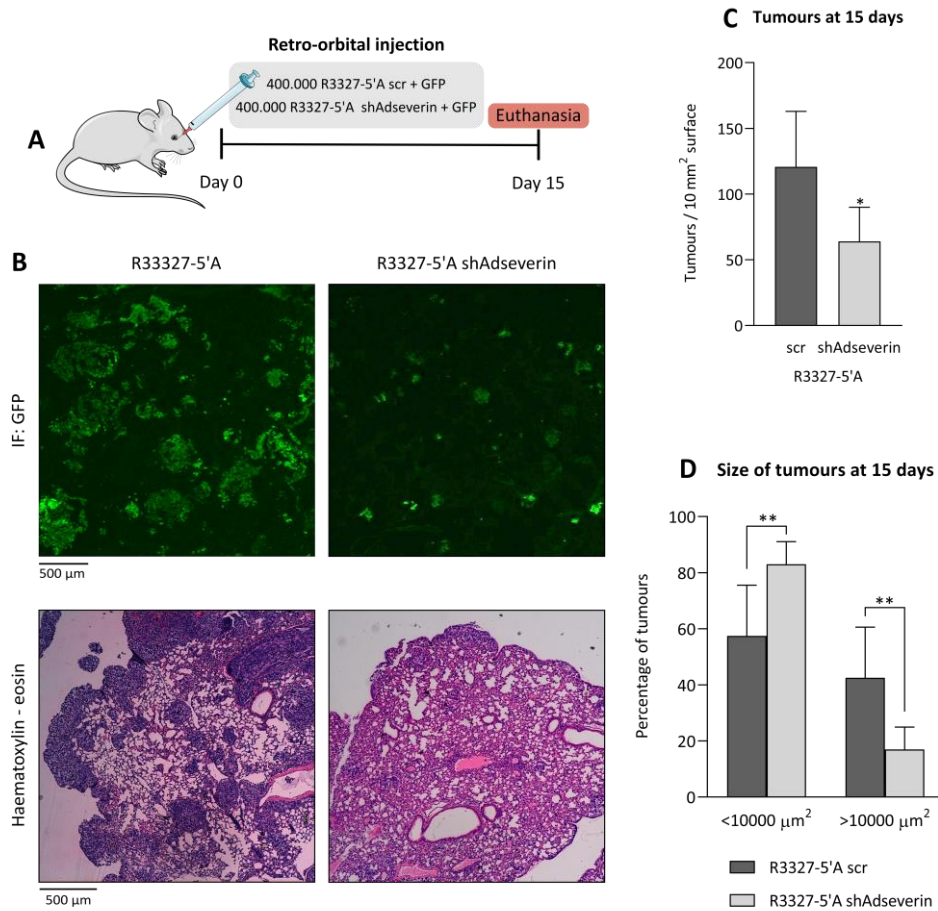
Figure 28. *Cells with Adseverin downregulated formed lesser and smaller tumours in vivo than wild-type cells.* **A)** R3327-5'A cells were infected with scramble shRNA and GFP or with an anti-Adseverin shRNA (shAdseverin) and GFP. Seventy-two hours later, cells were injected retro-orbitally into SCID mice, and the animals were euthanised fifteen days post-injection. **B)** Two weeks after injection, one lung of each mouse was cryopreserved and processed for immunofluorescence, and the other lung was paraffined and processed for haematoxylin-eosin staining. Above, there is an immunofluorescence anti-GFP for tumour (green) detection. Below, there is a haematoxylin-eosin staining, where tumours are stained in dark purple. Immunofluorescence images were acquired by confocal microscopy and haematoxylin-eosin images with phase-contrast microscopy. **C)** From immunofluorescences of seven different scramble shRNA (scr) R3327-5'A lungs and seven different R3327-5'A shAdseverin lungs, we counted the green tumours. The number of tumours is relative to 10 mm^2 of lung tissue. Data are the mean ± SEM, and statistical significance (n=7) was determined by Student t-test (*p≤0.05). **D)** From the same images in C, we measured the area of the green tumours by using the ImageJ software. Data are the mean ± SEM, and statistical significance (n=7) was determined by two-way ANOVA (**p≤0.01).

Once we characterised the Adseverin downregulation in cells, we wanted to explore how these cells behaved in the *in vivo* model. So, we injected 400.000 R3327-5'A cells and 400.000 R3327-5'A shAdseverin cells in SCID mice. Fifteen days later, mice were euthanised and their lungs were obtained **(Figure 28A)**.

We observed that Adseverin-downregulated cells could generate significantly fewer tumours than R3327-5'A wild-type cells **(Figures 28B and 28C)**. Moreover, the formed tumours were much smaller than the ones generated by wild-type cells **(Figures 28B and 28D)**. Thus, these results suggest that Adseverin may be involved in the establishment and growth of metastatic nodules. Certainly, the correlation of Adseverin expression with tumour aggressiveness had already been documented (Lin et al. 2019; Liu et al. 2016). However, the relevance of this protein in metastatic colonisation had never been established before. This result validated our proteomic approach to discover new targets involved in metastasis.

CHAPTER 3.

β-GLUCAN SIGNALLING ON CELL CYCLE.

CYCLIN D1 AND RETINOBLASTOMA 1 DEPENDENCE

1. β-Glucan induces a temporary proliferation arrest in human dermal fibroblasts

β-Glucans are carbohydrate polymers which are present in cereals like barley and in the cell walls from yeast, fungi, and bacteria. Their composition is based on the linkage of glucose monomers through glycosidic bonds. β-Glucans have been associated to distinct biological functions. For instance, barley β-Glucan can induce cytokine production (Noss et al. 2013) and can affect the viability of tumorous cells (Choromanska et al. 2018).

In addition, some clinical trials have shown that topically-applied yeast β-Glucans enhance wound healing in diabetic ulcers (Medeiros et al. 2012; Zykova et al. 2014). It stimulates immune and non-immune cells, like HDFs, by promoting its proliferation and migration (Woo et al. 2010a) and consequently, favouring wound repair. However, there is a lack of information about the effects of this compound on cell cycle and proliferation. Hence, in collaboration with Drs. Moralejo and Guillen (ETSEA – Lleida) who produce barley β-Glucan (1→3),(1→4), we took an interest in a possible role of this polymer in the regulation of cell cycle and Cyclin D1 activity.

To address this issue, first we wanted to test if barley β-Glucan could alter HDF proliferation. We cultured HDF cells with different concentrations of β-Glucan and measured the number of cells at 24 hours, 48 hours, and 72 hours. Surprisingly, the treatment with 400 µg/mL of β-Glucan decreased the number of cells at 24 hours, although this effect was mitigated at 48 hours **(Figures 29A and 29B)**. We also checked cells viability through trypan blue incorporation, but there was no significant difference in the quantity of dead cells (less than 1%) between conditions **(Figure 29B)**. These results suggest the existence of a β-Glucan-dependent transient and short arrest in cell proliferation.

In order to confirm this proliferation arrest, we performed a BrdU incorporation analysis in which we cultured HDF in absence (control) or presence of 400 µg/mL of β-Glucan (treatment). Eight hours before processing the samples, we added 10 µM of BrdU into the media. We analysed the BrdU nuclear incorporation at 24 hours and 48 hours after β-Glucan treatment. As seen in **Figure 29C**, BrdU incorporation at 24 hours was reduced in cells treated

with β-Glucan in comparison to control cells, even though BrdU levels were clearly recovered after 48 hours **(Figure 29D)**. To ensure that the proliferation arrest was caused exclusively by β-Glucan, we performed a similar experiment using other different polymers such as methylcellulose and amylopectin at 400 µg/mL of concentration. These polymers did not decrease significantly the BrdU incorporation at 24 hours of incubation, suggesting that the short proliferation arrest that β-Glucan induces to HDF cells is specific **(Figure 29E)**.

Figure 29. ***Barley β-Glucan induces a transient and short proliferation arrest in HDF cells***. **A)** Ten thousand HDF cells were incubated with 0 µg/mL, 100 µg/mL, 200 µg/mL, or 400 µg/mL of barley β-Glucan, and the number of cells was measured at 24 hours, 48 hours, and 72 hours after β-Glucan addition. Data of three experiments was expressed as the mean ± SEM. Significance was determined by one-way ANOVA (*p<0.05) (**p<0.01). **B)** Three thousand cells were cultured with DMEM containing antibiotics and 10% FBS for 48 hours. After this time, cells were treated in absence (control) or presence of 400 µg/mL of β-Glucan and trypan blue negative cells (viable cells) were quantified at 0 hours, 24 hours, and 48 hours. Data of three experiments was expressed as mean ± SEM. Significance was determined by one-way ANOVA (**p<0.01) (ns>0.05). **C)** HDF cells were treated with nothing (control) or with 400 µg/mL of β-Glucan and cells were fixed and analysed by immunofluorescence anti-BrdU at 24 hours and 48 hours after β-Glucan treatment. Eight hours before the imaging, 10 µM BrdU was added into the medium. A representative BrdU-staining image is shown. **D)** From the data shown in C, green cells (BrdU-positive) and blue nuclei (Hoechst) were quantified with ImageJ. The percentage of BrdU-staining was quantified by counting BrdU-positive cells versus total nuclei. Data of three experiments was expressed as mean ± SEM. Significance was determined by one-way ANOVA (**p<0.01). **E)** HDF cells were treated in absence (control) or presence of 400 µg/mL of β-Glucan, methylcellulose, or amylopectin. Then, cells were fixed and analysed by immunofluorescence anti-BrdU at 24 hours after compounds incorporation. Eight hours before the imaging, 10 µM BrdU was added into the medium. Data from four independent experiments was expressed as mean ± SEM. Significance was determined by one-way ANOVA (*p<0.05).

A Cells proliferation

B Cells viability

C BrdU / Hoechst / β-Glucan / 0 µg/mL / 400 µg/mL / 24h

D BrdU incorporation

E BrdU incorporation
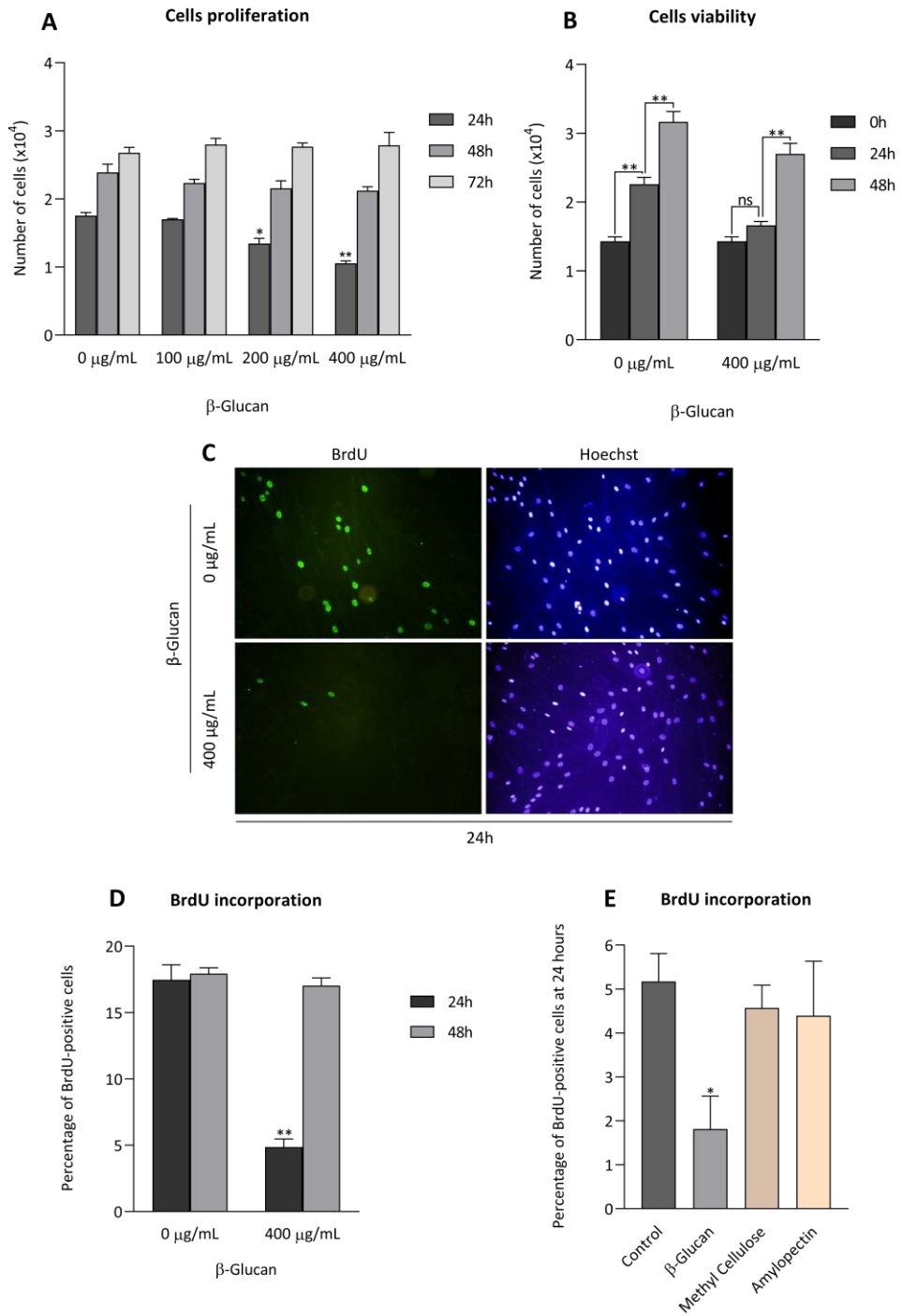
2. β-Glucan regulates cell cycle through Retinoblastoma 1-dependent and Cyclin D1-independent mechanisms

It is well established that Cyclin D1 and CDK4 are key regulators of the cell cycle entry. Cyclin D1 and CDK4 form a complex that phosphorylates and inactivates RB1, releasing the E2F factor and promoting the cell cycle entry and proliferation (Kato et al. 1993). Previous results showed that β-Glucan induced a short proliferation arrest and hence we sought to analyse the importance of β-Glucan in cell cycle entry.

First, we decided to analyse by immunoblot the expression of Cyclin D1 and CDK4 in β-Glucan treated HDF cells. Unexpectedly, these proteins were not downregulated neither at 12 hours nor at 24 hours after the addition of β-Glucan treatment **(Figure 30A)**. We also checked the levels of total and phosphorylated RB1 at Ser-780 (a phosphorylation site of Cyclin D1-CDK4 complex) at 24 hours after the incubation with β-Glucan, but they were not downregulated **(Figure 30B)**. Thus, these results suggested that Cyclin D1-CDK4 complex remained active in the presence of β-Glucan. Therefore, the β-Glucan could be participating in other steps of the cell cycle downstream of RB1.

Consequently, to investigate whether β-Glucan-dependent proliferation arrest was controlled by RB1, we downregulated RB1 (shRB1) expression in HDF cells **(Figure 30C)**. Then, we treated HDF shRB1 cells and HDF cells infected with scramble shRNA (control) with 400 μg/mL of β-Glucan during 24 hours, and performed a BrdU incorporation assay. Again, treated wild-type cells exhibited the proliferation arrest but, surprisingly, RB1 downregulated cells showed a similar ratio of BrdU incorporation than untreated cells **(Figure 30D)**, indicating that the temporary arrest caused by barley β-Glucan in HDF cells is dependent on RB1.

Despite these results, it has been previously described that under stress conditions, the phosphorylation of RB1 at Ser-249 and Thr-252 by p38 prevents the dissociation of RB1-E2F complex even if RB1 has been phosphorylated by CDK4 (Gubern et al. 2016). To determine whether the phosphorylation of p38 (active p38) in Thr-180 and Tyr-182 is involved in the transitory proliferation arrest, we performed an immunoblot against total and phosphorylated p38, using non-treated HDF cells as negative controls, HDF cells treated with

barley β-Glucan for 20 minutes, and HDF treated with NaCl for 20 minutes as a positive control of induced stress (Gubern et al. 2016).

As expected, we observed a rapid phosphorylation in p38 when it was induced by NaCl **(Figure 31A)**, even though we could not detect p38 phosphorylation after barley β-Glucan treatment **(Figures 31A and 31B)**. We performed a time course to check if the p38 phosphorylation occurred later in time after β-Glucan treatment, but we could not detect p38 phosphorylation at any time **(Figure 31B)**. Then, effects of β-Glucan on cell cycle may be on RB1 activity independently of p38.
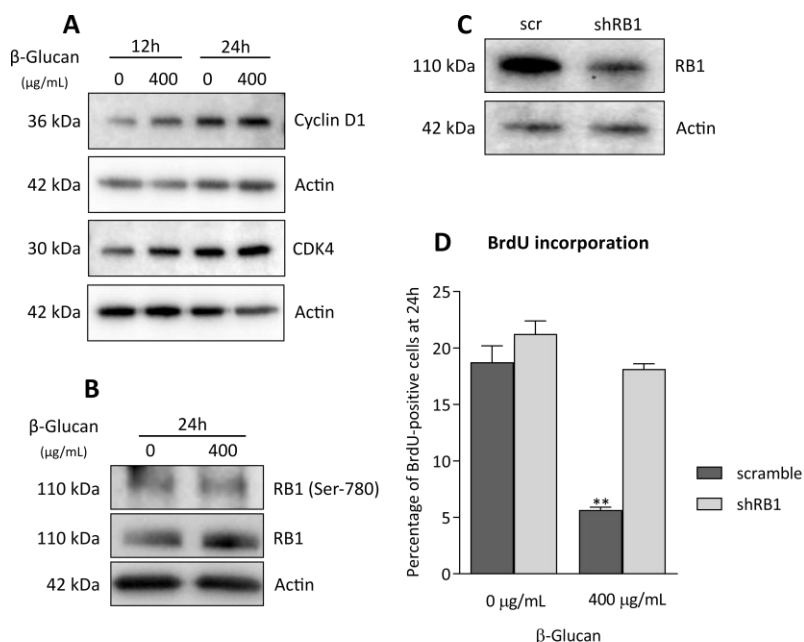
Figure 30. *The proliferation arrest induced by barley β-Glucan is dependent on RB1.* A) HDF cells were treated with anything (control) or with 400 μg/mL of barley β-Glucan for 12 hours and 24 hours, and total expression of Cyclin D1 and CDK4 was determined by immunoblot. Actin was used as a loading control. **B)** We used the same cells in A to analyse by immunoblot the expression levels of total and phosphorylated RB1 Ser-780 at 24 hours after β-Glucan addition. Actin was used as a loading control. **C)** HDF cells were infected with a scramble shRNA (scr) or an anti-RB1 shRNA (shRB1) and 72 hours later, an immunoblot was performed to analyse the RB1 levels. Actin was used as a loading control. **D)** The HDF from C were seeded and treated with 400 μg/mL of β-Glucan. Non-treated cells were used as a control. Twenty-four hours after the seeding, the BrdU incorporation assay was performed. The percentage of BrdU-positive cells was quantified by counting the BrdU-positive cells versus total nuclei with ImageJ. Data from three experiments are expressed as mean ± SEM. Significance was determined by one way ANOVA (**$p<0.01$).
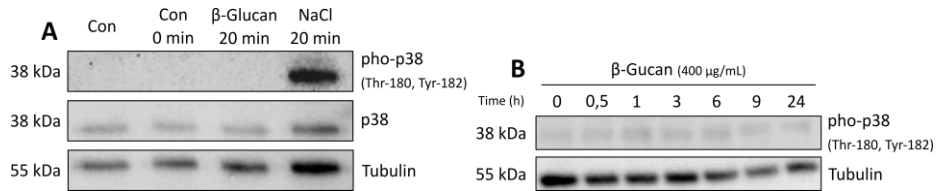
Figure 31. *The proliferation arrest induced by barley β-Glucan is not dependent on p38.* **A)** HDF cells were seeded for 48 hours under normal conditions (control). These cells were treated (con 0 min) with 400 µg/mL of β-Glucan or 500 mM of NaCl for 20 minutes. Then, an immunoblot anti-pho-p38 (Thr-180, Tyr-182), anti-p38, and anti-Tubulin was performed. Tubulin was used as a loading control. **B)** HDF were treated with β-Glucan for different times, and an immunoblot anti-pho-p38 (Thr-180, Tyr-182) was performed. Tubulin was used as a loading control.

3. β-Glucan regulates migration of human dermal fibroblasts

Being β-Glucan an inductor of a transitory proliferation arrest in HDF cells, we considered the possibility that, during this time, β-Glucan could be inducing other biological effects on these cells, such as migration.

To analyse this, we determined the migration of HDF cells in the presence and absence of β-Glucan by using Transwell assays **(see methods)**. We seeded HDF cells at the bottom of a Transwell membrane in the presence of medium without serum and either with or without 400 µg/mL of β-Glucan. On the other side of the filter, we placed medium with serum to attract the cells. Twenty-four hours after incubation, the cells were stained with Hoechst and we counted the cells that crossed the membrane from the lower to the upper side **(Figure 32A)**.

We observed that barley β-Glucan induced fibroblasts migration **(Figure 32B)**. Hence, during the first 24 hours after the treatment with β-Glucan, fibroblasts suffer a proliferation arrest and enhance their migration capacity at the same time.
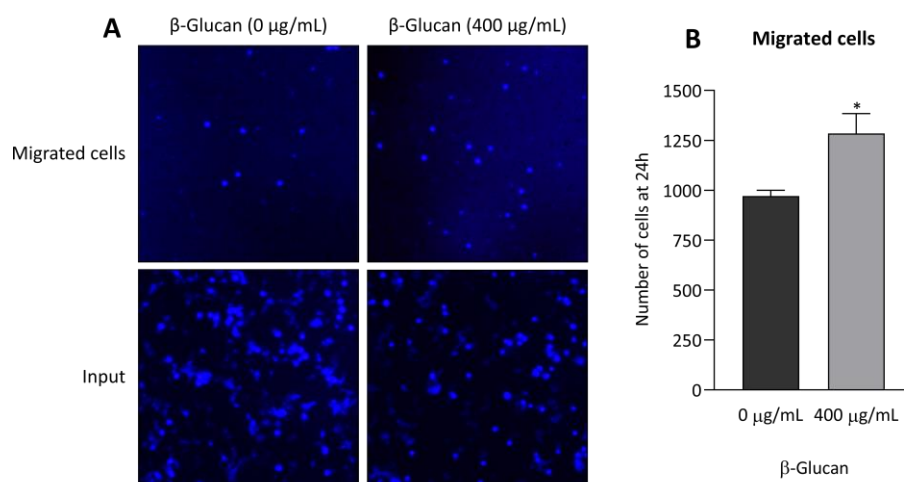
Figure 32. *Barley β-Glucan induces migration of HDF cells.* **A)** Representative image of a migration assay. HDF cells were seeded in Transwell filters in presence (400 µg/mL) or absence (0 µg/mL) of β-Glucan. Twenty-four hours later, migrated cells were fixed, stained with Hoechst, and quantified. A cotton applicator was used to remove the non-migrated cells. **B)** Quantification of migrated cells in A. Data from four experiments are expressed as mean ± SEM, and statistical significance was determined by Student t-test (*p<0.05).

4. β-Glucan improves wound closure *in vivo*

According to our results, barley β-Glucan promotes fibroblasts migration versus proliferation in primitive stages of treatment. Considering that one of the early responses in the wound healing process is fibroblasts migration to the wound, we suspected that barley β-Glucan could enhance *in vivo* wound closure.

To analyse this possibility, we performed a wound healing test using C57BL/6 mice. Under general anaesthesia and clean conditions, we did two full-thickness dorsal wounds on each mouse. Half of the mice were topically treated with water (control group), and the other half was topically treated with barley β-Glucan diluted in water (30 mg/mL). Wounds remained uncovered during all the treatment. β-Glucan was applied every three days, and we measured the wound area at the same time. Wounds of both groups of mice were almost totally closed 12 days after the injury **(Figure 33A)**, but the group treated with β-Glucan healed significantly faster than the control group **(Figure 33B)**. Therefore, these results suggest that β-Glucan is able to stimulate the wound healing process *in vivo*.
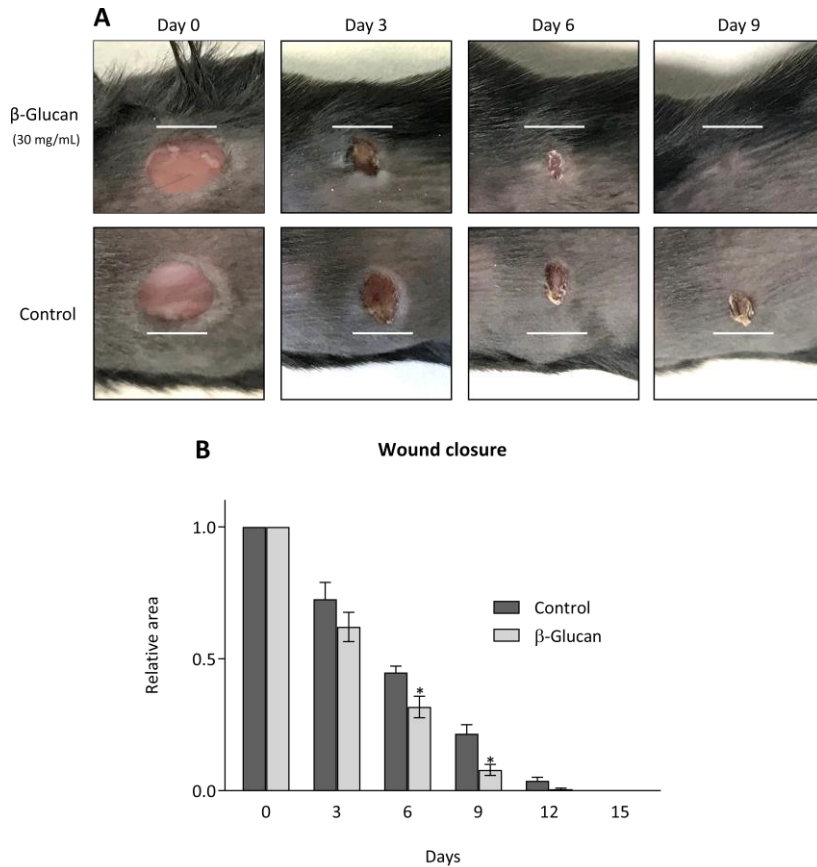
Figure 33. *Barley β-Glucan improves wound closure in vivo*. **A)** Wounds images of control and β-Glucan treated mice (30 mg/mL) at 0 days, 3 days, 6 days, and 9 days after the beginning of the treatment with β-Glucan or with water as a control. **B)** Measurements of the wound area. Data are expressed as mean ± SEM from β-Glucan-treated group (n=9) and from control group (n=6). Significance was determined by a two-way ANOVA test (*p<0.05).

In agreement with all these results, barley β-Glucan exerts a dual role by favouring a transitory arrest in cellular proliferation and inducing cellular migration. These effects could be of paramount importance in the regulation of wound healing.

DISCUSSION

ROLE OF THE CYCLIN D1 IN METASTASIS

Previous data showed the involvement of Cyclin D1 in the regulation of the metastatic colonisation process (Huang et al. 2009; Fusté et al. 2016a). This knowledge was in alignment with clinical data where the overexpression of Cyclin D1 was associated with metastatic cancer (Drobnjak et al. 2000). In these works, Cyclin D1 involvement in metastasis was observed in *in vivo* assays by injecting CTCs and macroscopically analysing the generated metastasis. Then, the predominant information is that Cyclin D1-deficient R3327-5'A cells generated fewer metastatic nodules in mice lungs than the wild-type cells (Fusté et al. 2016a). However, the metastatic colonisation from DTCs is developed in different steps by multiple mechanisms, even though the relevance of Cyclin D1 in those pathways is mainly unknown.

In this work, we wanted to improve the metastasis assay by adding GFP in the CTCs. Our purpose was to understand how cells disseminate, establish, and proliferate to form metastatic nodules in other parenchymal tissues. Due to the aggressiveness associated with the upregulation of Cyclin D1 in most cancers (Motokura et al. 1991) and the previous results of the metastasis assay we were based on, we expected R3327-5'A rat prostate tumour cells to disseminate further than R3327-5'A cells with downregulated Cyclin D1. In contrast, the reduction of Cyclin D1 levels in cells increased its ability to disseminate from blood vessels to lung parenchyma in mice euthanised two days after the injection of the cells, in comparison to R3327-5'A cells with conventional expression of Cyclin D1. R3327-5'A cells present characteristics of EMT (Luo et al. 1997), which explains the ability of these cells to migrate and invade other tissues (Pastushenko and Blanpain, 2019), compared to R3327-5'B cells, which are epithelial and cannot disseminate to the lung. The fact that decreased expression of Cyclin D1 had previously been associated with cell attachment and spreading (Fernández-Hernández et al. 2013; Fusté et al. 2016a) could explain that R3327-5'A with downregulated Cyclin D1 could extravasate easily from bloodstream to lung parenchyma.

On the other hand, it was of our interest to study how DTCs establish in the new tissue and start proliferating to form a metastatic nodule. To address this question, we analysed the number and size of the metastatic nodules in the lungs after an extended time following the injection (fifteen days). Consistently with the dissemination result, R3327-5'B cells did not

produce any metastasis because of its inability to extravasate into the lung. However, R3327-5'A wild-type cells generated more quantity and larger tumours than R3327-5'A with downregulated Cyclin D1. This fact contradicts what occurs on dissemination, but it is consistent with the previously published results. These data indicate that R3327-5'A wild-type cells establish efficiently in the lung parenchyma, whereas it is more challenging for the Cyclin D1 downregulated cells, which probably fail to survive during the first week. Hence, this suggests that Cyclin D1 has a role in metastatic nodule formation. This function of Cyclin D1 could be explained by two main aspects (He et al. 2007): first, it has been previously reported that human prostate tumour cells with Cyclin D1 overexpression can modify the tumour microenvironment to create a favourable condition for tumour establishment; second, high levels of Cyclin D1 enhance cell proliferation facilitating faster tumour growth, resulting in the presence of larger tumours.

In this work, we also wanted to understand how Cyclin D1 regulates both metastatic nodule establishment and growth. One of the best-characterised functions of Cyclin D1 is its association with CDK4 to control nuclear transcription factors that lead to cell proliferation (Malumbres and Barbacid, 2005). Thus, Cyclin D1-CDK4 phosphorylates and inhibits the RB1 releasing the E2F-mediated transcriptional program.

Nevertheless, several studies widely propose a cytoplasmic role of Cyclin D1 because of its interaction with cytoplasmic proteins such as Filamin A (Zhong et al. 2010) and Ral GTPases (Fernández et al. 2011). Furthermore, Fusté et al. (2016a) demonstrated that Cyclin D1-CDK4 complexes were located in fibroblasts and tumour cell membranes, where they could control cell migration, spreading, and invasion through Paxillin phosphorylation at Ser-83 and Rac1 GTPase activation. Moreover, a phosphomimetic allele of Ser-83 of Paxillin recovered the formation of metastasis in Cyclin D1 downregulated cells (Fusté et al. 2016a), indicating that Cyclin D1 regulates metastatic nodules through Paxillin.

However, since Cyclin D1-nuclear canonical function is the cell cycle and proliferation regulation through RB1, we cannot discard that Cyclin D1 could regulate DTCs establishment and growth in the lung through RB1. Hence, we generated an R3327-5'A cell line deficient in RB1 (R3327-5'A RB1$^{-/-}$). These cells with wild-type Cyclin D1 or Cyclin D1 downregulated were injected into mice, and the number and size of metastatic tumours were assessed after

fifteen days. The study exhibited that mice injected with R3327-5'A RB1$^{-/-}$ with Cyclin D1 downregulated had less quantity of tumours than the mice injected with R3327-5'A RB1$^{-/-}$ with wild-type Cyclin D1, indicating that the establishment of the metastatic nodules is independent of RB1. However, the size of tumours in both conditions was quite similar, suggesting that RB1 is necessary for tumour growth. Considering all this information, it could be possible that Cyclin D1 regulates survival and establishment of DTCs through Paxillin and nodule growth through RB1 **(Figure 34)**.

The R3327-5'A RB1$^{-/-}$ clones obtained through the CRISPR/Cas9 technique showed the same ability as wild types to start forming colonies *in vitro*, whereas they displayed a tendency to reduce proliferation. This result was unexpected given the fact that RB1 is a tumour suppressor gene. Thus, its loss has been widely associated with enhanced proliferation and the appearance of many cancer disorders like breast cancer (Knudsen et al. 2015), small-cell lung cancer (Niederst et al. 2015), or Retinoblastoma cancer during childhood (Mendoza and Grossniklaus, 2015). Additionally, the loss of RB1 in murine germinal centre B cells provoke both hyperproliferation and cell death (He et al. 2016) and RB1 depletion in embryonic myoblasts induced cell death (Zacksenhaus et al. 1996). Conversely, the proliferation of some other cells does not seem to be affected when RB1 is depleted, such as cone and rod photoreceptor cells and induced pluripotent stem cells (Vooijs et al. 2002; Deng et al. 2020). All these data suggest a great variety of RB1 roles, which can be cell type-specific. Moreover, the combination of RB1 loss with other gene alterations may lead to different cell behaviour (Knudsen et al. 2015). Hence, the reduction in proliferation which we observed in the RB1 knocked-out R3327-5'A cells is not utterly bizarre.
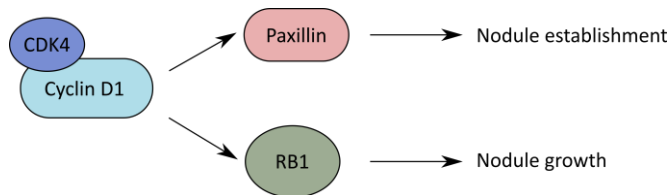
Figure 34. *Representative scheme of our hypothesis of metastasis regulation by Cyclin D1-CDK4.* Cyclin D1 can promote the establishment of metastatic nodules through the regulation of Paxillin, whereas it may control the metastatic nodule growth through RB1.

DESCRIBING NEW BIOMARKERS AND TARGETS OF METASTASIS

We were interested in detecting secreted proteins that may favour the generation of metastasis through regulating the tumour microenvironment in the lung. There are different proteomic studies of the association between tumour microenvironment and metastasis in the literature. Most of them use exosome isolation from biopsy or from body fluids (blood and urine), comparing metastatic versus non-metastatic patients (Qu et al. 2021; Wang et al. 2020). Another approach is to use the TIF obtained from biopsies containing both secreted proteins and secreted vesicles such as exosomes (Celis et al. 2004). Our approach is based on the collection of TIF, not from biopsies of human tumours, but using a metastatic colonisation model. In mice, we mimic the DTC colonisation process and acquire metastatic lungs. We applied this approach to obtain amplification of the quantity of secreted proteins, expecting that those proteins would be representative of the different steps of metastatic colonisation.

From this work, as expected, we have detected enriched extracellular proteins in the metastatic condition. Validating our approach, some of these proteins had been previously involved in cancer and metastasis, both by favouring the tumour microenvironment or enhancing cell migration and invasion.

For instance, Tenascin-C has been reported to be decisive in the tumour microenvironment. It promotes osteosarcoma cancer cells migration and induces metastatic progression to the lung (Sun et al. 2018). Moreover, it significantly influences many cancers invasive fronts, such as melanoma, breast, and colorectal cancers, hence providing poor clinical outcomes (Lowy and Oskarsson, 2015). S100B is an inflammatory molecule that participates in the establishment of a pre-metastatic niche, and it is used as a marker of metastasis in melanoma and lung, brain, breast, and ovarian cancers, among others (Pang et al. 2012; Yen et al. 2018; Ertekin et al. 2020).

Interestingly, we have found that the TIF in the metastatic condition was also enriched with cytoskeleton proteins. The presence of cytoskeleton proteins in metastasis samples of melanoma has been related to migration and escaping from the primary tumour (Shapanis et al. 2020). In contrast, it has also been described that the cytoskeleton proteins are depleted in metastasis samples of the liver in comparison to the primary tumour, the

colorectal carcinoma (Fahrner et al. 2021). This difference may be related to the cancer type or the metastatic stage. In our approach, the cells used (R3327-5'A) were prostate cancer cells. Wang et al. (2020) has recently reviewed the latest proteomic studies of exosomes from urine, plasma, and cell culture media for prostate cancer. Nevertheless, the enrichment in cytoskeleton proteins was not reported. Perhaps, our different approach has allowed us to stand out the presence of cytoskeleton proteins in the metastatic lungs.

Among the cytoskeleton proteins obtained, we selected two Actin-binding proteins such as Fascin and Adseverin. In agreement with our data, it has been described that Fascin promotes filopodia formation and is associated with metastatic induction in colorectal and gastric carcinomas (Tan et al. 2013). Adseverin (also named Scinderin) has been reported to modulate breast cancer and gastric cancer cells growth and invasion (Liu et al. 2016; Tanic et al. 2019a). Moreover, the expression of Adseverin correlates with tumour aggressiveness (Lin et al. 2019), but the relevance of this protein in metastatic colonisation has not been established yet. Therefore, among the different candidates, we decided to initiate the functional studies with Adseverin.

Regarding Adseverin, we show two main results in this work. First, this protein is present in the TIF of metastatic lungs and is secreted by tumorous cells. Second, Adseverin promotes metastatic colonisation of CTCs. The secretion of Adseverin by tumour cells has not been proved before. There are data from only two proteomic analyses describing the presence of Adseverin in exosomes from ovarian cancer cell lines (Liang et al. 2013) and urine (Gonzales et al. 2009) in humans. These data are consistent with our results finding Adseverin in the extracellular medium. However, we have identified Adseverin in the TIFs analysis but not in the exosomes-isolated fraction of the TIF. Consequently, we contemplate the possibility of some technical problems during the exosomes analysis, such as in the protein obtaining or the exosome isolation and lysis. Nonetheless, we have corroborated the secretion of Adseverin in the secretome analysis of R3327-5'A cells.

We obtained the secretomes from R3327-5'A and R3327-5'B *in vitro* cultured cells and tested the presence of Adseverin by immunoblot. These tumour cells expressed and released Adseverin into the media. Nevertheless, R3327-5'A cells presented increased levels of this protein in comparison to R3327-5'B cells, consistently with the fact that R3327-5'A cells are

more metastatic (Lai et al. 2018a). Moreover, we checked Adseverin staining in normal and metastatic lung tissue by immunohistochemistry and detected that this protein was only present in the metastatic nodules, indicating that its secretion into the TIF is tumour-dependent. This finding suggests that Adseverin is being secreted to regulate the tumorous microenvironment and thus favouring the metastatic niches establishment. However, no extracellular function of Adseverin has been reported and whether there is any cell receptor that binds Adseverin, remains unknown at the moment **(see below)**.

Our *in vivo* results show that Adseverin-downregulated R3327-5'A cells generate smaller and much fewer tumours in mice lungs than the control cells. The reduction in the number of nodules suggests that Adseverin would regulate the efficacy of DTCs to establish a nodule. Another possibility is that this Actin-binding protein would alter the extravasation process and dissemination of CTCs. It has been reported that Adseverin regulates the assemblage of Actin Filaments at the leading edge of the neutrophiles, denoting a direct role of Adseverin in the regulation of cells migration (Glogauer et al. 2021). Furthermore, the downregulation of Adseverin reduced the migration capacity in dental pulp cells and a human gastric cell line (Li et al. 2015; Chen et al. 2014). Thus, Adseverin may have a key role in tumorous cells' extravasation. However, further experiments are needed to determine if Adseverin has a role in regulating the ability of the cells to disseminate from the bloodstream to the lung parenchyma.

Adseverin downregulation reduced the average size of the nodules. This data is consistent with the reduced subcutaneous tumour size that Adseverin-downregulated human prostatic cancer cells (PC3) generate in comparison to PC3 wild-type cells (Lai et al. 2018b). Overall, in academic literature, we can find different works correlating the expression of Adseverin with the metastatic response. For instance, samples from patients with liver metastasis showed overexpression of Adseverin (Lin et al. 2019). In this work, we have contributed with new data showing that Adseverin may regulate metastatic colonisation.

One of the questions which arise from this work is how Adseverin controls metastatic colonisation. Adseverin is a filamentous Actin severing protein that belongs to the Gelsolin family (Trifaró et al. 1992). Under resting conditions, it is attached to Phosphatidylinositol 4,5-Biphosphate (PIP_2) from the plasmatic membrane through two binding sites located into

Adseverin's first and second domains. It has been demonstrated that during cell stimulation and cytosolic Ca^{2+} increase, Adseverin disengages from the plasma membrane to interact and cleave filamentous Actin (Trifaró et al. 2000). Then, as aforementioned, the regulation of the Actin filaments dynamics and consequently the processes such as migration may help explain the role of Adseverin in extravasation and dissemination.

Interestingly, we observed that Adseverin-downregulated R3327-5'A cells became bigger and flattened than wild-type cells at the confluence. Morphological changes in Adseverin-silenced cells have been previously described, even though some of them are opposite to what happened to our R3327-5'A cells. For instance, Adseverin depletion in breast adenocarcinoma human cells (MCF-7) decreased the cell surface area and reduced the cell length extensions (Tanic et al. 2019b), and the silencing in osteoclasts reduced the cell size but did not affect the surface morphology (Cao et al. 2017), suggesting that the cell shape changes due to Adseverin can be tissue-specific. In any case, the alterations in cell morphology in R3327-5'A Adseverin-deficient cells could explain its lack of ability to disseminate.

Another possible effect of Adseverin in metastasis would be related to its role in regulating exocytosis. Adseverin is mainly found in tissues with a highly secretory activity, and it has been previously reported that it exerts a role in exocytosis regulation (Trifaró et al. 1992). The Actin cytoskeleton interacts not only with plasma membranes but with some organelles, like secretory vesicles (Jockusch et al. 1977). Moreover, it has been described that filamentous Actin is generally located in the cell surface acting as a barrier to the secretory vesicles, avoiding their binding to the plasmatic membrane. Hence, it is further suggested that the Actin severing capacity of Adseverin is needed to break the Actin barrier, helping the secretory vesicles to reach the plasmatic membrane and fuse to it (Schafer and Cooper, 1995). We have seen that Adseverin depleted cells had more vesicles in their cytoplasm, which is consistent with the role of Adseverin in the exocytosis regulation. Then, the involvement of Adseverin in the guidance of exocytosis could lead to the creation of a favourable environment in the lung for DTCs establishment.

Finally, we described that Adseverin could regulate metastatic nodule growth **(see above)**. Moreover, we observed that the downregulation of Adseverin caused a remarkable

reduction in R3327-5'A cells proliferation and a decrease in the number and size of established colonies *in vitro*. This result was consistent with previous works describing the role of Adseverin promoting cell proliferation in human prostate cells, human lung carcinoma cells, and human breast carcinoma cells (Wang et al. 2014; Liu et al. 2015; Jian et al. 2018). Conversely, the expression of Adseverin in hepatocellular carcinoma cells restrains cell proliferation (Zhou et al. 2020).

However, the mechanism by which Adseverin influences cell proliferation is unknown. It has been described that the expression of some cell cycle regulators is modified when Adseverin is downregulated. For instance, in human prostate cells, cell cycle inhibitors such as p16 and p21 are upregulated, whereas Cyclin A expression is decreased (Wang et al. 2014), and p21 is increased in Adseverin-silenced human lung carcinoma cells (Liu et al. 2015). It is known that Adseverin depletion decreases the expression of EGFR in prostate cancer cells, and EGFR inhibits p27 through the Mitogen-activated protein Kinase Kinase / Extracellular signal-Regulated Kinase (MEK/ERK) signalling pathway (Lai et al. 2018b). In addition, MEK/ERK enhance Cyclin's D1 transcription (Musgrove, 2006). Therefore, it could be plausible that Adseverin could affect proliferation by regulating the cell cycle machinery through EGFR signalling. R3327-5'A cells show elevated levels of phosphorylated ERK (our unpublished results), but we do not know whether this is related to EGFR signalling alone. We consider it conceivable that the effects of Adseverin in R3327-5'A cells could be mediated by EGFR/ERK signalling, which would require future experiments.

β-GLUCAN SIGNALLING ON CELL CYCLE. CYCLIN D1 AND RETINOBLASTOMA 1 DEPENDENCE

The results of our work indicate that barley β-Glucan promotes an arrest in the proliferation of HDF cells. Conversely to our findings, previous projects showed that β-Glucan induces proliferation in diverse cell types (Majtan and Jesenak, 2018). Even though it seems contradictory, both ideas could be correct if we consider that we have observed a short arrest of proliferation 24 hours after β-Glucan addition, but also a total recovery after 48 hours, which means that an increase of proliferation occurs between the 24 hours and 48 hours. This result had not been previously detected because a predominant part of reports testing β-Glucan effects has analysed proliferation at long-term. However, data from two independent reports must be taken into consideration, since they manifest that fungal β-Glucan may reduce the proliferation of HDF and rat cells 24 hours after treatment (Woo et al. 2010b).

A second aspect is that, in our hands, the treatment with β-Glucan recovered but did not enhance HDF cells proliferation at 48 hours. Conversely, some published reports manifest that β-Glucan at similar concentrations enhances proliferation over long periods of time (Woo et al. 2010b). These antagonistic data could be explained due to the different cells used as a model and the variety of β-Glucans applied as treatment. For instance, and as in our data, a work reported that fungal (1→3),(1→6)-β-Glucan did not exacerbate long-term proliferation in HDFs (Son et al. 2007) but promoted a long-term proliferation response in the connective tissue of mouse cells (Son et al. 2005). So, we conclude that barley β-Glucan can promote short-term and long-term responses in the proliferation of HDF cells.

We have detected that the short arrest in the proliferation of HDF induced by β-Glucan is RB1-dependent. RB1 is a tumour suppressor protein that negatively regulates the cell cycle entry, and it is hyperphosphorylated and inactivated by Cyclin D1-CDK4/6 and Cyclin E-CDK2 complexes. Once inhibited, RB1 releases the transcriptional factor E2F, which promotes cell cycle genes transcription and proliferation **(Figure 35A)** (Sherr and Roberts, 2004). The fact that the sole RB1 downregulation rescues the proliferation arrest in the presence of β-Glucan, strongly suggests that Cyclin-CDK complexes would be unaffected by β-Glucan. In agreement with this, the RB1 protein remains phosphorylated in the presence of β-Glucan. Furthermore, the expression of Cyclin D1 and CDK4 were unaltered after β-Glucan addition.

Then, the mechanism of action of the β-Glucan should affect directly the RB1 functionality **(Figure 35A)**.
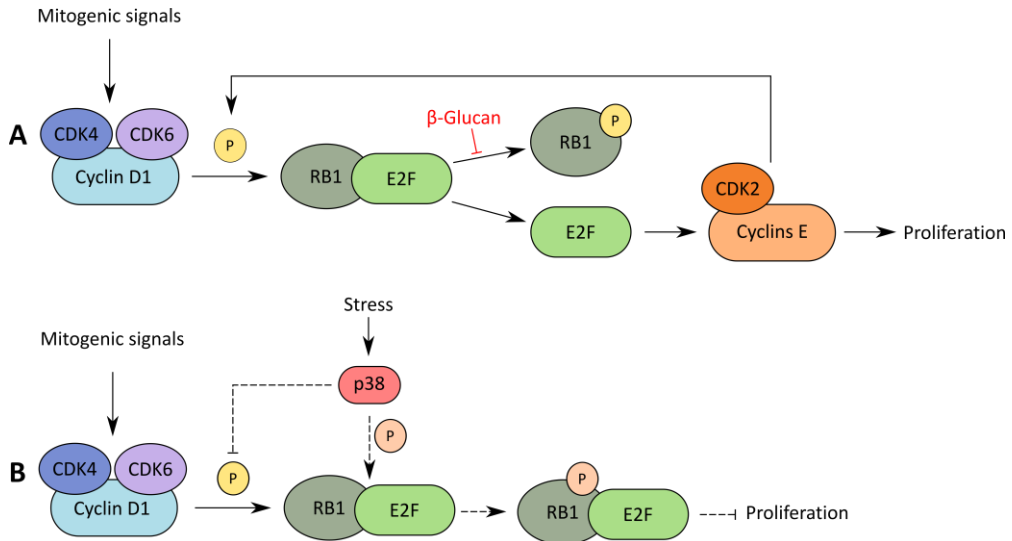
Figure 35. *Representative scheme of the regulation of Cyclin D1 - RB1 axis.* **A)** Mitogenic signals promote the association of Cyclin D1-CDK4/6 complexes that phosphorylate and inhibit RB1, favouring the release of the transcription factor E2F. In its turn, E2F induces the expression of Cyclins E, which, together with CDK2, hyperphosphorylate RB1. Red arrows indicate putative signalling pathways affected by barley β-Glucan. **B)** Stress causes the activation of p38, which phosphorylates RB1 at Ser-249 and Thr-252, blocking the effect of CDKs phosphorylation on RB1 and preventing the E2F release.

It has been described that under conditions of osmotic stress, p38 kinase is active and phosphorylates RB1 at Ser-249 and Thr-252 (Gubern et al. 2016). This p38-phosphorylation blocks the effect of the CDK phosphorylation of RB1 preventing the release of E2F **(Figure 35B)**. Despite this, the arrest on proliferation that we observe cannot be dependent on osmotic stress, as we do not perceive p38 activation either at short or long times. Furthermore, we could not detect the proliferation arrest when HDF cells were treated with amylopectin or methylcellulose, suggesting that the proliferation arrest we report is not because of osmotic stress caused by glucose polymers. Hence, we presume that the HDFs response to barley β-Glucan treatment could be dependent on β-Glucan specific receptors.

Accordingly, Yamaguchi et al. 2021 have recently described that fungal β-Glucan stimulates the agglomeration of neutrophils in the early stages of the wound healing process in mice through the activation of Dectin-1 receptors. They have also reported that Dectin-1 receptors appear in the skin fibroblasts of mice after the injury. The induction of these receptors may trigger signalling pathways that may alter the functionality of RB1, even though no pathways have been identified yet.

Previous reports showed that fungal β-Glucans favoured wound healing *in vitro* and *in vivo* (Majtan and Jesenak, 2018). The wound healing process requires that cells like fibroblasts to move into the injury by the coordination of various processes, such as cellular adhesion and migration. Later they proliferate and produce extracellular matrix (Stadelmann et al. 1998). In accordance, we describe that barley β-Glucan promotes HDF cells migration 24 hours after treatment *in vitro*, and we demonstrate that the topical application of barley β-Glucan in C57BL/6 mice skin lesions promotes the acceleration of wound healing. Therefore, we conclude that barley β-Glucan induces an RB1-dependent transient arrest in HDF cells proliferation, and at the same time triggers dermal fibroblasts migration. This double effect has not been reported yet in literature. In addition, we corroborate *in vivo* the efficacy of β-Glucans in the healing of wounds. Hence, it could have a clinical use as a treatment for sores or opened wounds.

CONCLUSIONS

FIRST. Cyclin D1 negatively regulates the dissemination of R3327-5'A circulating cells.

SECOND. Cyclin D1 regulates both the survival and establishment of disseminated tumour cells, and the metastatic nodule growth.

THIRD. The mechanism by which Cyclin D1 regulates survival and establishment of disseminated tumour cells is Retinoblastoma 1-independent. In contrast, the regulation of metastatic nodule growth by Cyclin D1 is Retinoblastoma 1-dependent.

FOURTH. The tumour interstitial fluid from metastatic lungs is enriched in cytoskeleton proteins.

FIFTH. The cytoskeleton proteins Fascin and Adseverin are secreted from tumour cells.

SIXTH. Adseverin regulates both the survival and establishment of disseminated tumour cells, and the metastatic nodule growth.

SEVENTH. Barley β-Glucan induces a short temporary arrest in human fibroblasts in a Retinoblastoma 1-dependent manner.

EIGHT. Barley β-Glucan positively regulates human fibroblasts migration.

NINETH. Barley β-Glucan improves the healing of wounds in mice.

BIBLIOGRAPHY

Agrawal, G.K; Jwa, N-S; Lebrun, M-H; Job, D; and Rakwal, R. 2010. "Plant Secretome: Unlocking Secrets of the Secreted Proteins." Proteomics 10 (4): 799–827.
https://doi.org/10.1002/pmic.200900514

Alao, John P. 2007. "The Regulation of Cyclin D1 Degradation: Roles in Cancer Development and the Potential for Therapeutic Invention." Molecular Cancer 6 (24): 1–16.
https://doi.org/10.1186/1476-4598-6-24

Allen, W. E; Jones, G. E; Pollard, J. W; and Ridley A. J. 1997. "Rho, Rac and Cdc42 Regulate Actin Organization and Cell Adhesion in Macrophages." Journal of Cell Science 110 (6): 707–20.
https://pubmed.ncbi.nlm.nih.gov/9099945/

Amanatullah, D. F; Reutens, A. T; Zafonte, B. T; Maofu, F; Mani, S; and Pestell, R. G. 2000. "Cell-Cycle Dysregulation and the Molecular Mechanisms of Prostate Cancer." Epidemiology 10461: 372–90.
https://doi.org/doi: 10.2741/amanatullah

Arnold, A; and Papanikolau, A. 2005. "Cyclin D1 in Breast Cancer Pathogenesis." Journal of Clinical Oncology 23 (18): 4215–24.
https://doi.org/10.1200/JCO.2005.05.064

Baldin, V; Lukas, J; Marcote, M. J; Pagano, M; and Draetta, G. 1993. "Cyclin D1 Is a Nuclear Protein Required for Cell Cycle Progression in G1." Genes and Development 7 (5): 812–21.
https://doi.org/10.1101/gad.7.5.812

Barrangou, R; Fremaux, C; Deveau, H; Richards, M; Boyaval, P; Moineau, S; Romero, D. A; Horvath, P. 2007. "CRISPR Provides Acquired Resistance Against Viruses in Prokaryotes." Science 315 (5819): 1709-1712.
https://doi.org/10.1126/science.1138140

Basha, R. Y; Sampath Kumar, T. S; and Doble, M. 2017. "Electrospun Nanofibers of Curdlan (β-1,3 Glucan) Blend as a Potential Skin Scaffold Material." Macromolecular Materials and Engineering 302 (4): 1–9.
https://doi.org/10.1002/mame.201600417

Bateman, Alex. 2019. "UniProt: A Worldwide Hub of Protein Knowledge." Nucleic Acids Research 47 (D1): D506–515.
https://doi.org/10.1093/nar/gky1049

Bendris, N; Lemmers, B; and Blanchard, J. M. 2015. "Cell Cycle, Cytoskeleton Dynamics and beyond: The Many Functions of Cyclins and CDK Inhibitors." Cell Cycle 14 (12): 1786–98.
https://doi.org/10.1080/15384101.2014.998085

Besson, A; Gurian-West, M; Schmidt, A; Hall, A; and Roberts, J. M. 2004. "P27Kip1 Modulates Cell Migration through the Regulation of RhoA Activation." Genes and Development 18: 862–76.
https://doi.org/10.1101/gad.1185504

Bienvenu, F; Jirawatnotai, S; Elias, J. E; Meyer, C. A; Mizeracka, K; Marson, A; et al. 2010. "Transcriptional Role of Cyclin D1 in Development Revealed by a Genetic-Proteomic Screen." Nature 463 (7279): 374–78.
https://doi.org/10.1038/nature08684

Brabletz, T; Jung, A; Reu, S; Porzner, M; Hlubek, F; Kunz-Schughart, L. A; Knuechel, R; Kirchner, T and Weinberg, R. A. 2001. "Variable-Catenin Expression in Colorectal Cancers Indicates Tumor Progression Driven by the Tumor Environment." PNAS 98 (18): 10356–61.
https://doi.org/doi: 10.1073/pnas.171610498

Cao, Y;Wang, Y; Sprangers, S; Picavet, D. I; Glogauer, M; McCulloch, C. A; and Everts, V. 2017. "Deletion of Adseverin in Osteoclasts Affects Cell Structure but Not Bone Metabolism." Calcified Tissue International 101 (2): 207–16.
https://doi.org/10.1007/s00223-017-0271-6

Casini, A; Olivieri, M; Petris, G; Montagna, C; Reginato, G; Maule, G; Lorenzin, F; et al. 2018. "A Highly Specific SpCas9 Variant Is Identified by in Vivo Screening in Yeast." Nature Biotechnology 36 (3): 265–71. https://doi.org/10.1038/nbt.4066

Celià-Terrassa, T; and Kang, Y. 2018. "Metastatic Niche Functions and Therapeutic Opportunities." Nature Cell Biology. Nature Cell Biology 20 (8) 868-877. https://doi.org/10.1038/s41556-018-0145-9

Celis, J. E; Gromov, P; Cabezón, T; Moreira, J .M. A; Ambartsumian, N; Sandelin, K; Rank, F; and Gromova, I. 2004. "Proteomic Characterization of the Interstitial Fluid Perfusing the Breast Tumor Microenvironment." Molecular and Cellular Proteomics. 3 (4) 327-344. https://doi.org/10.1074/mcp.M400009-MCP200

Cemeli, T; Guasch-Vallés, M; Nàger, M; Felip, I; Cambray, S; Santacana, M; Gatius, S; et al. 2019. "Cytoplasmic Cyclin D1 Regulates Glioblastoma Dissemination." Journal of Pathology 248 (4): 501–13. https://doi.org/10.1002/path.5277

Chen, H. Y; Shen, C. H; Tsai, Y. T; Lin, F.C; Huang, Y. P; and Chen, R. H. 2004. "Brk Activates Rac1 and Promotes Cell Migration and Invasion by Phosphorylating Paxillin." Molecular and Cellular Biology 24 (24): 10558–72. https://doi.org/10.1128/mcb.24.24.10558-10572.2004

Chen, Q; Boire, A; Jin, X; Valiente, M; Er, E. E; Lopez-Soto, A; Jacob, L. S; et al. 2016. "Carcinoma-Astrocyte Gap Junctions Promote Brain Metastasis by CGAMP Transfer." Nature 533 (7604): 493–98. https://doi.org/10.1038/nature18268

Chen, Q. F; Chang, L; Su, Q; Zhao, Y; and Kong, B. 2021. "Clinical Importance of Serum Secreted Clusterin in Predicting Invasive Breast Cancer and Treatment Responses." Bioengineered 12 (1): 278–85.

https://doi.org/10.1080/21655979.2020.1868732

Chen, X. M; Guo, J. M; Lian, P; Mao, L. G; Feng, W. Y; Le, D. H; and Li, K. Q. 2014. "Suppression of Scinderin Modulates Epithelial Mesenchymal Transition Markers in Highly Metastatic Gastric Cancer Cell Line SGC 7901." Molecular Medicine Reports 10 (5): 2327–33. https://doi.org/10.3892/mmr.2014.2523

Choromanska, A; Kulbacka, J; Harasym, J; Oledzki, R; Szewczyk, A; and Saczko, J. 2018. "High - and Low-Molecular Weight Oat Beta-Glucan Reveals Antitumor Activity in Human Epithelial Lung Cancer." Pathology and Oncology Research 24 (3): 583–92. https://doi.org/10.1007/s12253-017-0278-3

D'Amico, M; Hulit, J; Amanatullah, D. F; Zafonte, B. T; Albanese, C; Bouzahzah, B; Fu, M; et al. 2000. "The Integrated-Linked Kinase Regulates the Cyclin D1 Gene through Glycogen Synthase Kinase 3β and CAMP-Responsive Element-Binding Protein-Dependent Pathways." Journal of Biological Chemistry 275 (42): 32649–57. https://doi.org/10.1074/jbc.M000643200

Deakin, N. O; and Turner, C. E. 2008. "Paxillin Comes of Age." Journal of Cell Science 121: 2438–44. https://doi.org/10.1242/jcs.018044

Deltcheva, E; Chylinski, K; Sharma, C. M; Gonzales, K; Chao, Y; Pirzada, Z. A; Eckert, M. R; Vogel, J; Charpentier, E. 2011. "CRISPR RNA maturation by trans-encoded small RNA and host factor RNase III." Nature 471 (7340): 602-607. https://doi.org/10.1038/nature09886

Deng, X; Iwagawa, T; Fukushima, M; and Watanabe, S. 2020. "Characterization of Human-Induced Pluripotent Stem Cells Carrying Homozygous RB1 Gene Deletion." Genes to Cells 25 (7): 510–17. https://doi.org/10.1111/gtc.12771

Deshmukh, A. P; Vasaikar, S. V; Tomczak, K; Tripathi, S; den Hollander, P; Arslan, E; Chakraborty, P; et al. 2021. "Identification of EMT Signaling Cross-Talk and Gene Regulatory Networks by Single-Cell RNA Sequencing." PNAS 118 (19): 1–10. https://doi.org/https://doi.org/10.1073/pnas.210 2050118

Diehl, J. A; Zindy, F; and Sherr, C. J. 1997. "Inhibition of Cyclin D1 Phosphorylation on Threonine-286 Prevents Its Rapid Degradation via the Ubiquitin-Proteasome Pathway." Genes and Development 11: 957–72. https://doi.org/doi: 10.1101/gad.11.8.957

Donato, R; Sorci, G; Riuzzi, F; Arcuri, C; Bianchi, R; Brozzi, F; Tubaro, C; and Giambanco, I. 2009. "S100B's Double Life: Intracellular Regulator and Extracellular Signal." Biochimica et Biophysica Acta - Molecular Cell Research. https://doi.org/10.1016/j.bbamcr.2008.11.009

Drobnjak, M; Osman, I; Scher, H. I; Fazzari, M; and Cordon-Cardo, C. 2000. "Overexpression of Cyclin D1 Is Associated with Metastatic Prostate Cancer to Bone." Clinical Cancer Research 6 (5): 1891–95. https://pubmed.ncbi.nlm.nih.gov/10815912/

Eguchi, T; Sogawa, C; Ono, K; Matsumoto, M; Tran, M. T; Okusha, Y; Lang, B. J; Okamoto, K; and Calderwood, S. K. 2020. "Cell Stress Induced Stressome Release Including Damaged Membrane Vesicles and Extracellular HSP90 by Prostate Cancer Cells." Cells 9 (3): 1-24. https://doi.org/10.3390/cells9030755

Ertekin, S. S; Podlipnik, S; Ribero, S; Molina, R; Rios, J; Carrera, C; Malvehy, J; and Puig, S. 2020. "Monthly Changes in Serum Levels of S100B Protein as a Predictor of Metastasis Development in High-Risk Melanoma Patients." Journal of the European Academy of Dermatology and Venereology 34 (7): 1482–88. https://doi.org/10.1111/jdv.16212

Evans, T; Rosenthal, E. T; Youngblom, J; Distel, D; and Hunt, T. 1983. "Cyclin: A Protein Specified by Maternal MRNA in Sea Urchin Eggs That Is Destroyed at Each Cleavage Division." Cell 33 (2): 389–96. https://doi.org/10.1016/0092-8674(83)90420-8

Fahrner, M; Bronsert, P; Fichtner-Feigl, S; Jud, A; and Schilling, O. 2021. "Proteome Biology of Primary Colorectal Carcinoma and Corresponding Liver Metastases." Neoplasia (United States) 23 (12): 1240–51. https://doi.org/10.1016/j.neo.2021.10.005

Fernández, R. M. H; Ruiz-Miró, M; Dolcet, X; Aldea, M; and Garí, E. 2011. "Cyclin D1 Interacts and Collaborates with Ral GTPases Enhancing Cell Detachment and Motility." Oncogene 30: 1936–46. https://doi.org/10.1038/onc.2010.577

Fernández-Hernández, R; Rafel, M; Fusté, N. P; Aguayo, R. S; Casanova, J. M; Egea, J; Ferrezuelo, F; and Garí, E. 2013. "Cyclin D1 Localizes in the Cytoplasm of Keratinocytes during Skin Differentiation and Regulates Cell-Matrix Adhesion." Cell Cycle 12 (15): 2510–17. https://doi.org/10.4161/cc.25590

Fusté, N. P; Fernández-Hernández, R; Cemeli, T; Mirantes, C; Pedraza, N; Rafel, M; Torres-Rosell, J; et al. 2016a. "Cytoplasmic Cyclin D1 Regulates Cell Invasion and Metastasis through the Phosphorylation of Paxillin." Nature Communications 7: 1-24. https://doi.org/10.1038/ncomms11581

Fusté, N. P; Castelblanco, E; Felip, I; Santacana, M; Fernández-Hernández, R; Gatius, S; Pedraza, N; et al. 2016b. "Characterization of Cytoplasmic Cyclin D1 as a Marker of Invasiveness in Cancer." Oncotarget 7 (19): 26979–91. https://doi.org/doi: 10.18632/oncotarget.8876

Gallanis, G; Ramon, T; Pericas, I; Riegel, A. T; and Pohlmann, P. R. 2021. "An Evaluation of Palbociclib

as a Breast Cancer Treatment Option: A Current Update." Expert Opinion on Pharmacotherapy 22 (3): 281–90. https://doi.org/10.1080/14656566.2020.1838485

Gao, D; Joshi, N; Choi, H; Ryu, S; Hahn, M; Catena, R; Sadik, H; et al. 2012. "Myeloid Progenitor Cells in the Premetastatic Lung Promote Metastases by Inducing Mesenchymal to Epithelial Transition." Cancer Research 72 (6): 1384–94. https://doi.org/10.1158/0008-5472.CAN-11-2905

Ghajar, C. M; Peinado, H; Mori, H; Matei, I. R; Evason, K. J; Brazier, H; Almeida, D; et al. 2013. "The Perivascular Niche Regulates Breast Tumour Dormancy." Nature Cell Biology 15 (7): 807–17. https://doi.org/10.1038/ncb2767

Glogauer, J; Sun, C; Wang, Y; and Glogauer, M. 2021. "The Actin-Binding Protein Adseverin Mediates Neutrophil Polarization and Migration." Cytoskeleton 78 (5): 206–13. https://doi.org/10.1002/cm.21684

Gonzales, P. A; Pisitkun, T; Hoffert, J. D; Tchapyjnikov, D; Star, R. A; Kleta, R; Wang, N. S; and Knepper, M. A. 2009. "Large-Scale Proteomics and Phosphoproteomics of Urinary Exosomes." Journal of the American Society of Nephrology 20 (2): 363–79. https://doi.org/10.1681/ASN.2008040406

Gubern, A, Joaquin, M; Marquès, M; Maseres, P; Garcia-Garcia, J; Amat, R; González-Nuñez, D; et al. 2016. "The N-Terminal Phosphorylation of RB by P38 Bypasses Its Inactivation by CDKs and Prevents Proliferation in Cancer Cells." Molecular Cell 64 (1): 25–36. https://doi.org/10.1016/j.molcel.2016.08.015

Gupta, G. P; and Massagué, J. 2006. "Cancer Metastasis: Building a Framework." Cell 127 (4): 679–95. https://doi.org/10.1016/j.cell.2006.11.001

Guttridge, D. C; Albanese, C; Reuther, J. Y; Pestell, R. G; and Baldwin, A. S. 1999. "NF-KB Controls Cell Growth and Differentiation through Transcriptional Regulation of Cyclin D1." Molecular and Cellular Biology 19 (8): 5785–99. https://doi.org/10.1128/mcb.19.8.5785

Hall, A. 2009. "The Cytoskeleton and Cancer." Cancer and Metastasis Reviews. 28 (1-2): 5-14. https://doi.org/10.1007/s10555-008-9166-3

Hashimoto, Y; Parsons, M; and Adams, J. C. 2007. "Dual Actin-Bundling and Protein Kinase C-Binding Activities of Fascin Regulate Carcinoma Cell Migration Downstream of Rac and Contribute to Metastasis." Molecular Biology of the Cell 18 (11): 4591–4602. https://doi.org/10.1091/mbc.E07-02-0157

He, Y; Franco, O. E; Jiang, M; Williams, K; Love, H. D; Coleman, I. M; Nelson, P. S; and Hayward, S. W. 2007. "Tissue-Specific Consequences of Cyclin D1 Overexpression in Prostate Cancer Progression." Cancer Research 67 (17): 8188–97. https://doi.org/10.1158/0008-5472.CAN-07-0418

He, Z; O'Neal, J; Wilson, W. C; Mahajan, N; Luo, J; Wang, Y; Su, M. Y; et al. 2016. "Deletion of Rb1 Induces Both Hyperproliferation and Cell Death in Murine Germinal Center B Cells." Experimental Hematology 44 (3): 1–10. https://doi.org/10.1016/j.exphem.2015.11.006

Heckl, D; Kowalczyk, M. S; Yudovich, D; Belizaire, R; Puram, R. V; McConkey, M.E; Thielke, A; Aster, J. C; Regev, A; and Ebert, B. L. 2014. "Generation of Mouse Models of Myeloid Malignancy with Combinatorial Genetic Lesions Using CRISPR-Cas9 Genome Editing." Nature Biotechnology 32 (9): 941–46. https://doi.org/10.1038/nbt.2951

Horibata, S; Rogers, K. E; Sadegh, D; Anguish, L. J; McElwee, J. L; Shah, P; Thompson, P. R; and Coonrod, S. A. 2017. "Role of Peptidylarginine Deiminase 2

(PAD2) in Mammary Carcinoma Cell Migration." BMC Cancer 17 (1): 1–14. https://doi.org/10.1186/s12885-017-3354-x

Huang, H; de Hu, Y; Li, N; and Zhu, Y. 2009. "Inhibition of Tumor Growth and Metastasis by Non-Small Cell Lung Cancer Cells Transfected with Cyclin D1-Targeted SiRNA." Oligonucleotides 19 (2): 151–61. https://doi.org/10.1089/oli.2008.0174

Hulsen, T; de Vlieg, J; and Alkema, W. 2008. "BioVenn - A Web Application for the Comparison and Visualization of Biological Lists Using Area-Proportional Venn Diagrams." BMC Genomics 9 (488): 1–6. https://doi.org/10.1186/1471-2164-9-488

Hymowitz, S. G; and Malek, S. 2018. "Targeting the MAPK Pathway in RAS Mutant Cancers." Cold Spring Harbor Perspectives in Medicine 8 (11): 1–16. https://doi.org/10.1101/cshperspect.a031492

Jian, W; Zhang, X; Wang, J; Liu, Y; Hu, C; Wang, X; and Liu, R. 2018. "Scinderin-Knockdown Inhibits Proliferation and Promotes Apoptosis in Human Breast Carcinoma Cells." Oncology Letters 16 (3): 3207–14. https://doi.org/10.3892/ol.2018.9009

Jiang, W; Jia, Q; Liu, L; Zhao, X; Tan, A; Ma, N; and Zhang, H. 2011. "S100B Promotes the Proliferation, Migration and Invasion of Specific Brain Metastatic Lung Adenocarcinoma Cell Line." Cell Biochemistry and Function 29 (7): 582–88. https://doi.org/10.1002/cbf.1791

Jockusch, B; Burger, M; Prada, M; Richards, J; Chaponnier, C; and Gabbiani, C. 1977. "α-Actinin Attached to Membranes of Secretory Vesicles." Nature Publishing Group 270: 628–29. https://doi.org/10.1038/270628a0

Ishino, Y; Shinagawa, H; Makino, K; Amemura, M; Nakata, A. 1987. "Nucleotide Sequence of the iap Gene, Responsible for Alkaline Phosphatase Isozyme Conversion in *Escherichia coli,* and Identification of the Gene Product." Journal of Bacteriology 169 (12): 5429-5433. https://doi.org/10.1128/jb.16912.5429-433.1987

Karagiannis, G. S; Pavlou, M. P; and Diamandis, E. P. 2010. "Cancer Secretomics Reveal Pathophysiological Pathways in Cancer Molecular Oncology." Molecular Oncology 4 (6): 496–510. https://doi.org/10.1016/j.molonc.2010.09.001

Kato, J; Matsushime, H; Hiebert, S. W; Ewen, M. E; and Sherr, J. C. 1993. "Direct Binding of Cyclin D to the Retinoblastoma Gene Product (PRb) and PRb Phosphorylation by the Cyclin D-Dependent Kinase CDK4." Genes and Development 7 (3): 331–42. https://doi.org/10.1101/gad.7.3.331

Kawakami, K; Fujita, Y; Kato, T; Mizutani, K; Kameyama, K; Tsumoto, H; Miura, Y; Deguchi, T; and Ito, M. 2015. "Integrin B4 and Vinculin Contained in Exosomes Are Potential Markers for Progression of Prostate Cancer Associated with Taxane-Resistance." International Journal of Oncology 47 (1): 384–90. https://doi.org/10.3892/ijo.2015.3011

Keerthikumar, S; Chisanga, D; Ariyaratne, D; al Saffar, H; Anand, S; Zhao, K; Samuel, M; et al. 2016. "ExoCarta: A Web-Based Compendium of Exosomal Cargo." Journal of Molecular Biology 428 (4): 688–92. https://doi.org/10.1016/j.jmb.2015.09.019

Kim, J. H; Lee, S. R; Li, L. H; Park, H. J; Park, J. H; Lee, K. Y; Kim, M. K; Shin, B. A; and Choi, S. Y. 2011. "High Cleavage Efficiency of a 2A Peptide Derived from Porcine Teschovirus-1 in Human Cell Lines, Zebrafish and Mice." PLoS ONE 6 (4): 1–8. https://doi.org/10.1371/journal.pone.0018556

Knudsen, E. S; McClendon, A. K; Franco, J; Ertel, A; Fortina, P; and Witkiewicz A. K. 2015. "RB Loss Contributes to Aggressive Tumor Phenotypes in MYC-Driven

Triple Negative Breast Cancer." Cell Cycle 14 (1): 109–22. https://doi.org/10.4161/15384101.2014.967118

Knudsen, K. E; Diehl, J. A; Haiman, C. A; and Knudsen, E. S. 2006. "Cyclin D1: Polymorphism, Aberrant Splicing and Cancer Risk." Oncogene 25 (11): 1620–28. https://doi.org/10.1038/sj.onc.1209371

Kozar, K; Ciemerych, M. A; Rebel, V. I; Shigematsu, H; Zagozdzon, A; Sicinska, E; Geng, Y; et al. 2004. "Mouse Development and Cell Proliferation in the Absence of D-Cyclins." Cell 118 (4): 477–91. https://doi.org/10.1016/j.cell.2004.07.025

Krishnamurti, U; and Silverman, J. F. 2014. "HER2 in Breast Cancer: A Review and Update." Advances in Anatomic Pathology 21 (2): 100–107. https://doi.org/10.1097/PAP.0000000000000015

Labelle, M; Begum, S; and Hynes, R. O. 2011. "Direct Signaling between Platelets and Cancer Cells Induces an Epithelial-Mesenchymal-like Transition and Promotes Metastasis." Cancer Cell 20 (5): 576–90. https://doi.org/doi: 10.1016/j.ccr.2011.09.009

Lai, X; Su, W; Zhao, H; Yang, S; Zeng, T; Wu, W; and Wang, D. 2018a. "Loss of Scinderin Decreased Expression of Epidermal Growth Factor Receptor and Promoted Apoptosis of Castration-Resistant Prostate Cancer Cells." FEBS Open Bio 8 (5): 743–50. https://doi.org/10.1002/2211-5463.12412

Li, X; Jiang, H; Huang, Y; Gong, Q; Wang, J; and Ling, J. 2015. "Expression and Function of the Actin-Severing Protein Adseverin in the Proliferation, Migration, and Differentiation of Dental Pulp Cells." Journal of Endodontics 41 (4): 493–500. https://doi.org/10.1016/j.joen.2014.11.030

Li, Z; Wang, C; Jiao, X; Lu, Y; Fu, M; Quong, A. A; Dye, C; et al. 2006a. "Cyclin D1 Regulates Cellular Migration

through the Inhibition of Thrombospondin 1 and ROCK Signaling." Molecular and Cellular Biology 26 (11): 4240–56. https://doi.org/10.1128/MCB.02124-05

Li, Z; Jiao, X; Wang, C; Ju, X; Lu, Y; Yuan, L; Lisanti, M. P; Katiyar, S; and Pestell, R. G. 2006b. "Cyclin D1 Induction of Cellular Migration Requires P27KIP1." Cancer Research 66 (20): 9986–94. https://doi.org/10.1158/0008-5472.CAN-06-1596

Liang, B; Peng, P; Chen, S; Li, L; Zhang, M; Cao, D; Yang, J; et al. 2013. "Characterization and Proteomic Analysis of Ovarian Cancer-Derived Exosomes." Journal of Proteomics 80 (March): 171–82. https://doi.org/10.1016/j.jprot.2012.12.029

Lin, Q; Li, J; Zhu, D; Niu, Z; Pan, X; Xu, P; Ji, M; Wei, Y; and Xu, J. 2019. "Aberrant Scinderin Expression Correlates with Liver Metastasis and Poor Prognosis in Colorectal Cancer." Frontiers in Pharmacology 10 (1183): 1–11. https://doi.org/10.3389/fphar.2019.01183

Liu, H; Shi, D; Liu, T; Yu, Z; and Zhou, C. 2015. "Lentivirus-Mediated Silencing of SCIN Inhibits Proliferation of Human Lung Carcinoma Cells." Gene 554 (1): 32–39. https://doi.org/10.1016/j.gene.2014.10.013

Liu, J. J; Chao, J. R; Jiang, M. C; Ng, S. Y; Yen, J. J; and Yang-Yen, H. F. 1995. "Ras Transformation Results in an Elevated Level of Cyclin D1 and Acceleration of G1 Progression in NIH 3T3 Cells." Molecular and Cellular Biology 15 (7): 3654–63. https://doi.org/10.1128/mcb.15.7.3654

Liu, J. J; Liu, J. Y; Chen, J; Wu, Y. X; Yan, P; Ji, C. D; Wang, Y. X; et al. 2016. "Scinderin Promotes the Invasion and Metastasis of Gastric Cancer Cells and Predicts the Outcome of Patients." Cancer Letters 376 (1): 110–17. https://doi.org/10.1016/j.canlet.2016.03.035

Liu, J; Lian, J; Chen, Y; Zhao, X; Du, C. Z; Xu, Y; Hu, H; Rao, H; and Hong, X. 2021. "Circulating Tumor Cells (CTCs): A Unique Model of Cancer Metastases and Non-Invasive Biomarkers of Therapeutic Response." Frontiers in Genetics. Frontiers Media S.A. https://doi.org/10.3389/fgene.2021.734595

Lowy, C. M; and Oskarsson, T. 2015. "Tenascin C in Metastasis: A View from the Invasive Front." Cell Adhesion and Migration. Taylor and Francis Inc. https://doi.org/10.1080/19336918.2015.1008331

Lu, F; Gladden, A. B; and Diehl, J. A. 2003. "Advances in Brief an Alternatively Spliced Cyclin D1 Isoform, Cyclin D1b, Is a Nuclear Oncogene 1." Cancer Research 63: 7056–61. https://pubmed.ncbi.nlm.nih.gov/14612495/

Luo, J; Sharma, N; Seftor, E. A; Larco, J; Heidger, P. M; Hendrix, M. J. C; and Lubaroff, D. M. 1997. "Heterogeneous Expression of Invasive and Metastatic Properties in a Prostate Tumor Model." Pathology Oncology Research 3 (4): 264–71. https://doi.org/doi: 10.1007/BF02904285

Majtan, J; and Jesenak, M. 2018. "β-Glucans: Multi-Functional Modulator of Wound Healing." Molecules 23 (4): 1–15. https://doi.org/10.3390/molecules23040806

Makridakis, M; and Vlahou, A. 2010. "Secretome Proteomics for Discovery of Cancer Biomarkers." Journal of Proteomics 73 (12): 2291–2305. https://doi.org/10.1016/j.jprot.2010.07.001

Malumbres, M; and Barbacid, M. 2005. "Mammalian Cyclin-Dependent Kinases." Trends in Biochemical Sciences 30 (11): 630–41. https://doi.org/10.1016/j.tibs.2005.09.005

Malumbres, M; Sotillo, R; Cerezo, A; Gala, J; Ortega, S; Dubus, P; and Barbacid, M. 2004. "Mammalian Cells Cycle without the D-Type Cyclin-Dependent Kinases Cdk4 and Cdk6." Cell 118: 493–504. https://doi.org/doi: 10.1016/j.cell.2004.08.002

Mao, L; Dai, J; Cao, Y; Bai, X; Sheng, X; Chi, Z; Cui, C; et al. 2021. "Palbociclib in Advanced Acral Melanoma with Genetic Aberrations in the Cyclin-Dependent Kinase 4 Pathway." European Journal of Cancer 148 (May): 297–306. https://doi.org/10.1016/j.ejca.2021.02.021

Marampon, F; Casimiro, M. C; Fu, M; Powell, M. J; Popov, V. M; Lindsay, J; Zani, B. M; et al. 2008. "Nerve Growth Factor Regulation of Cyclin D1 in PC12 Cells through a P21RAS Extracellular Signal-Regulated Kinase Pathway Requires Cooperative Interactions between Sp1 and Nuclear Factor B." Molecular Biology of the Cell 19: 2566–78. https://doi.org/10.1091/mbc.E06-12-1110

Massagué, J; and Obenauf, A. C. 2016. "Metastatic Colonization." Nature 529 (1): 298–306. https://doi.org/10.1038/nature17038

Massagué, J; Batlle, E; and Gomis, R. R. 2017. "Understanding the Molecular Mechanisms Driving Metastasis." Molecular Oncology 11 (1): 3–4. https://doi.org/10.1002/1878-0261.12024

Matas-Nadal, C; Bech-Serra, J. J; Guasch-Vallés, M; Fernández-Armenteros, J. M; Barceló, C; Casanova, J. M; de La Torre Gómez, C; Aguayo Ortiz, R; and Garí, E. 2020. "Evaluation of Tumor Interstitial Fluid-Extraction Methods for Proteome Analysis: Comparison of Biopsy Elution versus Centrifugation." Journal of Proteome Research 19 (7): 2598–2605. https://doi.org/10.1021/acs.jproteome.9b00770

Matsushime, H; Quelle, D. E; Shurtleff, S. A; Shibuya, M; Sherr, C. J; and Kato, J. Y. 1994. "D-Type Cyclin-Dependent Kinase Activity in Mammalian Cells."

Molecular and Cellular Biology 14 (3): 2066–76. https://doi.org/10.1128/mcb.14.3.2066

Matsuura, I; Denissova, N. G; Wang, G; He, D; Long, J; and Liu, F. 2004. "Cyclin-Dependent Kinases Regulate the Antiproliferative Function of Smads." Nature 430 (6996): 226–31. https://doi.org/10.1038/nature02679

Medeiros, S. D. V; Cordeiro, S. L; Cavalcanti, J. E. C; Melchuna, K. M; Lima, A. M. S; Filho, I. A; Medeiros, A. C; et al. 2012. "Effects of Purified Saccharomyces Cerevisiae (1→3)-β-Glucan on Venous Ulcer Healing." International Journal of Molecular Sciences 13 (7): 8142–58. https://doi.org/10.3390/ijms13078142

Mendoza, P. R; and Grossniklaus, H. E. 2015. "The Biology of Retinoblastoma." Progress in Molecular Biology and Translational Science 134: 503–16. https://doi.org/10.1016/bs.pmbts.2015.06.012

Meng, H; Tian, L; Zhou, J; Li, Z; Jiao, X; Li, W. W; Plomann, M; et al. 2011. "PACSIN 2 Represses Cellular Migration through Direct Association with Cyclin D1 but Not Its Alternate Splice Form Cyclin D1b." Cell Cycle 10 (1): 73–81. https://doi.org/10.4161/cc.10.1.14243

Mojica, F. J; Díez-Villaseñor, C; Soria, E; Juez, G. 2000. "Biological significance of a family of regularly spaced repeats in the genomes of Archea, Bacteria and mitochondria." Molecular Microbiology 36(1):244-6. https://doi.org/10.1046/j.1365-2958.2000.01838

Motokura, T; et al. 1991. "A Novel Cyclin Encoded by a Bcl1-Linked Candidate Oncogene." Nature 350: 512–15. https://doi.org/doi: 10.1038/350512a0

Murgai, M; Ju, W; Eason, M; Kline, J; Beury, D. W; Kaczanowska, S; Miettinen, M. M; et al. 2017. "KLF4-Dependent Perivascular Cell Plasticity Mediates Pre-Metastatic Niche Formation and Metastasis." Nature Medicine 23 (10): 1176–90. https://doi.org/10.1038/nm.4400

Musgrove, E. A. 2006. "Cyclins: Roles in Mitogenic Signaling and Oncogenic Transformation." Growth Factors 24 (1): 13–19. https://doi.org/10.1080/08977190500361812

Musgrove, E. A; Caldon, C. E; Barraclough, J; Stone, A; and Sutherland, R. L. 2011. "Cyclin D as a Therapeutic Target in Cancer." Nature Reviews Cancer 11 (8): 558–72. https://doi.org/10.1038/nrc3090

Nakajima, K; Inagawa, M; Uchida, C; Okada, K; Tane, S; Kojima, M; Kubota, M; et al. 2011. "Coordinated Regulation of Differentiation and Proliferation of Embryonic Cardiomyocytes by a Jumonji (Jarid2)-Cyclin D1 Pathway." Development 138 (9): 1771–82. https://doi.org/10.1242/dev.059295

Neuman, E; Ladha, M. H; Lin, N; Upton, T. M; Miller, S. J; Direnzo, J; Pestell, R. G; et al. 1997. "Cyclin D1 Stimulation of Estrogen Receptor Transcriptional Activity Independent of Cdk4." MOLECULAR AND CELLULAR BIOLOGY 17 (9): 5338–47. https://doi.org/doi: 10.1128/MCB.17.9.5338

Neumeister, P. 2003. "Cyclin D1 Governs Adhesion and Motility of Macrophages." Molecular Biology of the Cell 14 (5): 2005–15. https://doi.org/10.1091/mbc.02-07-0102

Niederst, M. J; Sequist, L. V; Joirier, J. T; Mermel, C. H; Lockerman, E. L; Garcia, A. R; Katayama, R; et al. 2015. "RB Loss in Resistant EGFR Mutant Lung Adenocarcinomas That Transform to Small-Cell Lung Cancer." Nature Communications 6: 6377–87. https://doi.org/10.1038/ncomms7377

Nogués, L; Benito-Martin, A; Hergueta-Redondo, M; and Peinado, H. 2018. "The Influence of Tumour-Derived Extracellular Vesicles on Local and Distal Metastatic Dissemination." Molecular Aspects of Medicine. 60: 15-26. https://doi.org/10.1016/j.mam.2017.11.012

Noss, I; Doekes, G; Thorne, P. S; Heederik, D. J; and Wouters, I. M. 2013. "Comparison of the Potency of a Variety of β-Glucans to Induce Cytokine Production in Human Whole Blood." Innate Immunity 19 (1): 10–19. https://doi.org/10.1177/1753425912447129

Paget, S. 1889. "Distribution of Secondary Growths in Cancer of the Breast." The Lancet 8 (2): 98–101. https://pubmed.ncbi.nlm.nih.gov/2673568/

Paltridge, J. L; Belle, L; and Khew-Goodall, Y. 2013. "The Secretome in Cancer Progression." Biochimica et Biophysica Acta - Proteins and Proteomics 1834 (11): 2233–41. https://doi.org/10.1016/j.bbapap.2013.03.014

Pang, X; Min, J; Liu, L; Liu, Y; Ma, N; and Zhang, H. 2012. "S100B Protein as a Possible Participant in the Brain Metastasis of NSCLC." Medical Oncology 29 (4): 2626–32. https://doi.org/10.1007/s12032-012-0169-0

Park, H. A; Brown, S. R; and Kim, Y. 2020. "Cellular Mechanisms of Circulating Tumor Cells during Breast Cancer Metastasis." International Journal of Molecular Sciences 21 (14): 1–19. https://doi.org/10.3390/ijms21145040

Pastushenko, I; and Blanpain, C. 2019. "EMT Transition States during Tumor Progression and Metastasis." Trends in Cell Biology 29 (3): 212-226. https://doi.org/10.1016/j.tcb.2018.12.001.

Pastushenko, I; Brisebarre, A; Sifrim, A; Fioramonti, M; Revenco, T; Boumahdi, S; van Keymeulen, A; et al. 2018. "Identification of the Tumour Transition States Occurring during EMT." Nature 556 (7702): 463–68. https://doi.org/10.1038/s41586-018-0040-3

Peinado, H; Alečković, M; Lavotshkin, S; Matei, I; Costa-Silva, B; Moreno-Bueno, G; Hergueta-Redondo, M; et al. 2012. "Melanoma Exosomes Educate Bone Marrow Progenitor Cells toward a Pro-Metastatic Phenotype through MET." Nature Medicine 18 (6): 883–91. https://doi.org/10.1038/nm.2753

Peinado, H; Lavotshkin, S; and Lyden, D. 2011. "The Secreted Factors Responsible for Pre-Metastatic Niche Formation: Old Sayings and New Thoughts." Seminars in Cancer Biology 21 (2): 139–46. https://doi.org/10.1016/j.semcancer.2011.01.002

Pópulo, H; Lopes, J. M; and Soares, P. 2012. "The MTOR Signalling Pathway in Human Cancer." International Journal of Molecular Sciences 13 (2): 1886–1918. https://doi.org/10.3390/ijms13021886

Price, T. T; Burness, M. L; Sivan, A; Warner, M. J; Cheng, R; Lee, C. H; Olivere, L; et al. 2016. "Dormant Breast Cancer Micrometastases Reside in Specific Bone Marrow Niches That Regulate Their Transit to and from Bone." Science Translational Medicine 8 (340): 1–23. https://doi.org/10.1126/scitranslmed.aad4059

Qie, S and Diehl, J. A. 2016. "Cyclin D1, Cancer Progression and Opportunities in Cancer Treatment." Physiology & Behavior 176 (1): 139–48. https://doi.org/10.1016/j.physbeh.2017.03.040

Qu, X; Leung, T. C. N; Ngai, S. M; Tsai, S. N; Thakur, A; Li, W. K; Lee, Y; et al. 2021. "Proteomic Analysis of Circulating Extracellular Vesicles Identifies Potential Biomarkers for Lymph Node Metastasis in Oral Tongue Squamous Cell Carcinoma." Cells 10 (9): 1–16. https://doi.org/10.3390/cells10092179

Quail, D. F; and Joyce, J. A. 2013. "Microenvironmental Regulation of Tumor Progression and Metastasis." Nature Medicine. https://doi.org/10.1038/nm.3394

Quandt, E; Ribeiro, M. P. C; and Clotet, J. 2019. "Atypical Cyclins: The Extended Family Portrait." Cellular and Molecular Life Sciences. Springer. https://doi.org/10.1007/s00018-019-03262-7

Rabouille, C. 2017. "Pathways of Unconventional Protein Secretion." Trends in Cell Biology. Elsevier Ltd. https://doi.org/10.1016/j.tcb.2016.11.007

Ramos-García. 2016. "An Update on the Implications of Cyclin D1 in Oral Carcinogenesis." Oral Disease 23 (7): 897–912. https://doi.org/10.1111/ijlh.12426

Ran, F. A; Hsu, P. D; Wright, J; Agarwala, V; Scott, D. A; Zhang, F. "Genome engineering using the CRISPR-Cas9 system." Nature Protocols 8(11): 2281-2308. https://doi.org/10.1038/nprot.2013.143

Rane, S. G; Dubus, P; Mettus, R. V; Galbreath, E. J; Boden, G; Reddy, E. P; and Barbacid, M. 1999. "Loss of Cdk4 Expression Causes Insulin- Deficient Diabetes and Cdk4 Activation Results in β -Islet Cell Hyperplasia." Nature Genetics 22 (1): 44–52. https://doi.org/doi: 10.1038/8751

Resnitzky, P; et al. 1996. "The Ultrastructure of Mantle Cell Lymphoma and Other B-Cell Disorders with Translocation t (11 ; 14)(Q13 ; Q32)." British Journal of Haematology 94 (2): 352–61. https://doi.org/doi: 10.1046/j.1365-2141

Schafer, D. A; and Cooper, J. A. 1995. "Control of Actin Assembly at Filament Ends." Annual Review of Cell and Developmental Biology 11: 497–518. https://doi.org/doi: 10.1146/annurev.cb.11.1101 95.002433

Schneider, C.A; Rasband, W. S; and Eliceiri, K. W. 2012. "NIH Image to ImageJ: 25 Years of Image Analysis." Nat Methods 9 (7): 671–75. https://doi.org/doi: 10.1038/nmeth.2089

Schwartz, M. A; and Assoian, R. K. 2001. "Integrins and Cell Proliferation: Regulation of Cyclin-Dependent Kinases via Cytoplasmic Signaling Pathways." Journal of Cell Science 114 (14): 2553–60. https://pubmed.ncbi.nlm.nih.gov/11683383/

Shapanis, A; Lai, C; Sommerlad, M; Parkinson, E; Healy, E; and Skipp, P. 2020. "Proteomic Profiling of Archived Tissue of Primary Melanoma Identifies Proteins Associated with Metastasis." International Journal of Molecular Sciences 21 (21):1–13. https://doi.org/10.3390/ijms21218160

Sherr, C. J. 1993. "Mammalian G1 Cyclins Review." Cell 73: 1059–65. https://doi.org/10.1016/0092-8674(93)90636 -5

Sherr, C. J; and Roberts, J. M. 1999. "CDK Inhibitors: Positive and Negative Regulators of G1-Phase Progression." Genes and Development 13 (12): 1501–12. https://doi.org/10.1101/gad.13.12.1501

Sherr, C. J; and Roberts, J. M. 2004. "Living with or without Cyclins and Cyclin-Dependent Kinases." Genes and Development 18 (22): 2699–2711. https://doi.org/10.1101/gad.1256504.cycle

Shibue, T; and Weinberg, R. A. 2017. "EMT, CSCs, and Drug Resistance: The Mechanistic Link and Clinical Implications." Nature Reviews Clinical Oncology. Nature Publishing Group 14 (10): 611-629. https://doi.org/10.1038/nrclinonc.2017.44

Shtutman, M; Zhurinsky, J; Simcha, I; Albanese, C; D'Amico, M; Pestell, R; and Ben-Ze'ev., A 1999. "The Cyclin D1 Gene Is a Target of the β-Catenin/LEF-1 Pathway." Proceedings of the National Academy of

Sciences of the United States of America 96 (10): 5522–27. https://doi.org/10.1073/pnas.96.10.5522

Sicinska, E; Aifantis, I; Cam, L. L; Swat, W; Borowski, C; Yu, Q; Ferrando, A. A; et al. 2003. "Requirement for Cyclin D3 in Lymphocyte Development and T Cell Leukemias." Cancer Cell 4 (6): 451–61. https://doi.org/10.1016/S1535-6108(03)00301-5

Sicinski, P; Donaher, J. L; Geng, Y; Parker, S. B; Gardner, H; Park, M. Y; Robker, R. L; et al. 1996. "Cyclin D2 Is an FSH-Responsive Gene Involved in Gonadal Cell Proliferation and Oncogenesis." Nature 384 (6608): 470-474. https://doi.org/10.1038/384470a0

Sicinski, P; Donaher, J. L; Parker, S. B; Li, T; Fazeli, A; Gardner, H; Haslam, S. Z; Bronson, R. T; Elledge, S. J; and Weinberg, R. A. 1995. "Cyclin D1 Provides a Link between Development and Oncogenesis in the Retina and Breast." Cell 82 (4): 621–30. https://doi.org/10.1016/0092-8674(95)90034-9

Singh, S; and Solecki, D. J. 2015. "Polarity Transitions during Neurogenesis and Germinal Zone Exit in the Developing Central Nervous System." Frontiers in Cellular Neuroscience 9 (62): 1–8. https://doi.org/10.3389/fncel.2015.00062

Sleeman, J. P 2012. "The Metastatic Niche and Stromal Progression." Cancer and Metastasis Reviews 31 (3–4): 429–40. https://doi.org/10.1007/s10555-012-9373-9

Son, H. J; Bae, H. C; Kim, H. J; Lee, D. H; Han, D. W; and Park, J. C. 2005. "Effects of β-Glucan on Proliferation and Migration of Fibroblasts." Current Applied Physics 5 (5): 468–71. https://doi.org/10.1016/j.cap.2005.01.011

Son, H. J; Han, D. W; Baek, H. S; Lim, H. R; Lee, M. H; Woo, Y. I and Park, J.C. 2007. "Stimulated TNF-α Release in Macrophage and Enhanced Migration of Dermal Fibroblast by β-Glucan." Current Applied Physics 7 (suppl.1): 33–36. https://doi.org/10.1016/j.cap.2006.11.010

Stadelmann, W. K; Digenis, A. G; and Tobin, G. R. 1998. "Physiology and Healing Dynamics of Chronic Cutaneous Wounds." American Journal of Surgery 176 (2 A): 26S-38S. https://doi.org/10.1016/S0002-9610(98)00183-4

Steinbichler, T. B; Dudás, J; Riechelmann, H; and Skvortsova, I. I. 2017. "The Role of Exosomes in Cancer Metastasis." Seminars in Cancer Biology. Academic Press. https://doi.org/10.1016/j.semcancer.2017.02.006

Streit, M; Velasco, P; Riccardi, L; Spencer, L; Brown, L. F; Janes, J; Lange-Asschenfeldt, B; et al. 2000. "Thrombospondin-1 Suppresses Wound Healing and Granulation Tissue Formation in the Skin of Transgenic Mice." The EMBO Journal 19 (13): 3272–82. https://doi.org/10.1093/emboj/19.13.3272

Sumrejkanchanakij, P; Tamamori-Adachi, M; Matsunaga, Y; Eto, K; and Ikeda, M. K. 2003. "Role of Cyclin D1 Cytoplasmic Sequestration in the Survival of Postmitotic Neurons." Oncogene 22 (54): 8723–30. https://doi.org/10.1038/sj.onc.1206870

Sun, Z; Schwenzer, A; Rupp, T; Murdamoothoo, D; Vegliante, R; Lefebvre, O; Klein, A; Hussenet, T; and Orend, G. 2018. "Tenascin-C Promotes Tumor Cell Migration and Metastasis through Integrin A9b1–Mediated YAP Inhibition." Cancer Research 78 (4): 950–61. https://doi.org/10.1158/0008-5472.CAN-17-1597

Szklarczyk, D; Gable, A. L; Nastou, K. C; Lyon, D; Kirsch, R; Pyysalo, S; Doncheva, N. T et al. 2021. "The STRING Database in 2021: Customizable Protein-Protein Networks, and Functional Characterization of

User-Uploaded Gene/Measurement Sets." Nucleic Acids Research 49 (D1): D605–12. https://doi.org/10.1093/nar/gkaa1074

Tan, V. Y; Lewis, S. J; Adams, J. C; and Martin, R. M. 2013. "Association of Fascin-1 with Mortality, Disease Progression and Metastasis in Carcinomas: A Systematic Review and Meta-Analysis." BMC Medicine 11 (52): 1–17. https://doi.org/10.1186/1741-7015-11-52

Tanic, J; Wang, Y; Lee, W; Coelho, N.M; Glogauer, M; and McCulloch, C. A. 2019a. "Adseverin Modulates Morphology and Invasive Function of MCF7 Cells." Biochimica et Biophysica Acta - Molecular Basis of Disease 1865 (10): 2716–25. https://doi.org/10.1016/j.bbadis.2019.07.015

Thiery, J. P; Acloque, H; Huang, R. Y. J; and Nieto, M. A. 2009. "Epithelial-Mesenchymal Transitions in Development and Disease." Cell. https://doi.org/10.1016/j.cell.2009.11.007

Trifaró, J. M; Rodríguez del Castillo, A; and Vitale, M. L. 1992. "Molecular Neurobiology Dynamic Changes in Chromaffin Cell Cytoskeleton as Prelude to Exocytosis." Neurochemical Research 6 (4): 339–56. https://doi.org/doi:10.1023/a:1007503919265

Trifaró, J. M, Rosé, S. D; and Marcu, M. G. 2000. "Scinderin, a Ca 2+-Dependent Actin Filament Severing Protein That Controls Cortical Actin Network Dynamics during Secretion*." Neurochemical Research 25 (1): 133–44. https://doi.org/doi: 10.1023/a:1007503919265

Varga, J; and Greten, F. R. 2017. "Cell Plasticity in Epithelial Homeostasis and Tumorigenesis." Nature Cell Biology. 19 (10): 1133-1141. https://doi.org/10.1038/ncb3611

Velasco-Velázquez, M. A; Li, Z; Casimiro, M; Loro, E; Homsi, N; and Pestell, R. G. 2011. "Examining the Role of Cyclin D1 in Breast Cancer." Future Oncology Journal 7 (6): 753–65. https://doi.org/10.2217/fon.11.56

Vermeulen, K; van Bockstaele, D. R; and Berneman, Z. N. 2003. "The Cell Cycle: A Review of Regulation, Deregulation and Therapeutic Targets in Cancer." Cell Proliferation 36 (3): 131–49. https://doi.org/10.1046/j.1365-2184.2003.00266

Vivanco, I; and Sawyers, C. L. 2002. "The Phosphatidylinositol 3-Kinase-AKT Pathway in Humancancer." Nature Reviews Cancer 2 (7): 489–501. https://doi.org/10.1038/nrc839

Vooijs, M; te Riele, H; van der Valk, M; and Berns, A. 2002. "Tumor Formation in Mice with Somatic Inactivation of the Retinoblastoma Gene in Interphotoreceptor Retinol Binding Protein-Expressing Cells." Oncogene 21: 4635–45. https://doi.org/10.1038/sj.onc

Wagner, M; and Wiig, H. 2015. "Tumor Interstitial Fluid Formation, Characterization, and Clinical Implications." Frontiers in Oncology 5 (115): 1–12. https://doi.org/10.3389/fonc.2015.00115

Wang, D; Sun, S. Q; Yu, Y. H; Wu, W. Z; Yang, S. L; and Tan, J. M. 2014. "Suppression of SCIN Inhibits Human Prostate Cancer Cell Proliferation and Induces G0/G1 Phase Arrest." International Journal of Oncology 44 (1): 161–66. https://doi.org/10.3892/ijo.2013.2170

Wang, L; Song, G; Zhang, X; Feng, T; Pan, J; Chen, W; Yang, M; et al. 2017. "PADI2-Mediated Citrullination Promotes Prostate Cancer Progression." Cancer Research 77 (21): 5755–68. https://doi.org/10.1158/0008-5472.CAN-17-0150

Wang, Y. T; Shi, T; Srivastava, S; Kagan, J; Liu, T; and Rodland, K. D. 2020. "Proteomic Analysis of

Exosomes for Discovery of Protein Biomarkers for Prostate and Bladder Cancer." Cancers. MDPI AG. https://doi.org/10.3390/cancers12092335

Wells, A; Yates, C; and Shepard, C. R. 2008. "E-Cadherin as an Indicator of Mesenchymal to Epithelial Reverting Transitions during the Metastatic Seeding of Disseminated Carcinomas." Clinical and Experimental Metastasis 25 (6): 621-628. https://doi.org/10.1007/s10585-008-9167-1

Wong, C. W, Shientag L. A; Yu, J; Dong, Y; Kao, G; Al-Mehdi, A. B; Bernhard, E. J; and Muschel, R. J. 2001. "Apoptosis: An Early Event in Metastatic Inefficiency 1." Cancer Research 61 (1): 333–38. https://pubmed.ncbi.nlm.nih.gov/11196183/

Woo, Y. I; Park, B. J; Kim, H. L; Lee, M. H; Kim, J; Yang, Y; Kim, J. J; Tsubaki, K; Han, D. W; and Park, J. C. 2010a. "The Biological Activities of (1,3)-(1,6)-β-D-Glucan and Porous Electrospun PLGA Membranes Containing β-Glucan in Human Dermal Fibroblasts and Adipose Tissue-Derived Stem Cells." In Biomedical Materials. Vol. 5. Institute of Physics Publishing. https://doi.org/10.1088/1748-6041/5/4/044109

Xijin, G; Dongmin, S; and Yao, R. 2020. "ShinyGO: A Graphical Gene-Set Enrichment Tool for Animals and Plants." Bioinformatics 36 (8): 2628–29. https://doi.org/10.5281/zenodo.1451847

Xiong, Y; Connolly, T; Futcher, B; and Beach, D. 1991. "Human D-Type Cyclin." Cell 65 (4): 691–99. https://doi.org/10.1016/0092-8674(91)90100-D

Yamaguchi, K; Kanno, E; Tanno, H; Sasaki, A; Kitai, Y; Miura, T; Takagi, N; et al. 2021. "Distinct Roles for Dectin-1 and Dectin-2 in Skin Wound Healing and Neutrophilic Inflammatory Responses." Journal of Investigative Dermatology 141 (1): 164-176.e8. https://doi.org/10.1016/j.jid.2020.04.030

Yen, M. C; Huang, Y. C; Kan, J. Y; Kuo, P. L; Hou, M. F; and Hsu, Y. L. 2018. "S100B Expression in Breast Cancer as a Predictive Marker for Cancer Metastasis." International Journal of Oncology 52 (2): 433–40. https://doi.org/10.3892/ijo.2017.4226

Zacksenhaus, E; Jiang, Z; Chung, D; Marth, J. D; Phillips, R. A; and Gallie, B. L. 1996. "PRb Controls Proliferation, Differentiation, and Death of Skeletal Muscle Cells and Other Lineages during Embryogenesis." Genes and Development 10 (23): 3051–64. https://doi.org/doi: 10.1101/gad.10.23.3051

Zhang, L; Fried, F. B; Guo, H; and Friedman, A. F. 2008. "Cyclin-Dependent Kinase Phosphorylation of RUNX1/AML1 on 3 Sites Increases Transactivation Potency and Stimulates Cell Proliferation." Blood 111: 1193–1200. https://doi.org/10.1182/blood-2007-08

Zhong, Z; Yeow, W-S; Zou, C; Wassell, R; Wang, C; Pestell, R. G; Quong, J. N; and Quong. A. A. 2010. "Cyclin D1/Cyclin Dependent Kinase 4 Interacts with Filamin A and Affects the Migration and Invasion Potential of Breast Cancer Cells." Cancer Research 70 (5): 2105–14. https://doi.org/10.1158/0008-5472.CAN-08-1108

Zhou, B; Chen, T. W; Jiang, Y. B; Wei, X. B; de Lu, C; Li, J. J; Xie, D; and Cheng, S. Q. 2020. "Scinderin Suppresses Cell Proliferation and Predicts the Poor Prognosis of Hepatocellular Carcinoma." Oncology Letters 19 (3): 2011–20. https://doi.org/10.3892/ol.2020.11262

Zykova, S. N; Balandina, K. A; Vorokhobina, N. V; Kuznetsova, A. V; Engstad, R; and Zykova, T. A. 2014. "Macrophage Stimulating Agent Soluble Yeast β-1,3/1,6-Glucan as a Topical Treatment of Diabetic Foot and Leg Ulcers: A Randomized, Double Blind, Placebo-Controlled Phase II Study." Journal of Diabetes Investigation 5 (4): 392–99. https://doi.org/10.1111/jdi.12165

ANNEX

PUBLICATIONS

Barley β-Glucan accelerates wound healing by favoring migration versus proliferation of human dermal fibroblasts

Fusté NP*, **Guasch M***, Guillen P*, Anerillas C, Cemeli T, Pedraza N, Ferrezuelo F, Encinas M, Moralejo M, Garí E.

*Authors contributed equally to this work

Carbohydr Polym. 2019 Apr 15; 210:389-398. doi: 10.1016/j.carbpol.2019.01.090. Epub 2019 Jan 28.

Cytoplasmic Cyclin D1 regulates glioblastoma dissemination

Cemeli T, **Guasch-Vallés M**, Nàger M, Felip I, Cambray S, Santacana M, Gatius S, Pedraza N, Dolcet X, Ferrezuelo F, Schuhmacher AJ, Herreros J, Garí E.

J Pathol. 2019 Apr 7; 248(4):501-513. doi: 10.1002/path.5277. Epub 2019 May 16.

Evaluation of Tumor Interstitial Fluid-Extraction Methods for Proteome Analysis: Comparison of Biopsy Elution versus Centrifugation

Matas-Nadal C, Bech-Serra JJ, **Guasch-Vallés M**, Fernández-Armenteros JM, Barceló C, Casanova JM, de la Torre Gómez C, Aguayo Ortiz R, Garí E.

J Proteome Res. 2020 Jul 2; 19(7):2598-2605. doi: 10.1021/acs.jproteome.9b00770. Epub 2020 Jan 8.